

Some pages of this thesis may have been removed for copyright restrictions.

If you have discovered material in Aston Research Explorer which is unlawful e.g. breaches copyright, (either yours or that of a third party) or any other law, including but not limited to those relating to patent, trademark, confidentiality, data protection, obscenity, defamation, libel, then please read our [Takedown policy](#) and contact the service immediately (openaccess@aston.ac.uk)

Synthesis and application of novel probes for the detection of cysteine sulphenic acids

Shibani Nissansala Ratnayake

Doctor of Philosophy

Aston University

March 2015

©Shibani N Ratnayake, 2015

Shibani Nissansala Ratnayake asserts her moral right to be identified as the author of this thesis

This copy of the thesis has been supplied on condition that anyone who consults it is understood to recognise that its copyright rests with its author and that no quotation from the thesis and no information derived from it may be published without appropriate permission or acknowledgement.

Aston University

Synthesis and application of novel probes for the detection of cysteine sulphenic acids

Shibani Ratnayake

Doctor of Philosophy

2015

Cysteine is a thiol containing amino acid that readily undergoes oxidation by reactive oxygen species (ROS) to form sulphenic (R-SOH) sulphinic (RSO₂H) and sulphonic (RSO₃H) acids. Thiol modifications of cysteine have been implicated as modulators of cellular processes and represent significant biological modifications that occur during oxidative stress and cell signalling. However, the different oxidation states are difficult to monitor in a physiological setting due to the limited availability of experimental tools. Therefore it is of interest to synthesise and use a chemical probe that selectively recognises the reversible oxidation state of cysteine sulphenic acid to understand more about oxidative signalling. The aim of this thesis was to investigate a synthetic approach for novel fluorescent probe synthesis, for the specific detection of cysteine sulphenic acids by fluorescence spectroscopy and confocal microscopy. N-[2-(Anthracen-2-ylamino)-2-oxoethyl]-3,5-dioxocyclohexanecarboxamide was synthesised in a multistep synthesis and characterised by nuclear magnetic resonance spectroscopy. The optimisation of conditions needed for sulphenic acid formation in a purified protein using human serum albumin (HSA) and the commercially available biotin tagged probe 3-(2,4-dioxocyclohexyl)propyl-5-((3aR,6S,6aS)-hexahydro-2-oxo-1H-thieno[3,4-d]imidazol-6-yl)pentanoate (DCP-Bio1) were identified. This approach was extended to detect sulphenic acids in Jurkat T cells and CD4⁺ T cells pre- and post-stimulus. Buthionine sulfoximine (BSO) was used to manipulate the endogenous antioxidant glutathione (GSH) in human CD4⁺ T cells. Then the surface protein thiol levels and sulphenic acid formation was examined. T cells were also activated by the lectin phytohaemagglutinin-L (PHA-L) and formation of sulphenic acid was investigated using SDS-PAGE, western blotting and confocal microscopy. Resting Jurkat cells have two prominent protein bands that have sulphenic acid modifications whereas resting CD4⁺ T cells have an additional band present. When cells were treated with BSO the number of bands increased whereas activation reduced the number of proteins that were modified. The identities of the protein bands containing sulphenic acids were explored by mass spectrometry. Cysteine oxidation was observed in redox, metabolic and cytoskeletal proteins. In summary, a novel fluorescent probe for detection of cysteine sulphenic acids has been synthesised alongside a model system that introduces cysteine sulphenic acid in primary T cells. This probe has potential application in the subcellular localisation of cysteine oxidation during T cell signalling.

Key words: Sulphenic acid, HSA, CD4⁺ T cells, DCP-Bio1, BSO

Dedication:

I would like to dedicate this thesis to my loving husband Ajitha Ratnayake and to my wonderful parents for supporting me throughout my PhD.

Acknowledgements:

Firstly I would like to thank my supervisors Prof Helen R Griffiths and Dr Eric Lattmann for their continuous support. I would also like to thank Dr Mike Davis for all his guidance in the chemistry laboratory. I would like to thank Charlotte Bland for her assistance in confocal and fluorescence microscopy. Lastly I would like to thank all my colleagues in lab 364 and 358 for their continuous help and support. Mass spectrometry was done by Dr Andrew Creese at the University of Birmingham.

On a personal note I would like to thank my lovely friends Matt, Pranav and Baptiste for all the laughs in the lab and being there for me when times were tough. All the discussions we had during the last four years both academically and non -academically is much appreciated. A special thanks to Baptiste for all the help with my chemistry chapter.

I would like to thank Rita, Iru, Rach and Justin for their support and help. I would like to thank Helen for all her guidance and support throughout this PhD. I wouldn't be here today if not for the guidance I have had over the years from my loving parents. Thank you both so much. Last but not least my wonderful husband who put up with me all this time specially the last six months through the stress of thesis writing.

Table of Contents

Title Page	
Summery	1
Dedication	2
Acknowledgements	3
List of Contents	4
List of Figures	8
List of Tables	11
Abbreviations	12
Chapter 1.0: General introduction	20
1.1 Reactive oxygen species:.....	21
1.2 Cysteine:.....	22
1.2.1 Cysteine sulphenic acids:.....	25
1.2.2 Cysteine sulphinic and sulphonic acids:.....	29
1.3 Cysteine sulphenic acids in proteins:.....	30
1.4 Tools to detect cysteine sulphenic acid formation in proteins:.....	32
1.5 Inflammation and the immune system:.....	49
1.5.1 T cell maturation and sub populations:.....	51
1.5.2 T cell activation and TCR signalling:.....	53
1.5.3 Oxidative stress in the immune system:.....	56
1.6 Aims and objectives:.....	59
Chapter 2.0 Materials and methods	60
2.1 Materials:.....	61
2.2 Methods:.....	62
2.2.1 Jurkat E6.1 T Cell culture:.....	62
2.2.2 Trypan blue cell counting and cell viability:.....	62
2.2.3 Sodium dodecyl sulphate polyacrylamide gel electrophoresis (SDS-PAGE):.....	63
2.2.4 The bicinchoninic acid (BCA) assay:.....	67
2.2.5 Glutathione (GSH) assay:.....	68
2.2.6 Flow cytometry:.....	70
Chapter 3.0 Detection of sulphenic acid in human serum albumin (HSA)	71
3.1 Preface:.....	72
3.2 Introduction:.....	73
3.2.1 Thiol oxidation:.....	73
3.2.2 Human serum albumin:.....	73
3.2.3 Sulphenic acid in human serum albumin:.....	75
3.3 Materials and methods:.....	76
3.3.1 HSA sample preparation for dot blot and western blotting and mass spectrometry:	76

3.3.2	Glutathione preparation for mass spectrometry:	76
3.3.3	Protein Enzyme Linked Sulphenyl Probe Assay (ELSPA):	77
3.3.4	Dot blot for sulphenic acid on HSA:	78
3.3.5	SDS-PAGE and western blotting for sulphenic acid on HSA:	79
3.3.6	Coomassie staining:	79
3.3.7	HSA preparation for mass spectrometry:	79
3.3.8	In-gel protein digestion for mass spectrometry:	80
3.3.9	Peptide sequencing using mass spectrometry:	81
3.4	Results:	83
3.4.1	Detection of glutathione (GSH) modifications by mass spectrometry:	83
3.4.2	Optimisation of hydrogen peroxide concentrations for sulphenic acid formation determined by ELSPA:	85
3.4.3	Visualisation of sulphenic acid formation on HSA by dot bot:	90
3.4.4	Effect of different concentrations of DCP-Bio1 on sulphenic acid formation in HSA:	91
3.4.5	HSA treatment with different concentrations of hydrogen peroxide:	93
3.4.6	The effect of iodoacetamide on sulphenic acid formation in HSA:	95
3.4.7	Detection of sulphenic acid modifications of HSA by mass spectrometry:	97
3.5	Discussion:	99
Chapter 4.0 Protein sulphenic acid formation in Jurkat T cells and human CD4+ T cells....		103
4.1	Preface:	104
4.2	Introduction:	105
4.3	Materials and Methods:	107
4.3.1	Isolation of peripheral blood mononuclear cells (PBMC):	107
4.3.2	Negative isolation of human CD4+ T cells:	108
4.3.3	Flow cytometric assay for cell surface CD4+ analysis:	109
4.3.4	Modulation of cellular CD4+ T cell thiol levels:	109
4.3.5	Preparation of cells for flow cytometry to detect surface thiols:	109
4.3.6	Effect of BSO on surface thiols using 5,5'-dithiobis(2-nitrobenzoic acid) (DTNB) assay:	110
4.3.7	Cell lysate preparation for GSH assay:	111
4.3.8	Activation of T cells by PHA-L and PHA-P:	111
4.3.9	Quantification of interleukin-2 (IL-2):	111
4.3.10	Flow cytometry for the detection of T cell activation:	112
4.3.11	Protein sulphenic acid extraction in Jurkat T cells and human CD4+ T cells: ...	113
4.3.12	Method development for protein sulphenic acid extraction using Jurkat T cell line:	115

4.3.13 T cell sample preparation for mass spectrometry:.....	117
4.3.14 Confocal Microscopy:	118
4.3.15 Data analysis:.....	118
4.4 Results:.....	119
4.4.1 Isolation of BPMC s and CD4+ T cells from 20 mL of blood:	119
4.4.2 Purity of negatively isolated human CD4+ T cells using flow cytometry:	120
4.4.3 The effect of GSH synthetase inhibitor, buthionine sulfoximine (BSO) on CD4+ T cell viability:.....	121
4.4.4 Effect of buthionine sulfoximine on CD4+ T cell total GSH level:	122
4.4.5 Effect of BSO on surface thiols of CD4+T cells:.....	123
4.4.6 Effect of PHA-L and PHA-P on cell viability:.....	125
4.4.7 Effect of PHA-L and PHA-P on CD4 + T cell activation:	126
4.4.8 Effect of PHA-P and PHA-L on T cells using IL-2 ELISA:	127
4.4.9 Protein sulphenic acid modifications in Jurkat E6.1 T cells:.....	128
4.4.10 CD4+ T cell protein sulphenic acid modifications:.....	131
4.4.11 BSO treated CD4+ T cell protein sulphenic acid modifications:	133
4.4.12 BSO and PHA-L treated CD4+ T cell protein sulphenic acid modifications:....	135
4.4.13 PHA-L treated CD4+ T cell protein sulphenic acid modifications:.....	137
4.4.14 Mass spectrometry identification of protein bands containing sulphenic acid modifications:.....	139
4.4.15 Cell imaging:	145
4.5 Discussion:	147
Chapter 5.0 Synthesis of novel compounds for the detection of cysteine sulphenic acids....	152
5.1 Preface:.....	153
5.2 Introduction:.....	154
5.2.1 Strategy for the synthesis of fluorescent probe:	156
5.3 Materials and methods:	157
5.3.1 Materials:	157
5.3.2 Methods:.....	158
5.4 Results and discussion:	169
5.4.1 Retrosynthetic approach for fluorescent probe to detect sulphenic acid:	169
5.4.2 First synthesis of synthon 3	170
5.4.3 Second strategy for the synthesis of synthon 3.....	172
5.4.4 Synthesis of synthon 2.....	175
5.4.5 Synthesis of the probe	176
5.4.6 Synthesis of sulphenic acid detecting magnetic probe:	182
Chapter 6.0 General discussion	184

6.1 Discussion:	185
6.2 Conclusion:	190
6.3 Future work:	190
7.0 References	191

List of Figures:

Figure number and title	Page number
1.1 Different oxidation states of cysteine in a biological system	23
1.2 Tautomers of sulphenic acid	25
1.3 Electrophilic reactions of sulphenic acids	27
1.4 Nucleophilic reactions of sulphenic acids	28
1.5 S-Alkylation of sulphenic acid by dimedone	34
1.6 Schematic for the synthesis of DCP-MCC and DCP-MAB	35
1.7 Fluorescent and affinity based probes to detect cysteine sulphenic acids	38
1.8 Synthesis of DAz-1	43
1.9 Chemical structure of DAz-2	45
1.10 Development of T cells	52
1.11 Schematic representation of TCR signalling	55
2.1 Schematic representation of protein transfer to PVDF membrane	66
3.1 Schematic representation of b and y ions	82
3.2 Disulphide bond formation in glutathione is increased by hydrogen peroxide	84
3.3 Increasing hydrogen peroxide concentration increases sulphenic acid modification in HSA	86
3.4 Effect of DCP-Bio1 concentration on detection of sulphenic acid formation in HSA with hydrogen peroxide	87
3.5 Treatment conditions affect the detection of sulphenic acids	89
3.6 Sulphenic acid formation can be detected on dot blot	90
3.7 HSA sulphenic acid modifications with different concentrations of DCP-Bio1	92
3.8 Increasing hydrogen peroxide concentrations increases sulphenic acid modifications in HSA	94
3.9 Sulphenic acid formation is prevented by the addition of iodoacetamide	96
3.10 The formation of sulphenic acid is detected by mass spectrometry	98
4.1 Schematic representation of centrifuged whole blood in lymphoprep® density gradient	107
4.2 The reaction between thiol and 5,5'-dithiobis(2-nitrobenzoic) acid	110
4.3 Schematic representation of the approach for isolation of sulphenic acid modified proteins	114
4.4 Determination of DCP-Bio1 concentration required for sulphenic acid	116

	detection in Jurkat T cells	
4.5	PBMC and CD4+ T cells recovered from 20 mL blood	120
4.6	Purity of negatively isolated CD4+ T cells	121
4.7	Buthionine sulfoximine (BSO) treatment of CD4+ T cells does not affect T cell viability	122
4.8	Pre-incubation with buthionine sulfoximine (BSO) affects the total glutathione (GSH) levels in CD4+ T cells	123
4.9	Buthionine Sulfoximine (BSO) pre-incubation with CD4+ T cells reduces surface thiol levels	125
4.10	PHA-L and PHA-P treatment decreases with cell viability	126
4.11	T cell activation markers are increased by increasing concentrations of PHA-L and PHA-P	127
4.12	PHA-L increases IL-2 secretion	128
4.13	Schematic presentation of isolation of sulphenic acid modified proteins	130
4.14	Protein sulphenic acid modifications in Jurkat E6.1 T cells	131
4.15	Protein sulphenic acid modifications in resting CD4+ T cells	133
4.16	Sulphenic acid modifications in buthionine sulfoximine (BSO) treated T cells	135
4.17	Protein sulphenic acid modifications with BSO and PHA-L treated T cells	137
4.18	Protein sulphenic acid modifications after 5 µg/mL for 24 hours	139
4.19	Detection of protein thiols and sulphenic acid in CD4+ T cells	147
5.1	General structure of the fluorescent probe	157
5.2	Excitation spectrum of N-[2-(anthracen-2-ylamino)-2-oxoethyl]-3,5-dioxocyclohexanecarboxamide in DMSO	168
5.3	Schematic representation of retrosynthetic approach for fluorescent probe1	170
5.4	Reaction conditions for the synthesis of 2-amino-N-(anthracen-2-yl) acetamide	171
5.5	Reaction mechanism for the formation of amine	172
5.6	Reaction mechanism for mixed anhydride formation	173
5.7	Reaction conditions for the synthesis of 2-amino-N-(anthracen-2-yl) acetamide via synthetic route 2	174
5.8	¹ H NMR spectrum of 2-amino-N-(anthracen-2-yl) acetamide	175
5.9	Tautomeric structures of 3,5-diketohexahydrobenzoic acid in solution	177
5.10	Protection of 3,5- diketohexahydrobenzoic acid	178
5.11	¹ H NMR spectrum of 3-methoxy-5-oxocyclohex-3-ene-1-carboxylic acid	179
5.12	Reaction conditions for the synthesis of N-[2-(anthracen-2-ylamino)-2-oxoethyl]-3,5-dioxocyclohexanecarboxamide	180

5.13	¹ H NMR of N-[2-(anthracen-2-ylamino)-2-oxoethyl]-3,5-dioxocyclohexanecarboxamide	182
5.14	Infrared spectra of magnetic bead product with magnetic bead starting material	183
5.15	Infrared spectra comparison of starting material with material cleaved of with 2 M HCl	184
6.1	Schematic representation of T cells	190

List of Tables:

Table number and title	Page number
2.1 Buffers and reagents used for SDS-PAGE	63
2.2 Reagents for polyacrylamide gels	65
2.3 Combination of chemicals needed to prepare a standard curve to determine protein concentration	67
2.4 List of reagents required for the GSH assay	68
2.5 Combination of reagents required for the standard curve to determine total GSH level	69
3.1 Reagents required for the ELSPA	77
4.1 Reagents and quantities used for isolation of CD4+ T cells	108
4.2 Results of protein identifications for the 25 kDa band	141
4.3 Results of protein identifications for 40 kDa band	142
4.4 Results of protein identifications for the 45 kDa band	143
4.5 Results of protein identifications for the 50 kDa band	144
4.6 Results of protein identifications for the 65 kDa band	145
5.1 Hydrogenation using different catalysts	176

Abbreviations:

ACN	Acetonitrile
ADAP	Adhesion and degranulation promoting adaptor protein
AhpC	Alkyl hydroperoxide reductase subunit C
AhpE	Alkyl hydroperoxide reductase subunit E
Akt2	v-Akt murine thymoma viral oncogene homolog 2
ANOVA	Analysis of variance
AP-1	Activator protein-1
APC	Antigen presenting cells
APC	Allophycocyanin
APS	Ammonium persulphate
BAPNA	N- α -Benzoyl-L-arginine-4-nitroanilide hydrochloride
BCA	Bicinchoninic acid
BCP	Bacterioferritin comigratory protein
Biotin-HPDP	N-[6-(Biotinamido)hexyl]-3'-(2'-pyridyldithio)propionamide
Boc	Tert-butyloxycarbonyl
BSA	Bovine serum albumin
BSO	Buthionine sulfoximine
CD3	Cluster of differentiation 3
CD4	Cluster of differentiation 4
CD8	Cluster of differentiation 8
CD25	Cluster of differentiation 25
CD28	Cluster of differentiation 28
CD44	Cluster of differentiation 44
CD40 L	Cluster of differentiation 40 ligand
CD80	Cluster of differentiation 80

CD86	Cluster of differentiation 86
c-Kit	Stem cell growth factor receptor
Cys	Cysteine
DAz-1	N-(3-Azidopropyl)-3,5-dioxocyclohexanecarboxamide
DAz-2	4-(3-Azidopropyl) cyclohexane-1,3-dione
DC	Direct current
DC	Dendritic cells
DCC	Dicyclohexylcarbodiimide
CID	Collision induced dissociation
DCP-Bio1	3-(2,4-Dioxocyclohexyl)propyl-5-((3aR,6S,6aS)-hexahydro-2-oxo-1H-thieno[3,4-d]imidazole-6-yl)pentanoate
DCP-Bio2	5-((3aR,6S,6aS)-Hexahydro-2-oxo-1H-thieno[3,4-d]imidazole-6-yl)-N-((1-(3-(2,4-dioxocyclohexyl)propyl)-1H-1,2,3-triazol-4-yl)methyl)pentanamide
DCP-Bio3	3-(2,4-Dioxocyclohexyl)propyl-4-(5-((3aR,6S,6aS)-hexahydro-2-oxo-1H-thieno[3,4-d]imidazole-6-yl)pentanamide)butylcarbamate
DCP-FL1	Fluoresceinamine-5'-N-[2,4-dioxocyclohexyl)propyl]carbamate
DCP-FL2	Fluoresceinamine-5'-N-[3-((1-(3-(2,4-dioxocyclohexyl)propyl)-1H-1,2,3-triazol-4-yl)methyl)urea
DCP-MAB	3-(2,4-Dioxocyclohexyl) propyl-2-(methylamino)benzoate
DCP-MCC	3-(2,4-Dioxocyclohexyl)propyl-7-methoxy-2-oxo-2H-chromen-3-ylcarbamate
DCP-Rho1	Rhodamine B[4-[3-(2,4-dioxocyclohexyl)propyl]carbamate]piperazine amide
DCP-Rho2	Rhodamine B-3-(2,4-dioxocyclohexyl) propyl-4-oxo-4-(piperazin-1-yl) butylcarbamate
DIAD	Diisopropyl azodicarboxylate
DIEA	N,N-Diisopropylethylamine
DMF	Dimethylformamide

DMSO	Dimethyl sulphoxide
DNA	Deoxyribonucleic acid
DPPA	Diphenyl phosphorazide
DTNB	5,5'-Dithiobis(2-nitrobenzoic) acid
DTT	Dithiothreitol
EDC	1-Ethyl-3-(3-dimethylaminopropyl)carbodiimide
EDTA	Ethylenediaminetetraacetic acid
EGF	Epidermal growth factor
EGFR	Epidermal growth factor receptor
ELISA	Enzyme linked immunosorbent assay
ELSPA	Enzyme linked sulphenyl probe assay
ESI-MS	Electrospray ionisation mass spectroscopy
FBS	Foetal bovine serum
FITC	Fluorescein isothiocyanate
FS	Forward scatter
GADS	GRB2 related adaptor protein
GAPDH	Glyceraldehyde-3-phosphate dehydrogenase
GCL	Glutamate cysteine ligase
GPx	Glutathione peroxidase
GPx3	Glutathione peroxidase 3
GRB2	Growth factor receptor bound protein 2
GSH	Glutathione
GSR	Glutathione reductase
GSSG	Glutathione disulphide
H ₂ O ₂	Hydrogen peroxide
HCl	Hydrochloric acid

HRP	Horseradish peroxidase
HSA	Human serum albumin
HSC	Hematopoietic stem cell
H ₂ SO ₄	Sulphuric acid
IAM	Iodoacetamide
IFN- γ	Interferon- γ
IL-1 β	Interleukin 1 beta
IL-2	Interleukin 2
IL-4	Interleukin 4
IL-5	Interleukin 5
IL-6	Interleukin 6
IL-10	Interleukin 10
IL-12	Interleukin 12
IL-17	Interleukin 17
IL-18	Interleukin 18
IL-21	Interleukin 21
IL-22	Interleukin 22
IL-35	Interleukin 35
ITAM	Immunoreceptor tyrosine-based activation motif
ITK	Interleukin-2-inducible T cell kinase
LAT	Linker of activated T cells
Lck	Lymphocyte-specific protein tyrosine kinase
LDA	Lithium diisopropyl amide
LT- α	Lymphotoxin α
LTQ	Linear trap quadrupole
MALDI	Matrix assisted laser desorption ionisation

MAPK	Mitogen activated protein kinase
MES	2-[N-Morpholino]ethane sulphonic acid
MHC-I	Major histocompatibility complex class I
MHC-II	Major histocompatibility complex class II
MP	Mobile phase
NaCl	Sodium chloride
NADH	Nicotinamide adenine dinucleotide
NADPH	Nicotinamide adenine dinucleotide phosphate
Na ₃ VO ₄	Sodium vanadate
NBD-Cl	4-Chloro-7-nitrobenzo-2-oxa-1,3-diazole
N-Boc-GABA	γ-(Boc-Amino)butyric acid,4-(tert-Butoxycarbonylamino)butyric acid
NCK1	Non-catalytic region of tyrosine kinase adaptor protein 1
NEM	N-Ethylmaleimide
NH ₄ HCO ₃	Ammonium bicarbonate
NHS	N-Hydroxy succinamide
NK	Natural killer
NMR	Nuclear magnetic resonance
Nox	NADPH oxidase
O ₂ ⁻	Superoxide ion radical
OhrR	Organic hydroperoxide resistance regulator
OPD	O-Phenylenediamine
OxyR	Oxidative stress regulator
PBMC	Peripheral blood mononuclear cells
PBS	Phosphate buffered saline
PE	Phycoerythrin
PHA	Phytohaemagglutinin

PI	Positive ionisation
PLC γ	Phospholipase C γ 1
Prx1	Peroxiredoxin 1
Prx5	Peroxiredoxin 5
Prx6	Peroxiredoxin 6
Prxs	Peroxiredoxins
PrxQ	Peroxiredoxin Q
P/S	Penicillin/ Streptomycin
PTP	Protein tyrosine phosphatase
PTSA	p-Toluene sulphonic acid
PVDF	Polyvinylidene difluoride
RAG1	Recombination-activating gene 1
RAG2	Recombination activating gene 2
RBC	Red blood cells
RF	Radio frequency
R _f	Retention factor
RNS	Reactive nitrogen species
ROS	Reactive oxygen species
RPMI	Rosewell park memorial institute
RS \cdot	Thiyl radical
RS $^-$	Thiolate anion
RSNO	Nitrosothiols
RSNO ₂	Nitrothiols
RSOH	Sulphenic acid
RSO ₂ H	Sulphinic acid
RSO ₃ H	Sulphonic acid

RSOSR	Thiosulphinate
RSSR	Disulphide
SC	Side scatter
SDS-PAGE	Sodium dodecyl sulphate-polyacrylamide gel electrophoresis
SEM	Standard error mean
SHP-1	Src homology region 2 domain-containing phosphatase-1
SHP-2	Src homology region 2 domain-containing phosphatase-2
SLP-76	Lymphocyte cytosolic protein 2 domain containing leukocyte protein of 76kDa
SNO	S-Nitrosation
SSA	Sulphosalicylic acid
T-ALL	T cell acute lymphoblastic leukemia
TBAF	Tetrabutylammonium fluoride
TBDMS	Tert-Butydimethylsilyl ether
TBS	Tris buffered saline
TBST	Tris buffered saline tween -20
TBTU	O-(Benzotriazol-1-yl)-N,N,N',N'-tetramethyluronium tetrafluoroborate
Tc	T cytotoxic
TCR	T cell receptor
TEMED	N,N,N',N'-Tetramethylethane-1,2-diamine
TFA	Trifluoroacetic acid
TGF- β	Transforming growth factor beta
Th	T helper
Th1	T helper 1
Th2	T helper 2
Th17	T helper 17

THF	Tetrahydrofuran
TLC	Thin layer chromatography
TNF- α	Tumour necrosis factor alpha
TOF	Time of flight
Tpx	Lipid hydroperoxide peroxidase
Treg	T regulatory
TRX	Thioredoxin
UV	Ultraviolet
VAV1	Guanine nucleotide exchange factor
VHR	Vaccinia H1-related
Yap1	Yes associated protein 1
ZAP-70	Zeta chain associated protein kinase 70

Chapter 1.0: General introduction

1.1 Reactive oxygen species:

Reactive oxygen species (ROS) until recently were considered only to be toxic by-products of metabolism (1). They encompass a wide range of molecules and are mainly produced in the cells as by-products from the mitochondria during electron transport and from activated phagocytic cells. The sequential reduction of oxygen through the addition of electrons leads to formation of other species of ROS including hydrogen peroxide (H_2O_2), superoxide ion radicals ($\text{O}_2^{\cdot-}$) and hydroxyl radicals (OH^{\cdot}). When the balance between the production and clearance of these species is disrupted and ROS are overproduced the cells are said to be in oxidative stress. ROS can mediate effects such as cell proliferation and activation as well as consequences such as growth inhibition or cell death. Oxidative stress has been implicated in many human diseases such as atherosclerosis, cancer, neurodegenerative diseases and ageing (1, 2, 3). Many biomolecules including lipids, DNA and amino acid residues in proteins are susceptible to oxidation by various forms of ROS. Proteins containing more cysteine, tyrosine, tryptophan and methionine are especially vulnerable to oxidation.

1.2 Cysteine:

Cysteine (Cys) is a sulphur containing amino acid with the chemical formula of $\text{HO}_2\text{CCHNH}_2\text{CH}_2\text{SH}$. It has been found that the cysteine content of species is varied and that it increases with the complexity of the organism. This may be attributed to its relative reactivity compared to other amino acids especially with regards to oxidation (4, 5). The importance of cysteine lies in its sulphur containing functional group thiol or sulphhydryl group (-SH), which is unique to cysteine amongst other amino acids (6). Although the main components of all living organisms are carbon, nitrogen, oxygen and phosphorus, sulphur also plays an important role in biological systems. It occurs in all major classes of bio molecules including proteins, nucleic acids, sugars and metabolites (7). Sulphur is a group VIa second row element of the periodic table with an electronic configuration of $[\text{Ne}]3s^23p^4$. It shares many similarities in chemical reactivity with oxygen as they are of the same periodic group. However it can expand its valence shell to hold more than eight electrons owing to the availability of empty d-orbitals. This gives sulphur many distinct properties that are exploited in proteins and other molecules. The combination of low electronegativity and lone pair availability makes thiols better nucleophiles compared to alcohols. Therefore disulphide bonds (RS-SR) are more stable than peroxide bonds (RO-OR), which make disulphide bonds a key structural feature of proteins. Sulphur has many different oxidation states ranging from +6 to -2 in an oxidative environment (8). In cysteine, the sulphur atom is fully reduced with an oxidation state of -2. Therefore the thiol side chain is readily oxidised to give a variety of different post-translational modifications, some of which are shown in **Figure 1.1** below (9).

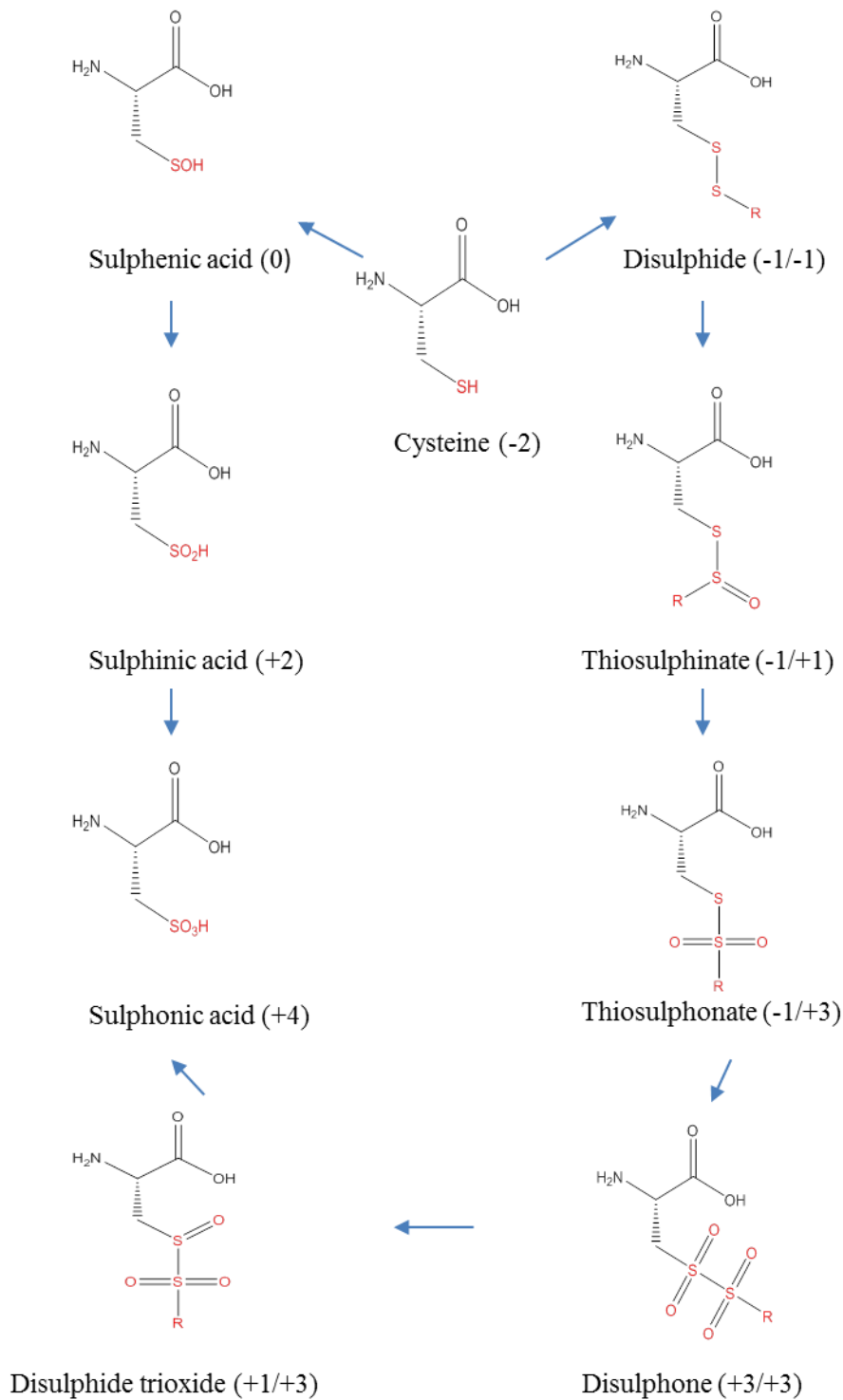


Figure 1.1: Different oxidation states of cysteine in a biological system. Sulphur has many different oxidation states ranging from +6 to -2. In cysteine sulphur is fully reduced and has an oxidation state of -2. When the cysteine thiol is oxidised it forms reversible modifications such as sulphenic acids and disulphide bonds or gets over oxidised to form irreversible modifications such as cysteine sulphonics acids.

The sulphur atom in a thiol group is electron rich and nucleophilic. Its reactivity is further increased in the deprotonated thiolate anion (RS^-) form. In this respect the thiol group is mildly acidic with a pKa value ranging from ~4-9 depending on the structure of the protein and the local environment (8, 10). The thiolate anion reacts with 'hard' electrophilic centres such as carbonyl or phosphoryl groups as well as with 'soft' electrophiles like saturated carbon. Due to its high reactivity the thiol group of cysteine plays a major role in many biological activities like catalysis, metal binding and in acting as a 'molecular switch' activating or deactivating cellular functions (8). One of the most commonly known oxidation reactions is the formation of the disulphide bond. The formation of disulphide bonds can progress via two general pathways. They can either be formed by condensation of a thiol with a sulphenic acid ($RSOH$) or by a thiol-disulphide exchange. Disulphide bonds are stable intermediates and are often involved in the conservation of the protein structure and function. However, disulphides can undergo nucleophilic cleavage, which is an important biological reaction (8, 10, 11). As the oxidation number of the sulphur atom in cysteine increases it becomes more positively charged, hence becoming less nucleophilic in nature. Therefore the higher oxidation states of cysteine are less stable energetically. The first product of cysteine oxidation is the formation of sulphenic acid (12).

1.2.1 Cysteine sulphenic acids:

The cysteine sulphenic acids (RSOH) (**Figure 1.1**) are unstable and have highly reactive functional groups, which have been viewed as intermediates to other higher oxidation state groups such as the sulphinic (RSO₂H) and sulphonic (RSO₃H) acid groups (2, 8, 11). Since they are generally too unstable to isolate it has been a challenge until recently to detect which was the correct tautomeric structure of sulphenic acid. According to spectroscopic evidence the prominent tautomer is the divalent sulphur tautomer **1** over the sulphoxide structure **2** both of which are shown in **Figure 1.2**. Studies using infrared spectroscopy on 1-anthraquinonesulphenic acid and 1,4-anthraquinonedisulphenic acid in solution have shown that the S-O bond is longer than that of the sulphoxide thus favouring the formation of tautomer **1** (13).

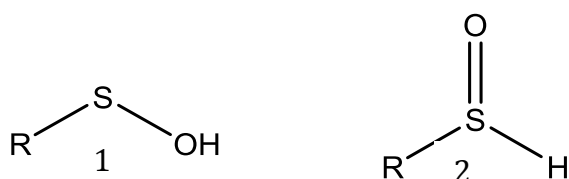


Figure 1.2: Tautomers of sulphenic acid. Sulphenic acids favour the formation of tautomer **1**, which has been confirmed by infrared spectrometry.

The oxidation state of sulphur in sulphenic acid is 0 and therefore it displays both electrophilic and nucleophilic reactivity. Even though the nucleophilic nature is weak in sulphenic acids, when there is a possibility for intermolecular hydrogen bond formation it can play an important role. The electrophilic nature of the sulphur atom in sulphenic acids can be demonstrated by several reactions. One of the most important discoveries was the reaction of 5,5-dimethyl-1,3-cyclohexanedione also known as dimedone which was discovered by Allison and co-workers in 1974. It reacts specifically with sulphenic acids in a condensation reaction where the sulphenic acid acts as an electrophile to yield the thioether derivative as shown below (**Figure 1.3, 1**) (14). Although the exact mechanism for this reaction is not

known it could proceed via a 1,4-addition or a direct substitution reaction (8). Sulphenic acids could also react with amines to form sulphenamides (**Figure 1.3, 2**). When the nitrogen atoms of the amides are in close proximity with the sulphur atom, the nitrogen can act as a nucleophile to form cyclic sulphenamides (**Figure 1.3, 3**) (15, 16). This five-member ring represents another form of a cysteine oxidation state that is resistant to further oxidation. The initial evidence for this species was crystallographic (17), therefore leaving some doubts to its relevance in a biological system. However, studies using model chemistry have better defined this cyclization reaction in the constrained setting of a protein active site (18). Recent studies of the peroxide sensitive transcriptional regulator, organic hydroperoxide resistance regulator (OhrR) from *Bacillus subtilis* support stable formation of the sulphenamide species in solution (19).

Sulphenic acids also react with other nucleophilic thiols to form disulphide bonds (4). The sulphenic acids, due to their instability can undergo rapid changes like condensation with another thiol group or with a small molecule thiol like glutathione (GSH) to form disulphide bonds. If two cysteinyl residues are close to each other within a molecule they will form intramolecular disulphide bonds. An intermolecular disulphide bond will form during the oxidation of different protein sulphhydryl groups if they are located in an environment on the surface of the protein, which will allow them to approach each other (20). Sulphenic acid formation and disulphide bond formation are reversible reactions which are important in maintaining a reduced cellular environment and are also a major component of the ROS-linked modulation of cell signalling pathways (2). Disulphide bond formation can stabilize extracellular proteins, protect against irreversible inactivation, modify structures to create, destroy or modulate functional sites, and ultimately regulate enzymatic or transcriptional activity of the proteins (1, 3, 8).

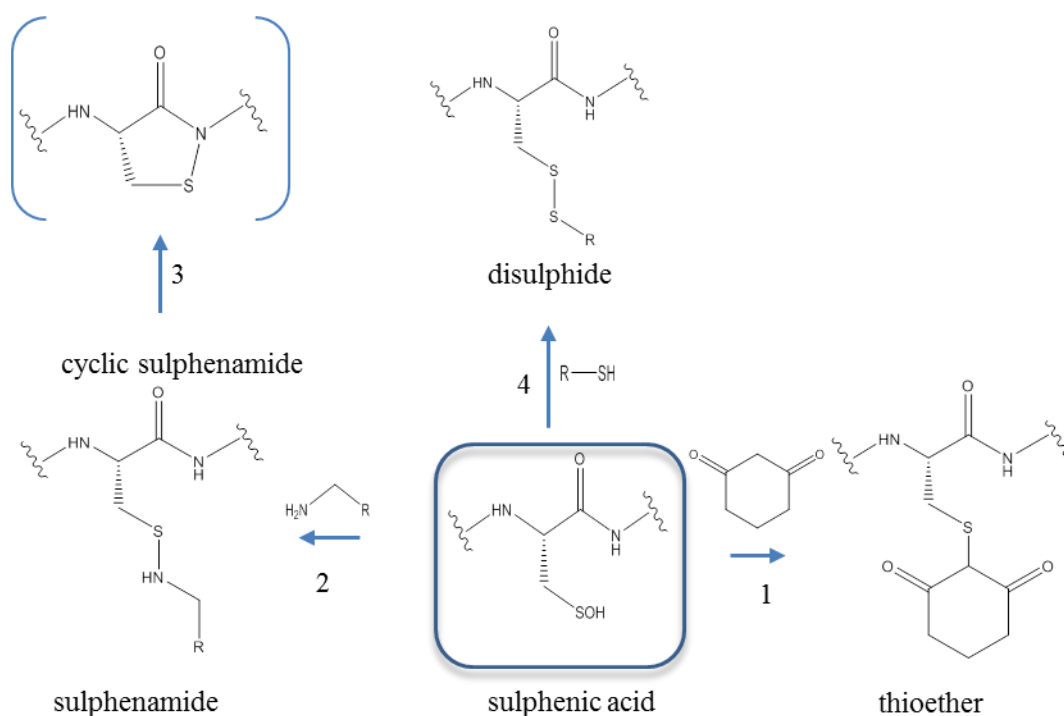


Figure 1.3: Electrophilic reactions of sulphenic acids. Sulphenic acids act as electrophiles and react with 1,3-cyclohexanedione to form a thioether product **1**. They can also react with the amines to form sulphenamides **2** and can form cyclic sulphenamides **3** with neighbouring nitrogen atoms. Disulphide bond formation **4** is an important biological function where sulphenic acids act as electrophiles.

In a number of reactions sulphenic acids act nucleophiles. In the case of sulphinic acid formation sulphenic acid acts as a nucleophile in its reaction with hydrogen peroxide (**Figure 1.4, 1**) (21). One important reaction that has also been used in the identification of sulphenic acids in biological systems is the nucleophilic substitution reaction on 4-chloro-7-nitrobenzo-2-oxa-1,3-diazole (NBD-Cl) (**Figure 1.4, 2**). Based on its unique spectral properties the identification of both thiols and sulphenic acids can be discriminated; this will be discussed in detail later in the chapter (7).

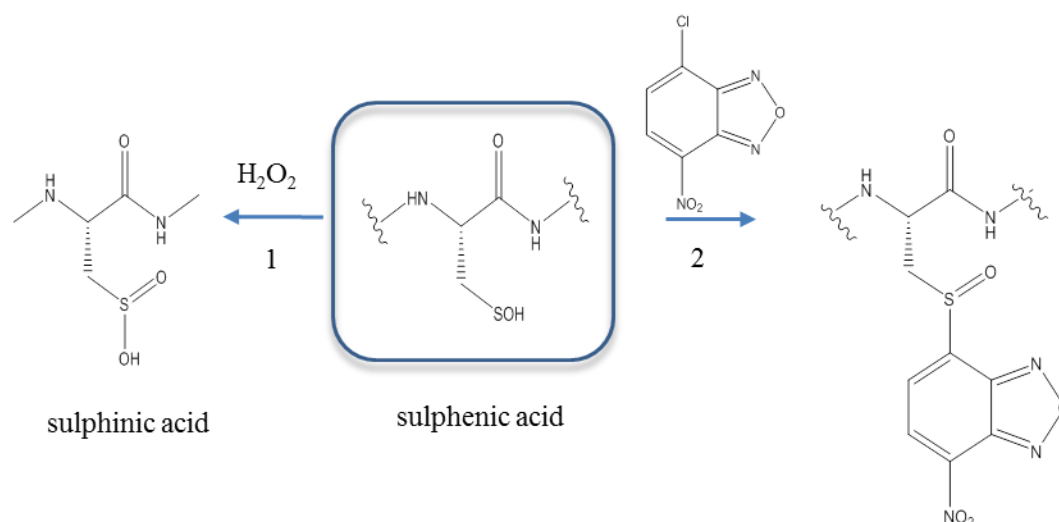


Figure 1.4: Nucleophilic reactions of sulphenic acids. Sulphenic acids can act as nucleophiles and react with hydrogen peroxide and form sulphinic acids **1** or react with halogenated compounds such as with NBD-Cl **2**.

Sulphenic acids are formed by the reaction of a thiol or a thiolate anion with many oxidants due to sulphur's nucleophilic character. One-electron oxidants such as O_2^- can react with the thiolate anion to produce thiyl radicals (R-S^\cdot), which then can form disulphide bonds with another thiolate accompanied by superoxide formation (21). Two electron oxidants such as hydrogen peroxide, peroxyxynitrite and hypochlorous acids also generate sulphenic acids (22, 23). Sulphenic acids may accumulate or undergo further oxidation to form more stable products such as sulphinic or sulphonic acids depending on the microenvironment and the level of oxidants present (2).

1.2.2 Cysteine sulphinic and sulphonic acids:

In addition to being key intermediates in the formation of disulphides sulphenic acids are also intermediates in the oxidation of thiols to sulphinic and sulphonic acids (**Figure 1.1**). Unlike sulphenic acids, sulphinic or sulphonic acid species do not undergo self-condensation reactions or react with thiol groups. They are stable oxidation products, which can be isolated and crystallised. The oxidation of sulphenic acids to sulphinic acids can occur enzymatically as well as in the presence of oxidants. For example, when the enzyme cysteamine oxygenase reacts on the thiol cysteamine it forms the sulphinic acid hypotaurine (24). Sulphinic acids have gained importance in the redox regulation of peroxiredoxin (25, 26, 27). It has two cysteines (peroxidatic and resolving) which are redox active, in its catalytic site which decompose hydrogen peroxide. When hydrogen peroxide is present, the peroxidatic cysteine at the active site is oxidised to sulphenic acid and then forms a disulphide bond with the resolving cysteine. However, when concentrations of hydrogen peroxide increase the sulphenic acid will oxidise further to form a sulphinic acid that inactivates the enzyme (25, 26, 27). Until recently it was thought that sulphinic acid formation was an irreversible protein modification. Although cysteine sulphinic acids cannot be reduced back to a thiol by molecules such as glutathione or thioredoxin (28) a highly selective enzyme called sulfiredoxin, which has been isolated from yeast can reduce the sulphinic acids back to the thiols (29, 30).

1.3 Cysteine sulphenic acids in proteins:

Recent research suggests that protein sulphenic acids can spontaneously form in unfolded proteins even in the absence of exogenously added oxidants with just the presence of oxygen and trace metals. These sulphenic acids act as intermediates in the formation of disulphide bonds in protein folding (31). The antioxidant properties of many proteins can be attributed to cysteine oxidation to sulphenic acids. Peroxiredoxins (Prxs) are the most abundant antioxidant enzymes in the cytosol and belong to the family of peroxidases. Prxs are very specific in recognising hydrogen peroxide, peroxyxynitrite and organic hydroperoxides. They are classified into six subfamilies consisting of Ahpc/Prx1, BCP/PrxQ, Prx5, Prx6, Tpx and AhpE (32). Over the years extensive research has been done to recognise their role as antioxidant and signalling molecules and their mechanism of action (33, 34). It has been predicted through kinetic experiments that under physiological conditions eukaryotic Prxs are responsible for the removal of about 90% of mitochondrial hydrogen peroxide (35) and reduction of almost all of the cytoplasmic H₂O₂ (36). Another important antioxidant enzyme is the glutathione peroxidase (GPx) (37) which play a role in the detoxification of hydrogen peroxide in the cells (38). The vast majority of non-vertebrate GPxs are cysteine homologues (2-CysGPxs) whereas mammalian GPxs are selenoproteins (SecGPxs) (39). Both of these families have similarities in that they share a common enzyme substitution system. The catalysis occurs between the enzymes and their substrates in a sequence of reactions rather than with the involvement of a central enzyme complex where all the substrates are bound at the same time. Normally a 2-cysPrx/2-cysGPx consists of 2 cysteine molecules. One cysteine is present in the active site known as the peroxidatic cysteine while the other is known as the resolving cysteine. When hydrogen peroxide is present in cells, initially the peroxidatic cysteine is oxidised to a cysteine sulphenic acid. But as it is highly reactive with other thiols it will rapidly form a disulphide bond with the resolving cysteine. These disulphides can be reduced back to cysteines residues by molecules such as thioredoxin (Trx), which is important to maintain the cellular antioxidant system (40). In addition to being intermediates in the

catalytic cycle of many antioxidant enzymes they also play a role in cell signalling and sensing oxidative stress (41). It has been proposed that sulphenic acid formation is involved in the inactivation of protein tyrosine phosphatases (PTP) by hydrogen peroxide. Tanner *et al* have demonstrated that purified PTPs such as vaccinia H1-related (VHR) and PTP1 are inhibited by hydrogen peroxide and that this inhibition is reversible with reducing agents such as dithiothreitol (DTT) or glutathione. Utilizing the electrophilic reagent 7-chloro-4-nitrobenzo-2-oxa-1,3-diazole (NBD-Cl), it was shown that a cysteine sulphenic acid intermediate (Cys-SOH) is formed after attack of the catalytic thiolate on H₂O₂ (42). Once formed, sulphenic acid modifications can act as a molecular switch to activate/deactivate proteins. For example, Zheng *et al* have shown that a redox sensitive disulphide is present in the active site of the transcription factor OxyR in *E.coli*, with both Cys199 and Cys208 being essential for transcriptional activation of OxyR (43). Disulphide bond formation between these two cysteines leads to a conformational change in the OxyR-DNA complex that in turn activates transcription. Hydrogen peroxide-oxidized Cys199 forms a Cys199SOH, which is condensed rapidly with the thiol of Cys208 to form the disulphide. It appears that this protein has the ability to detect hydrogen peroxides and other peroxidases (43).

1.4 Tools to detect cysteine sulphenic acid formation in proteins:

Interest in the identification of the cysteine sulphenic acids in proteins has grown over the last few decades as their importance in biological activities is becoming better known. Despite their importance in cellular processes such as redox regulation and enzyme catalysis only a limited set of tools are present to identify these species and most are only applicable to *in vitro* studies of isolated proteins. The fact that SOH is unstable and undergoes oxidation to higher oxidation states, absence of any UV-visible spectral properties and its small size makes it a challenge for detection. The majority of the data presented thus far rely on the reactivity of sulphenic acids with chemically selective probes. Both direct and indirect methods have been used for the detection of sulphenic acids in proteins (44).

Indirect methods rely on the changes in the redox state of cysteine by the loss of reactivity with thiol modifying reagents. The free thiol groups are blocked by alkylating agents such as N-ethylmaleimide (NEM) and iodoacetamide (IAM), two thiol specific alkylating agents that react readily with cysteine thiolate anions (45). The biotin-switch method, which was first developed to detect protein S-nitrosation (SNO) (46) consists of blocking the free cysteine thiol with methyl methanethiosulphonate, reduction of RSNO with ascorbate and labelling of thiols with biotin-HPDP which is a pyridyldithiol-biotin compound for labelling protein cysteines and other molecules that contain sulphhydryl groups. An adaptation of this method was used by Eaton and coworkers to detect protein sulphenic acids indirectly. Their method involved blocking the thiols with NEM, reduction of SOH with RSOH reducing agent sodium arsenite (47) and labelling of reduced thiols with biotin maleimide. This enables isolation of labelled proteins to be identified with SDS-PAGE and western blotting as well mass spectrometry analysis. The limitations of this method are that the selectivity of sodium arsenite has not been extensively studied and the fact that proteins undergo extensive treatments under denaturing conditions which could lead to false identifications of modifications (48). Another method used to identify protein sulphenic acids indirectly uses blocking thiols with alkylating agent iodoacetamide and the oxidising of remaining sulphenic

acids to sulphonic acids. These sulphonic acids are then identified using pervanadate. Sulphenic acids present on protein tyrosine phosphatases have been identified using this technique. Some of the drawbacks of using this method are that if all the thiols have not been blocked, this could lead to false positive signals (49, 50). The electrophilic probe NBD-Cl has also been used to detect sulphenic acid formation. The disadvantage to using this probe is that it is not selective as it can also react with thiols and in some instances with amines and phenols. NBD-Cl forms a sulfoxide with sulphenic acids, which has an absorbance maximum at 347 nm. The thiol reacts with NBD-Cl to form a thioether, which has an absorbance max at 420 nm. This shift in absorbance has been used to confirm the presence of sulphenic acids (51). However, there have been many cases where it has not been possible to detect this protein modification via the absorption maxima and the only way to positively identify sulphenic acids was via mass spectral analysis (52). Poole *et al* have used this technique to observe that sulphenic acid are formed as an intermediate in the C165S mutant of the AhpC peroxidase protein from *Salmonella typhimurium* as well as the flavoprotein NADH peroxidase of *Enterococcus faecalis* (52). A genetically-encoded probe has been used by Wood and researchers to trap sulphenic acid modified proteins in *E.coli*. The probe was a modification of the transcription factor yes associated protein 1 (Yap1) consisting of 85 amino acids of the cysteine rich C-terminal domain along with a His-tag for affinity purification. Of the three native cysteines, two were mutated leaving Cys598 to form disulphides with sulphenic acid modifications. With this method glutathione peroxidase3 (GPx3) has been identified as a redox sensing protein with an active cysteine Cys36, which forms a sulphenic acid intermediate (53).

Direct methods use small molecular probes that selectively react with one class of oxidative cysteine modification. The key challenge to this approach is to design a probe that is selective to the detection of the desired functional group. Investigating the role of sulphenic acids in proteins requires reagents for their detection (44). In 1974, Benitez and Allison presented the first evidence that adduct formation with 5,5-dimethyl-1,3-cyclohexadione (dimedone) could be used as a diagnostic tool to detect sulphenic acids in proteins such as glyceraldehyde-3-

phosphate dehydrogenase (GAPDH) (14). Although the exact mechanism for this reaction is not known it is believed to proceed via a direct substitution (**Figure 1.5**). Although chemical modifications of cysteine sulphenic acids by dimedone provide a useful way to tag these species, the lack of any spectral or affinity label associated with dimedone requires that detection be undertaken by mass spectrometry (3).

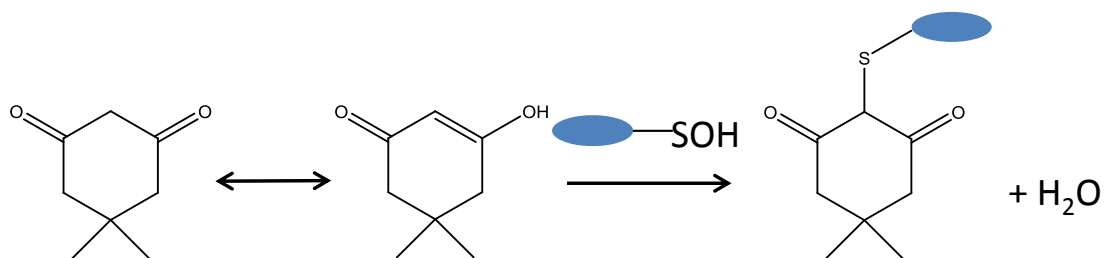


Figure 1.5: S-alkylation of a sulphenic acid by dimedone. Dimedone reacts with sulphenic acid via a direct substitution reaction.

In 2005, Poole *et al* provided a new tool for the isolation and identification of protein sulphenic acid by synthesis of a functionalised derivative of 1,3-cyclohexadione which is a dimedone like compound and linking this to two different fluorophores, isatoic acid and 7-methoxycoumarin to yield fluorescent probes. The synthesis of the two fluorescent probes 3-(2,4-dioxocyclohexyl)propyl-2-(methylamino)benzoate (DCP-MAB) and 3-(2,4-dioxocyclohexyl)propyl-7-methoxy-2-oxo-2H-chromen-3-ylcarbamate (DCP-MCC) are shown in **Figure 1.6** below (54).

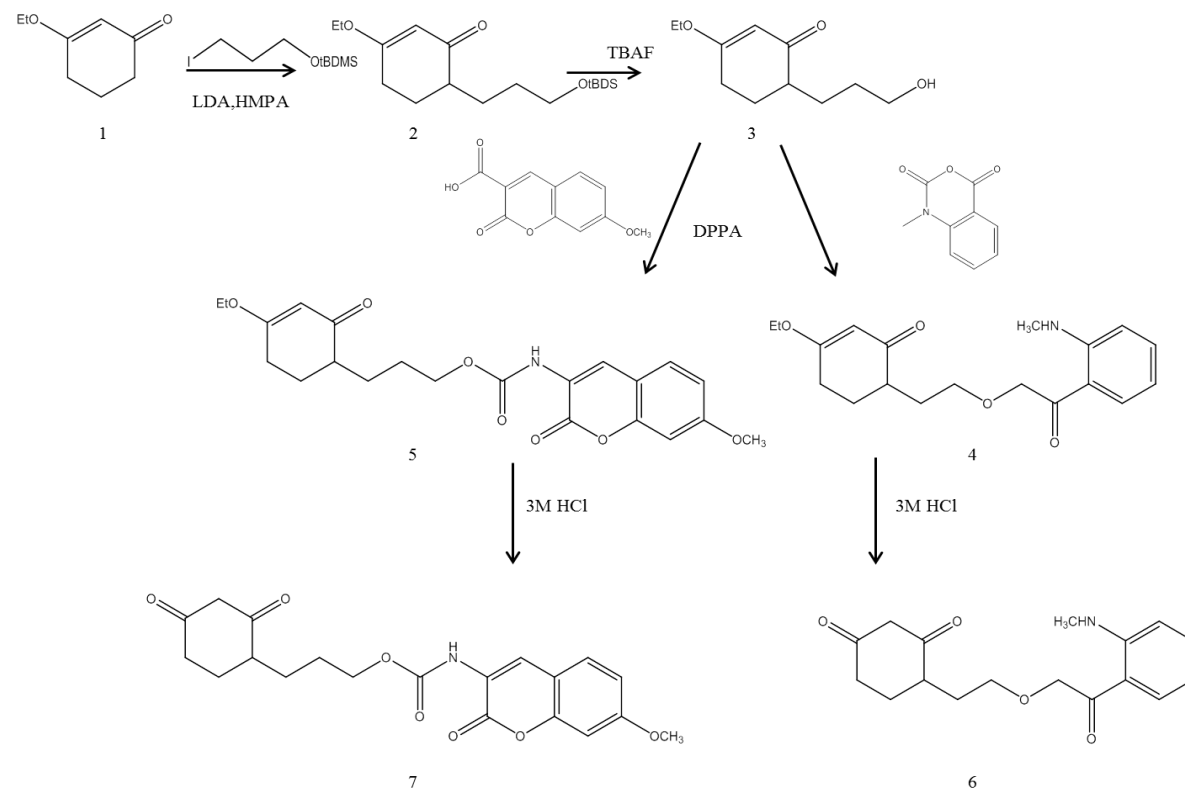
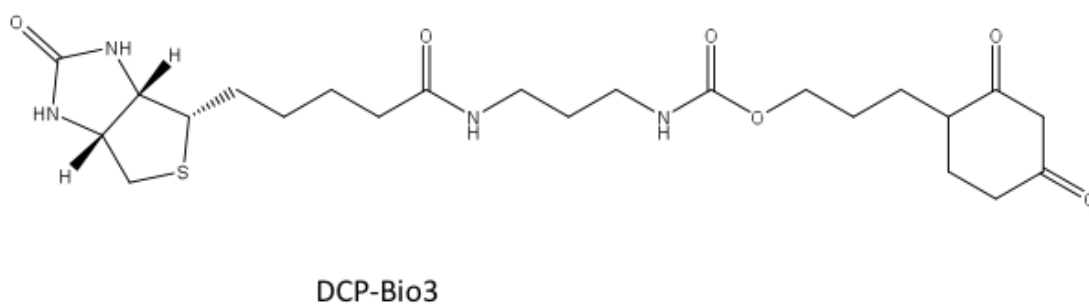
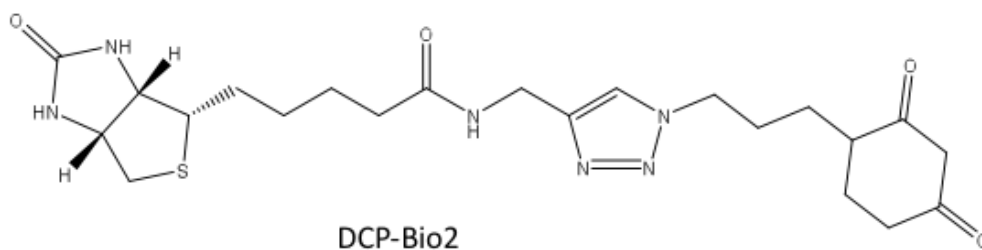
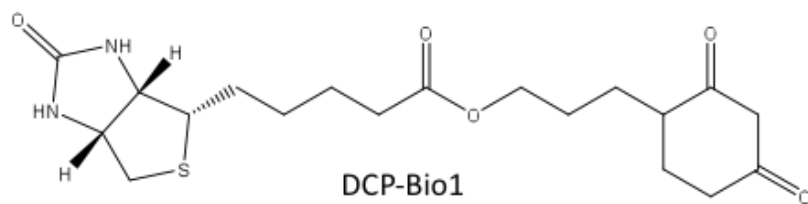
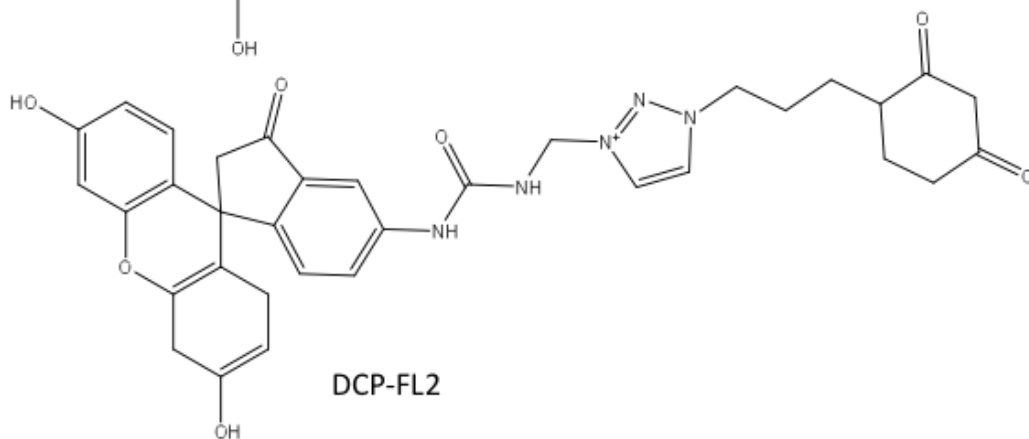
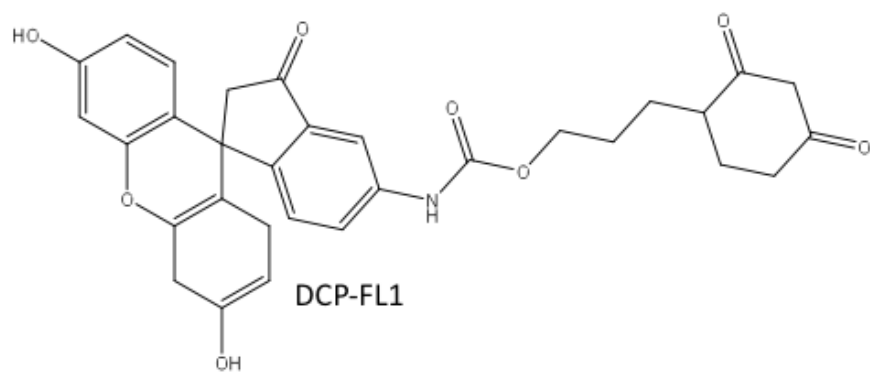


Figure1.6: Schematic for the synthesis of DCP-MCC (7) and DCP-MAB (6). The protected version of 1,3-cyclohexadione, 3-ethoxy-2-cyclohexen-1-one (1) is alkylated with tert-butyldimethylsilyl ether (TBDMS) protected 3-iodo-1-propanol yielded 3-ethoxy-6-(3-tert-butyldimethylsilyloxypropyl)-cyclohex-2-enone (2). Treatment of 2 with tetra-n-butylammonium fluoride (TBAF) removed the silyl group to give the alcohol, 3-ethoxy-6-(3-hydroxypropyl) cyclohex-2-enone (3). Condensation of 3 with N-methylisatoic anhydride produced 3-(4-ethoxy-2-oxocyclohex-3-enyl) propyl-2-(methylamino)benzoate (4). Heating 7-methoxycoumarin-3-carboxylic acid in the presence of diphenyl phosphorazidate (DPPA) yielded 3-(4-ethoxy-2-oxocyclohex-3-enyl) propyl-7-methoxy-2-oxo-2H-chromen-3-ylcarbamate (5). Treatment of products 4 and 5 with 3 M hydrochloric acid (HCl) yielded 6 (DCP-MAB) and 7 (DCP-MCC) respectively.

The protected version of 1,3-cyclohexadione, 3-ethoxy-2-cyclohexen-1-one (**Figure 1.6, 1**) was used by Poole *et al* as the starting material for both fluorescent probes. Alkylation of 1 with tert-butyldimethylsilyl ether (TBDMS) protected 3-iodo-1-propanol yielded 3-ethoxy-6-(3-tert-butyldimethylsilyloxypropyl)-cyclohex-2-enone (**Figure 1.6, 2**). Treatment of 2 with tetra-n-butylammonium fluoride (TBAF) removed the silyl group to give the alcohol, 3-ethoxy-6-(3-hydroxypropyl)cyclohex-2-enone (**Figure 1.6, 3**). This alcohol group provides the attachment site for the fluorophores. Condensation of 3 with N-methylisatoic anhydride produced 3-(4-ethoxy-2-oxocyclohex-3-enyl) propyl-2-(methylamino) benzoate (**Figure 1.6, 4**). Heating 7-methoxycoumarin-3-carboxylic acid in the presence of diphenyl phosphorazidate (DPPA) yielded 3-(4-ethoxy-2-oxocyclohex-3-enyl)propyl-7-methoxy-2-oxo-2H-chromen-3-ylcarbamate (**Figure 1.6, 5**). Treatment of products 4 and 5 with 3 M hydrochloric acid (HCl) yielded 6 (DCP-MAB) and 7 (DCP-MCC) respectively (54).

Once the probes were synthesised, Poole *et al* examined the reactivity toward protein sulphenic acid. The C165S mutant of AhpC, a cysteine based peroxidase from *Salmonella typhimurium* was purified and rapidly titrated with hydrogen peroxide of known concentration to convert the cysteine thiol group to its sulphenic acid form. The advantage of using the C165S mutant is that it only has one cysteine (Cys46), keeping the essentiality of a single active site cysteine for the reduction by peroxides as opposed to the wild type, which has a second cysteine (Cys165). Removal of the second cysteine allows sulphenic acid formation whereas if two thiol groups were present the Cys165 could react with the recently formed sulphenic acid of Cys46 to form the more stable disulphide bond of the oxidised enzyme (2, 54, 55). Both compounds formed adducts with the sulphenic but not the sulphinic or sulphonic acid forms of the peroxidase. This was confirmed by results from electrospray ionisation mass spectroscopy (ESI-MS). The sulphenic acid form of the protein either reacted with the reagents or were further oxidised and were therefore not observed. Although this was an advance towards sulphenic acid detection the absence of any affinity tags such as biotin meant that these probes could not be used in western blotting techniques as the probes could not be visualised.

The synthesis of seven new reagents through the attachment of fluorescein, rhodamine and biotin moieties to an alcohol functional group on a linker attached to 1,3-cyclohexadione was reported by Poole *et al* in 2007 (56). One major advantage over the previous two probes is that these probes are useful for detecting labelled proteins in polyacrylamide gels. The fluorescent probes can directly be observed both in solution and after gel electrophoresis. The reagents were also compatible with mass spectroscopic approaches to confirm covalent attachment and identify the specific site of modification. Furthermore the biotin-linked probes could be detected through western blotting type approaches as well as enabling affinity techniques for the isolation of modified proteins (56). **Figure 1.7** below shows the seven reagents based on 1,3-cyclohexadione.



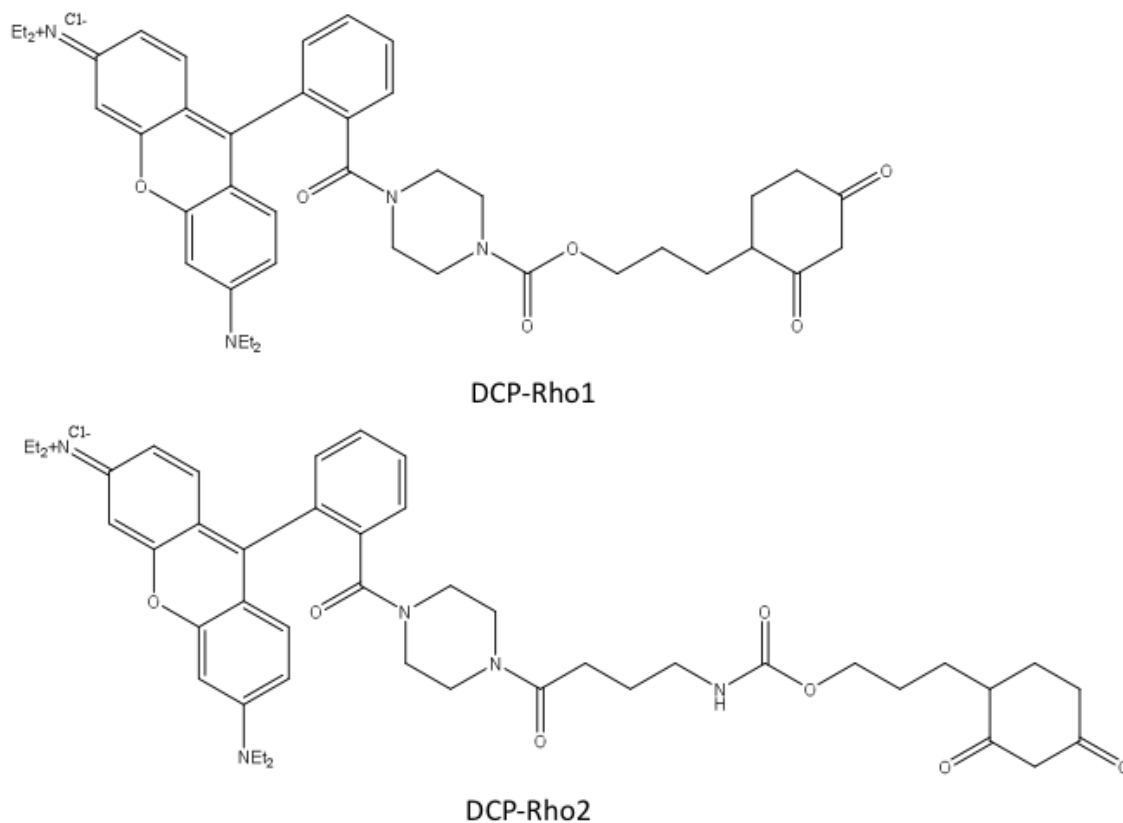


Figure 1.7: Fluorescent and affinity based probes to detect cysteine sulphenic acid. Four fluorescent probes DCP-FL1, DCP-FL2, DCP-Rho-1, DCP-Rho2 and three biotin tagged probes DCP-Bio1, DCP-Bio2 and DCP-Bio3 were synthesised and utilised to detect sulphenic acids in various proteins.

The experiments carried out to synthesise each of the probes by Poole and her colleagues are described below. The treatment of fluoresceinamine isomer with p-nitrophenyl chloroformate yielded fluoresceinamine-5'-N-(p-nitrophenyl)carbamate. This product was filtered and analysed by thin layer chromatography (TLC) and nuclear magnetic resonance (NMR) spectroscopy. Reacting this with the protected alcohol derivative of 1,3-cyclohexadione produced the protected fluorescein carbamate conjugate. Deprotection of the enol ether was achieved using 4 M HCl in 1,4-dioxane to give fluoresceinamine-5'-N-[2,4-dioxocyclohexyl]propyl] carbamate (DCP-FL1) (56).

The synthesis of fluoresceinamine-5'-N-[3-((1-3-(2,4-dioxocyclohexyl)propyl)-1H-1,2,3-triazol-4-yl)methyl]urea (DCP-FL2) involved the introduction of a urea linker propargylamine, which was added to fluoresceinamine-5'-N-(p-nitrophenyl)carbamate. The product, fluoresceinamine-5'-N-(3-propargyl)urea triethylamine salt, was precipitated and filtered off with the addition of triethylamine. In parallel, 3-ethoxy-6-(3-azidopropyl)cyclohex-2-enone was synthesised from 3-ethoxy-6-(3-hydroxypropyl)cyclohex-2-enone by adding diisopropyl azodicarboxylate (DIAD), triphenyl phosphate and diphenylphosphorazide (DPPA) in tetrahydrofuran (THF) at 0°C. Utilizing 'click' chemistry permitted the coupling of the azide compound of the alcohol with the propargyl urea to form fluoresceinamine-5'-N-[3-((1-3-(4-ethoxy-2-oxocyclohex-3-enyl)propyl)-1H-1,2,3-triazol-4-yl)methyl]urea. Acid deprotection with 3 M HCl yielded the final product DCP-FL2 (56).

The first biotinylated probe 3-(2,4-dioxocyclohexyl)propyl-5-((3aR,6S,6aS)-hexahydro-2-oxo-1H-thieno[3,4-d]imidazole-6-yl)pentanoate (DCP-Bio1), was generated with the coupling of biotin to the alcohol 3-ethoxy-6-(3-hydroxypropyl)-cyclohex-2-enone. The coupling was done using dicyclohexylcarbodiimide (DCC) as the coupling agent. Acid deprotonation of 3-(4-ethoxy-2-oxocyclohex-3-enyl)propyl-5-((3aR, 6S, 6aS)-hexahydro-2-oxo-1H-thieno[3, 4-d]imidazole-6-yl)pentanoate with HCl produced DCP-Bio1 in good yield (70%)

5-((3aR,6S,6aS)-hexahydro-2-oxo-1H-thieno[3,4-d]imidazole-6-yl)-N-((1-(3-(2,4-dioxocyclohexyl)propyl)-1H-1,2,3-triazol-4-yl)methyl)pentanamide (DCP-Bio2), was synthesised with biotin and incorporating propargylamine similar to the synthesis of DCP-FL2. 3-ethoxy-6-(3-azidopropyl)cyclohex-2-enone (synthesis procedure described previously for the synthesis of DCP-FL2) and 5-((3aR,6S,6aS)-hexahydro-2-oxo-1H-thieno[3,4-d]imidazol-6-yl)-N-(prop-2-ynyl)pentanamide were reacted together using click chemistry utilised in the synthesis of the fluorescein triazole conjugate. The final step involved acid deprotection yielding DCP-Bio2 (56).

The final biotin linked probe 3-(2,4-dioxocyclohexyl)propyl-4-(5-((3aR,6S,6aS)-hexahydro-2-oxo-1-H-thieno[3,4-d]imidazole-6-yl)pentanamide)butylcarbamate (DCP-Bio3) was synthesised incorporating a longer 'linker', 1,4-diaminobutane. The first step of the synthesis was the mono N-Boc protection of 1,4-diaminobutane. This is followed by the DCC coupling of biotin and BOC deprotection to give the amine hydrochloric acid salt, N-(4-aminobutyl)-5-((3aR,6S,6aS)-hexahydro-2-oxo-1H-thieno[3,4-d]imidazole-6-yl)pentanamide hydrochloric salt. 3-ethoxy-6-(3-hydroxylpropyl)cyclohex-2-enone and p-nitrophenyl chloroformate were reacted together to form 3-(4-ethoxy-2-oxocyclohex-3-enyl)propyl-4-nitrophenylcarbonate. This was coupled with the free amine of the hydrochloric acid salt to give the protected version of the biotin derivative 3-(4-ethoxy-2-oxocyclohex-3-enyl)propyl-4-(5-((3aR,6S,6aS)-hexahydro-2-oxo-1H-thieno[3,4-d]imidazole-6-yl)pentanamido)butylcarbamate. Deprotection of the compound resulted in the probe DCP-Bio3.

The synthesis of the rhodamine derivatives were explored because rhodamine B is known to be cell permeable (57) which would be advantageous for the detecting of intracellular sulphenic acids without cell lysis. The first step towards the synthesis of rhodamine B[4-[3-(2,4-dioxocyclohexyl)propyl]carbamate]piperazine amide (DCP-Rho1) was the synthesis of rhodamine B piperazide amide. This was done with the addition of piperazine and rhodamine B in trimethylaluminum under reflux. Coupling the compound with 3-(4-ethoxy-2-

oxocyclohex-3-enyl)propyl-4-nitrophenylcarbonate, which is described in the synthesis of DCP-Bio3 and deprotection proceeded to give the first rhodamine derivative DCP-Rho1.

The synthesis of the second rhodamine derivative, rhodamine B-3-(2,4-dioxocyclohexyl)propyl-4-oxo-4-(piperazin-1-yl)butylcarbamate (DCP-Rho2), was undertaken as described below. Rhodamine B piperazine amide was coupled using DCC to γ -(Boc-amino)butyric acid, 4-(tert-Butoxycarbonylamino)butyric acid (N-Boc GABA) to yield the extended protective derivative rhodamine B tert-butyl-4-oxo-4-(piperazin-1-yl)butylcarbamate. Deprotection of the N-Boc group with 4 M HCl and further coupling to the carbonate derivative 3-(4-ethoxy-2-oxocyclohex-3-enyl) propyl-4-nitrophenylcarbonate followed by enol ether deprotection yielded DCP-Rho2.

To test the reactivity of the probes Poole *et al* used the C165S mutant of AhpC as the choice protein because of its rapid formation of the sulphenic acid intermediate at the active site (Cys 46) upon oxidation by peroxides (55, 56, 57). The stabilized sulphenic acid forms of the proteins were then incubated with DMSO and the seven probes to yield the covalent protein adduct. These samples were analysed using electrospray ionisation mass spectroscopy. In each case the expected results and the observed results from the MS were very similar indicating the formation of adducts. The biotinylated probe DCP-Bio1 was used to detect sulphenic acid formations of protein tyrosine phosphatases (PTPs) SHP-1 and SHP-2 in cell lysates from CD8+ T cells (58). It has also been used to identify sulphenic acid modifications of the serine/threonine protein kinase Akt2 (59).

In 2008 Carroll *et al* (60) described a method that enabled live cell labelling of sulphenic acid modified proteins. A bifunctional probe N-(3-azidopropyl)-3,5-dioxocyclohexanecarboxamide referred to as DAz-1 (**Figure 1.8, 5**) was synthesised. It includes the nucleophile 1,3-cyclohexanedione (**Figure 1.8, 2**), a dimedone analogue that reacts selectively with sulphenic acids to form adducts. In addition DAz-1 also contains an azide “chemical handle” that can be selectively detected with phosphine reagents via the Staudinger ligation (62) for identification, enrichment and visualisation. The advantages of this probe over existing probes was that due to its small size, it could be favourably up taken

by cells and facilitate protein labelling. Furthermore because of the azide group, once introduced into proteins it could be tagged by a variety of affinity and fluorescent reagents (60). The synthesis of DAz-1 is outlined below in **Figure 1.8**.

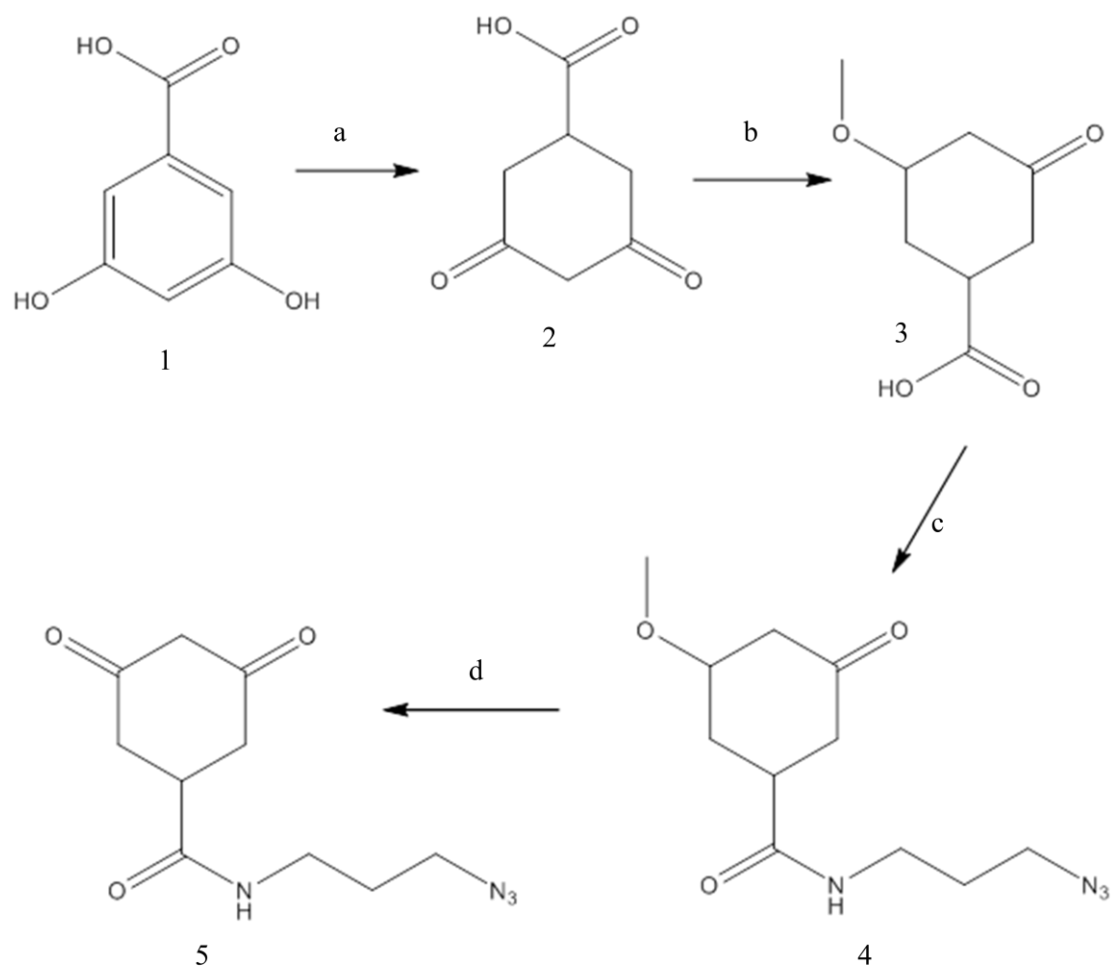


Figure 1.8: Synthesis of DAz-1. 3,5-dihydroxybenzoic acid **1** was hydrogenated to give the diketone **2** and protected as a methyl ether using PTSA and methanol for 10 minutes at room temperature. 3-azidopropylamine was coupled to compound **3** using TBTU/DIEA in DMF to provide the amide **4**. The synthesis was completed with the deprotection of the methoxy group with 2 M HCl.

Ni-catalysed hydrogenation (a) of 3,5-dihydroxybenzoic acid **1**, which is commercially available, gave the diketone **2** in 85% yield (61). To prevent undesired reactions at the ketone, it was protected as methyl ether **3** using p-toluene sulphonic acid (PTSA) and methanol for 10 minutes at room temperature (b). The coupling of the amine, 3-azidopropylamine was carried out with *O*-(Benzotriazol-1-yl)-*N,N,N',N'*-tetramethyluronium tetrafluoroborate (TBTU) and

N,N-diisopropylethylamine (DIEA) in dimethylformamide (DMF) (c) to provide the amide **4**. The synthesis of DAz-1 was completed through deprotection of methyl vinyl ether with 2 M HCl in THF (d) (60).

Experiments were carried out by Carroll and colleagues to test the ability of DAz-1 to bind specifically to protein sulphenic acids. Two model proteins were examined *in vitro*. Papain from *Carica papaya* which is the prototype cysteine endopeptidase has been studied comprehensively because of its homology with mammalian cysteine proteases. The oxidation of the active site Cys25 of papain induces a loss of enzymatic activity. Experiments were done to assess the modification at Cys25 by monitoring cleavage of the chromogenic substrate N α -benzoyl-L-arginine-4-nitroanilide hydrochloride (BAPNA). Untreated papain showed catalytic activity in the presence of BAPNA as the substrate. However when treated with a stoichiometric amount of hydrogen peroxide (H₂O₂) the protease activity was eliminated. Treatment of the oxidised papain sample with the reducing agent DTT led to the reactivation of enzymatic activity demonstrating that the Cys25 sulphenic acid was reduced to the thiol form. Having recognized that H₂O₂ and DTT can be used to modulate the activity of papain Cys25 the researchers then investigated the effect of DAz-1 on the assay. In the absence of hydrogen peroxide, the inclusion of DAz-1 had no effect on the enzymatic activity. However when the oxidised papain was treated with the probe the protease activity was abolished and this could not be reversed with the addition of DTT. These data suggested that a covalent modification of cysteine sulphenic acid and DAz-1 had occurred in papain. The selectivity of DAz-1 was also explored by western blot. Oxidised papain was incubated with the probe and subjected to labelling with phosphine-biotin (p-biotin) via the Staudinger ligation (62). The reactions were separated by electrophoresis and studied by streptavidin blotting. In the absence of oxidised papain no bands were detected by streptavidin blotting demonstrating the specificity of DAz-1 to detect sulphenic acid modified proteins (10).

The specificity of DAz-1 for sulphenic acid was then investigated with a different protein, human serum albumin (HSA) (10). HSA contains one free cysteine, Cys 34, 17 disulphide

bridges and is the most abundant protein in plasma (63). It has been demonstrated by Carballal and colleagues that Cys 34 in HSA oxidises to form a stable sulphenic acid (64). In the experiments carried out by Carroll and the research group the thiol and sulphenic acid content was assessed using 7-chloro-4-nitrobenzo-2-oxa-1,3-diazole (NBD-Cl). NBD-Cl is a non-fluorescent compound that upon the reaction with thiol groups or sulphenic acid groups (52) will emit distinctive signals. Reacting HSA with NBD-Cl yielded one major peak on the UV-Vis spectra at 347 nm and additional peak at 400 nm. This indicated that the NBD-Cl had formed adducts with both thiol and sulphenic acid groups. However, when DAz-1 was added to HSA prior to the addition of NBD-Cl the sulphenic peak at 347 nm disappeared leaving only the 400 nm thiol peak (10). The advantage of DAz-1 over existing probes is that it is a small molecule which is cell permeable therefore making it possible to detect sulphenic acids in intact cells. In this approach experiments were carried out on human T lymphoma cell line Jurkat. DAz-1 was incubated with Jurkat cells in increasing concentrations. After labelling the excess probe was washed off, cells lysed and the DAz-1 labelled proteins were detected after ligation with p-biotin. Through HRP-streptavidin western blotting it was shown that the intensity of DAz-1 labelling increased in a dose dependent manner thus demonstrating the cell permeability of DAz-1 (10).

The synthesis of 4-(3-azidopropyl)cyclohexane-1,3-dione (DAz-2) was reported by Carroll *et al* in 2009 (1). This was an analogue of DAz-1 with a propyl azide linker installed directly at the C4 position of the 1,3-cyclohexadione scaffolds. (**Figure 1.9**)

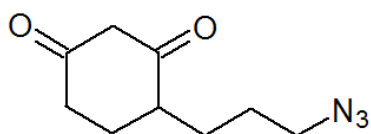


Figure 1.9: Chemical structure of DAz-2

Two synthetic routes are reported in the literature with a 10% yield of the final compound. Both routes begin with the protection of the reactive diketone of 1,3-cyclohexadione. The protected 3-ethoxy-cyclohex-2-enone was synthesised with I_2 in ethanol at room temperature. A lithium diisopropyl amide (LDA) solution was used to activate 3-ethoxycyclohex-2-enone for the alkylation with 3-iodo-tert-butyltrimethylsilyloxypropane to give 6-(3-tertbutyltrimethylsilyloxypropane)-3-ethoxycyclohex-2-enone. This compound was then deprotected with tetrabutylammonium fluoride (TBAF) to give 6-(3-hydroxypropyl)-3-ethoxycyclohex-2-enone. Via mesylation, the azide chemical handle was installed and subsequent nucleophilic displacement of the mesyl alcohol by sodium azide in a two-step reaction. The resulting 6-(3-azidopropyl)-3-ethoxycyclohex-2-enone was deprotected in the final step using ceric(IV) ammonium nitrate to give the final product DAz-2. The alternative route was attempted to reduce the number of synthetic steps. An LDA solution was used to activate the protected 3-ethoxycyclohex-2-enone for alkylation with 3-iodopropylazide to yield 6-(3-azidopropyl)-3-ethoxycyclohex-2-enone. This was then deprotected to give DAz-2 (1).

The hypothesis that DAz-2 would be more effective to detect sulphenic acid than DAz-1 was investigated using their reactivity to GAPDH. GAPDH is a glycolytic enzyme with an active site cysteine (Cys149) that is readily oxidized (14, 65). For these experiments, untreated or H_2O_2 treated GAPDH was reacted with DAz-1 and DAz-2. The azide tagged proteins were conjugated to phosphine-biotin and analysed by HRP-streptavidin Western blot. In reactions without H_2O_2 , faint labelling of GAPDH by the 2 probes was observed which was consistent with the high reactivity of Cys149. Control reactions carried out in the absence DAz-1 and DAz-2 showed no detectable protein labelling. Protein labelling of DAz-2 was notably more intense relative to DAz-1 (1). DAz-2 was also evaluated for sulphenic acid detection in living cells. The extent and selectivity of covalent modifications of sulphenic acid modified proteins were examined by performing Staudinger ligation in lysates from cells treated with azido-probe. Cells probed with both DAz-1 and DAz-2 showed similar protein labelling patterns although DAz-2 treated cells showed a higher intensity. These data showed that DAz-2 was

more sensitive to sulphenic acid detection (1). Another study by Carroll *et al* led to the development of a new set of sulphenic acid detecting probes DYn-1 and DYn-2 (66). In these two probes the linker to the dimedone molecule contains an alkyl group instead of an azide group which offer higher sensitivity compared to the reverse combination in DAz-1 and DAz-2. Another advantage of these over the existing probes were that they were synthesised in high yields and with less synthetic routes. When the two probes were tested for sulphenic acid labelling in a recombinant protein GPx3 it was revealed that DYn-2 detected more sulphenic acid modifications to DYn1. This could be due to steric hindrance during the click chemistry reactions (67). DYn-2 has been used to monitor sulphenic acid modifications during cell signalling. It was demonstrated that epidermal growth factor receptor (EGFR) goes through sulphenic acid modifications when epidermal growth factor (EGF) is added. Normally when EGF is bound to the extracellular domain of EGFR it leads to the activation of NADPH oxidase (Nox) that will generate hydrogen peroxide. While the intracellular domain of EGFR has six-cysteine residues only one cysteine (Cys797) is conserved. It was observed that it was this cysteine that was oxidised to sulphenic acid during endogenous production of hydrogen peroxide (68).

The main strategies employed so far for the synthesis of probes relies on the reactivity of dimedone or dimedone based derivatives. They are either linked to fluorophores for visualisation or use biotin tags for affinity purification. One particular disadvantage of using dimedone is that the derivatization process requires multiple synthetic steps and the overall yield is low. In 2011 Poole *et al* report the synthesis of 1,3-cyclopentanedione derived probes (69). They examined 4-(ethylthio)cyclopentane-1,3-dione, which could be used for the synthesis of sulphenic acid detection probes. One major advantage of this was the opportunity for direct conjugation to thiol-containing tags through a Michael addition. Furthermore fluorophores or affinity tags such as biotin could be incorporated in easy steps with high yields. To test the reactivity and selectivity towards cysteine sulphenic acids the C165S mutant of AhpC was used as the model protein. The cysteine active site was mildly oxidised and incubated with 4-(ethylthio)cyclopentane-1,3-dione, dimedone and 1,3-

cyclopentanedione respectively. These samples were then analysed by ESI-TOF MS. The results indicate that 1,3-cyclopentanedione reacts in a similar fashion to dimedone to detect sulphenic acids although kinetic studies have shown that this occurs about 20 times slower than the dimedone reaction (69). In summary, probes such as NBD-Cl that were first used to identify sulphenic acid modifications in proteins have the disadvantage of not being specific to sulphenic acids which could lead to false positive identifications. Although the probes synthesised by Poole and co-workers are cell permeable and have both affinity and fluorescence tags their synthesis is lengthy. While Daz-1 and Daz-2 are small molecules they have no affinity or fluorescent tags attached to them. Therefore additional molecules have to be synthesised and added to the experiments in order to be able to detect the modified sites.

1.5 Inflammation and the immune system:

Inflammation is the simplest mechanism by which the body defends itself against any damage or bacterial infection. The inflammatory responses are clinically characterised by the basic symptoms such as heat, pain, redness, swelling and result in loss of function. These symptoms are common in everyday life and are the result of cytokines and other inflammatory mediators acting on specific receptors on circulating cells and endothelial cells in the local blood vessels (70, 71). The immune system is responsible for these inflammatory responses and can be separated into two systems known as innate and adaptive immunity. The cross talk between these two systems is essential for the development of an effective immune response (70). The innate immune system accounts for a rapid non-specific response to pathogens or to cells that are injured or stressed (72). It is comprised of natural killer (NK) cells, macrophages, neutrophils, eosinophils, basophils and dendritic cells (DC). When pathogens such as bacteria and other microorganisms invade the human body an innate response is triggered with phagocytic neutrophils being the first to respond. This leads to the activation of neutrophils at the inflammation site leading to the release of cytokines. Cytokines are small proteins that are secreted by cells that act as mediators between cells. These include tumour necrosis factor- α (TNF- α), interleukins 1L-1 β , IL-4, IL-6, IL-10, IL-12, IL-18, chemokines and interferon- γ (IFN- γ). Cytokines may act on the cells that secrete them, on nearby cells or even on distant cells by which they can mediate signalling processors to recruit cells to the site of infection (73, 74).

The adaptive system comprises of T cells and B cells that are required for an effective immune response. Although it is slower to respond it is highly specific to the defined antigen and generation of immunological memory (72). Although T cells and B cells are the main cells involved in the adaptive system, DCs and macrophages from the innate system are needed to present antigens to naïve T cells. Cell-mediated immune responses occur due to T cells. When a specific antigen is presented by antigen presenting cells (APCs) to a T cell receptor (TCR) they become activated and differentiate into effector T cells. B cells are

responsible for the generation of antibodies. They do so by bearing an immunoglobulin receptor on the cell surface that is antigen specific. They phagocytize the antigen and activate specific T cells that will then induce the B cells to expand and differentiate into antibody producing cells (75). These antibodies are very specific to the antigen that trigger their production and will eventually lead to the removal of antigen. Once the immune response is over most of the activated T cells and B cells will die (70). However, a number of these cells will differentiate into memory cells so that when the body is exposed to the same antigen again it will trigger a faster secondary immune response (73).

1.5.1 T cell maturation and sub populations:

All blood cells including T cells arise from a type of cell called the hematopoietic stem cell (HSC). These cells are multipotent which mean that they can differentiate in various ways to generate different blood cells. Early on these HSCs differentiate to give rise to either a common lymphoid progenitor cell or a myeloid progenitor cell. The common lymphoid progenitor cells then give rise to T, B and natural killer cells and some of the dendritic cells. Developing T cells also known as thymocytes migrate from the bone marrow to the thymus where they undergo different maturation stages (**Figure 1.10**). In the early stages of thymocyte development they have not yet rearranged their T cell receptor (TCR) genes and don't express proteins such as RAG-1 and RAG-2 that are required for rearrangement. As maturation progresses expression of cell surface molecules such as c-Kit (stem cell growth factor receptor), CD44 (adhesion molecule involved in homing) and CD25 (α -chain of IL-2 receptor) occurs. When the cells stop expressing c-Kit, RAG-1 and RAG-2 gene expression is turned on thus beginning the rearrangement of the TCR genes. According to the TCR gene rearrangement two cell lineages namely $\alpha:\beta$ and $\gamma:\delta$ are produced (71). About 5% of T cells are $\gamma\delta$ and are characterised by the expression of $\gamma:\delta$ TCR at the cell surface. The $\alpha\beta$ cells express $\alpha:\beta$ TCR at the cells surface and after positive selections can either differentiate into CD4 or CD8 T cells (76). CD4 T cells also known as T helper (Th) cells can recognise antigens bound to major histocompatibility complex (MHC) class II (MHC-II) molecules whereas CD8 or cytotoxic T (Tc) cells recognise antigens which are bound to MHC class I (MHC-I) molecules. During the development of T cells about 98 % of thymocytes do not mature, either because they fail in making a productive TCR rearrangement or because they fail to survive thymic selection. If TCRs of T cells strongly interact with self-MHC then they are negatively selected and eliminated. Cells that recognise self-MHC molecules are positively selected and leave the thymus to circulate in the blood stream as resting T cells (71). T cells differ according to the markers expressed on the cell surface as well as their function. When a CD8 T cell comes into contact with an antigen via MHC-1 on APCs, they

turn into effector T cells. Their main function is to release cytotoxins such as granulysin, perforin and granzymes into infected cells. Once CD4 T cells are activated they can develop into a variety of cells that include Th1, Th2, Th17 and T regulatory (Treg) T cells. The development of these cells depends on the level and type of co-stimulation, the amount of antigen that is presented to them and the environment that surrounds them (77). Th1 cells secrete interferon- γ (IFN- γ) lymphotoxin- α (LT- α) and interleukin-2 (IL-2) and are important for the protection against intracellular pathogens such as macrophages that are infected. Th2 cells induce the proliferation of B cells leading to an immune response against extracellular pathogens. They secrete B cell growth factors, interleukin-4 (IL-4), interleukin-5 (IL-5) and CD40 ligand (CD40 L) (70, 78, 79). Th17 cells produce IL-17, IL-21 and IL-22 and act against extracellular bacteria and fungi. Treg cells protect the immune system against self-antigens and secrete transforming growth factor beta (TGF- β), IL-10 and IL-35 (79).

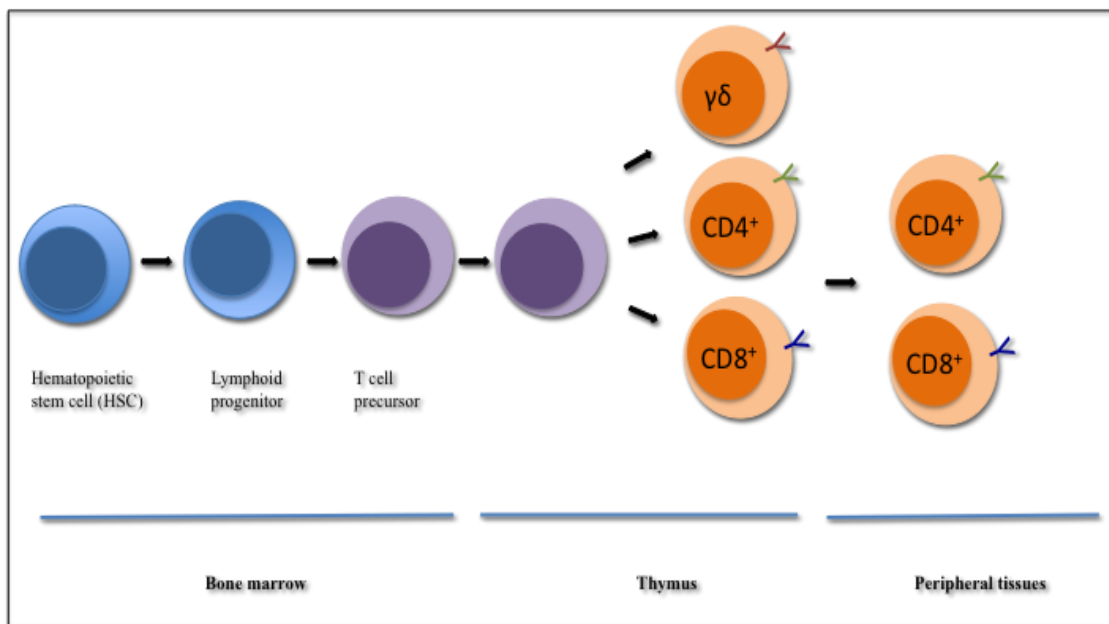


Figure 1.10: Development of T cells. T cell precursors arrive from the bone marrow via the blood stream into the thymus where they undergo development into mature CD8⁺, CD4⁺ or $\gamma\delta$ T cells. Then they are exported to the peripheral tissues where they can undergo antigen-induced activation into effector cells or memory cells.

1.5.2 T cell activation and TCR signalling:

Once the T cells are mature they enter the blood stream as naïve T cells and circulate in the periphery until they become activated. When an antigen interacts with a resting T cell it initiates a cascade of biological events that induces a T cell to enter the cell cycle, proliferate and differentiate into memory or effector cells. The contact between T cells and APCs is very specific and when they present an antigen to the naïve T cells they become activated. It is the T cell receptor located on the T cell surface that recognises specific antigens that are bound to MHC molecules at the surface of APCs (80). Co-stimulatory molecules such as CD80 and CD86 and chemical mediators expressed by antigen presenting cells are also needed to activate the T cells. The T cell receptor (TCR) is a trans-membrane protein that consists of an extracellular ligand-binding unit (α and β chains) and an intracellular signalling unit (γ , δ , ϵ , and ζ chains or the CD3 complex) (81). All these components are important for signal transduction. The T cell receptor associates with the CD3 unit to form a TCR-CD3 complex. The CD3 is a complex of five polypeptide chains that form three dimers. It consists of a heterodimer of γ and ϵ chains, heterodimers of δ and ϵ chains and a homodimer of two ζ chains or a heterodimer of ζ and β chains. The T cell receptor complex can therefore be conceived as a four-dimer complex. The cytoplasmic domains of the CD3 chains consist of the immunoreceptor tyrosine-based activation motif (ITAM). It has been shown that these sites interact with tyrosine kinases and that they play an important role in signal transduction (82).

Although the recognition of antigen-MHC complexes is mediated mainly by the TCR-CD3 complex, various other membrane molecules play an important role as accessories in antigen recognition and T cell activation. Once the MHC peptide has been engaged by the TCR it leads to clustering with co-receptors CD4 or CD8 where they bind to certain regions of the MHC molecule. This brings Lck, which is a protein tyrosine kinase associated with the cytoplasmic tails of the co-receptors into close proximity with the cytoplasmic region of the

TCR complex. The cytoplasmic tail of TCR contains immunoreceptor tyrosine based activation motifs (ITAMs), which are phosphorylated by the tyrosine kinase. This provides a docking site for zeta-chain-associated protein kinase 70 (ZAP-70) and it becomes activated. ZAP-70 in turn phosphorylates the membrane protein LAT (linker of activated T cells) and SLP-76 (SH-2 domain containing lymphocyte protein of 76kDa molecules). LAT acts as an anchor to signalling molecules such as GRB2 (growth factor receptor bound protein 2), GADS (GRB2 related adaptor protein), ADAP (adhesion and degranulation promoting adaptor protein), ITK (interleukin-2-inducible T cell kinase), PLC γ (phospholipase C γ 1), NCK1 (non-catalytic region of tyrosine kinase adaptor protein 1) and VAV1 (guanine nucleotide exchange factor). Several signalling pathways such as Ca²⁺, MAPK (mitogen activated protein kinase) (**Figure 1.11**) become activated resulting in the transport of transcription factors that are essential for gene expression and the growth and differentiation of T cells into effector cells leading to the removal of pathogens (81, 83).

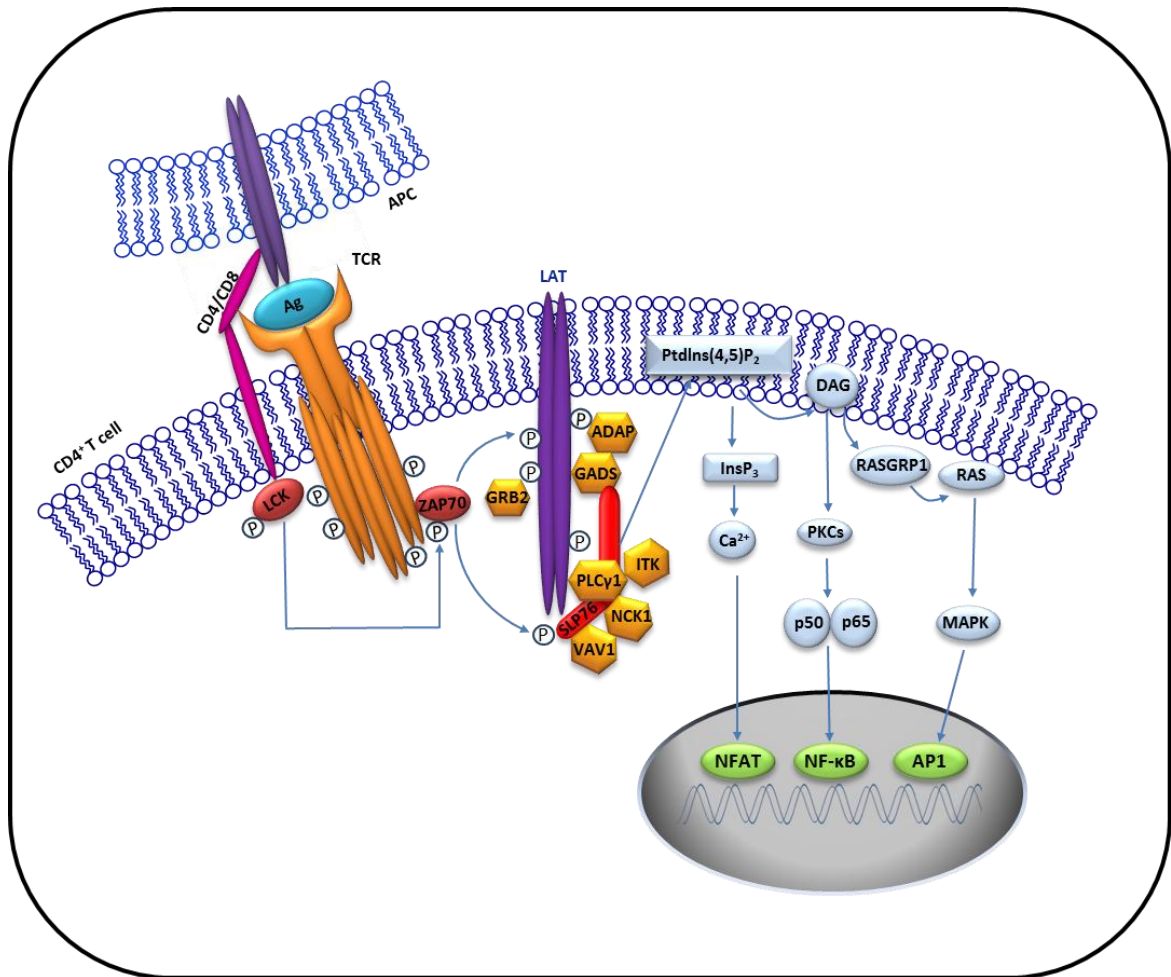


Figure 1.11: Schematic representation of TCR signalling. When an antigen is presented to the TCR via an APC and the MHC has been engaged, clustering with co-receptors CD4 or CD8 occurs. This brings Lck, which is a protein tyrosine kinase into close proximity with the cytoplasmic region of the TCR complex. The cytoplasmic tail of TCR contains immunoreceptor tyrosine based activation motifs (ITAMs), which are phosphorylated by the tyrosine kinase, leading to the activation of protein kinase 70 (ZAP-70). ZAP-70 in turn phosphorylates a membrane protein, LAT (linker of activated T cells) and SLP-76 (SH-2 domain containing lymphocyte protein of 76 kDa molecules). LAT acts as an anchor to signalling molecules such as GRB2 (growth factor receptor bound protein 2), GADS (GRB2 related adaptor protein), ADAP (adhesion and degranulation promoting adaptor protein), ITK (interleukin-2-inducible T cell kinase), PLC γ (phospholipase C γ 1), NCK1 (non-catalytic region of tyrosine kinase adaptor protein 1) and VAV1 (guanine nucleotide exchange factor). Several signalling pathways such as Ca²⁺, MAPK (mitogen activated protein kinase) and NF- κ B (nuclear factor- κ B) become activated resulting in the transport of transcription factors that are essential for gene expression and the growth and differentiation of T cells.

1.5.3 Oxidative stress in the immune system:

In recent years the effect of ROS and oxidative stress on immune cells and their roles in diseases has gained much interest. T cells play an important role in the adaptive immune response and their function is influenced by changes in the redox environment. Therefore the release of ROS during inflammation by activated granulocytes and macrophages or by stimulated T cells is important for the balance of T cell activation/inactivation and the regulation of immune outcomes (84). Cells have developed defence mechanisms that help protect against oxidative damage thus maintaining redox homeostasis. When cells are under oxidative stress these molecules alter their expression and this has an effect on the cellular function of T cells.

ROS are important for the activation and proliferation of T cells. A study by King and his research group have shown that when peripheral blood mononuclear cells (PBMCs) were reacted with the ROS generator 2,3-dimethoxy-1,4-naphthoquinone that Th1 phenotype was inhibited whereas the Th2 were promoted. This is indicative of the importance of a redox balance in the cells, which must be regulated for the maturation, and activation of T cells (85). The redox environment between the APC and T cell also plays a role in the activation of T cells. Upon activation T cells display increased cell surface thiols, which suggests that a reduced extracellular environment is needed for the activation of T cells (86). Enzymes such as superoxide dismutase (SOD) convert two peroxide anions into hydrogen peroxide and oxygen and catalase converts hydrogen peroxide into water and oxygen where it completes the detoxification process. SODs have three isoforms and are suggested as being important in preventing oxidative stress associated diseases (87, 88). SOD2 helps protect against superoxide anions, which are by products of respiration. A recent study using T cell specific SOD2 knockout mice has shown that when SOD2 is absent there is an increased level of superoxide production, which causes apoptosis and defects in T cell population resulting in immunodeficiency (89). Glutathione peroxidase (GPx) is another important group of antioxidants, which are responsible for reducing peroxides. They are capable of protecting

cells from damage against ROS to proteins, lipids and nucleic acids. (90). A study has recently shown that GPx1 deficient CD4+ T cells produced more ROS compared to normal T cells. It was also shown that GPx deficient cells are more susceptible to hydrogen peroxide induced apoptosis. When treated with anti IL-4 and anti IFN- γ antibody Th1 phenotype was evident and Th2 and Th17 were suppressed indicative that GPx1 is not only important in the redox balance of ROS but also in the regulation of Th1 cell proliferation and differentiation (91).

There are also a number of non-enzymatic antioxidant molecules that play an important part in the regulation of the redox balance in the cell. Two major systems that control the thiol redox state are the thioredoxin (Trx) and the glutathione systems. Trx-1 is a cytosolic protein that is present in all the cells but is also secreted to the surface of the cell upon cell activation (92, 93). Trx-1 is a 12 kDa protein that has several redox active cysteine residues. They are involved in cytokine expression (94, 95, 96), regulation of transcription factors such as NF- κ B and AP-1 (97) and act as an antioxidant and redox-regulating enzyme (98). A study by Shao *et al* (99) has shown that in patients with T cell acute lymphoblastic leukemia (T-ALL) higher lymphocyte count was associated with higher expression of Trx. In vitro studies have also shown that exogenous treatment with TRX increased proliferation of lymphocytes, which suggests that they are important in the proliferation of T cells (99). Glutathione (GSH) is one of the most powerful intra-cellular molecules that act as a defence against the negative effects of ROS. Glutathione is a thiol containing tri-peptide, which consists of L-glutamate, L-cysteine and glycine (100). The free thiol of cysteine serves as a target for ROS and GSH is converted to its oxidised form GSH disulphide (GSSG). It can be reduced again to its initial form (GSH) by a specific enzyme, glutathione reductase and reduced NADPH (101). Maintaining the GSH/GSSG ratio is vital to the cell survival as the level of glutathione is responsible how efficiently the cell can recover from oxidative damage (102, 103, 104, 105, 106, 107, 108, 109). Depletion of GSH levels in cells has been suggested to lead to the progression of certain diseases including HIV and arthritis (110, 111, 112).

In recent years the effect of ROS and oxidative stress on immune cells and their roles in diseases has gained much interest. T cells have an important role in the immune system and their function is influenced by changes in the redox balance. Various T cell subsets respond differently to oxidative stress and therefore can contribute to a variety of different immune responses (113). For T cells to become activated, a reduced environment is key and therefore the presence of an oxidative environment affects the activation of T cells, negatively (114). However, the range and kinetics of target protein oxidation in T cells which are able to act as molecular switches to activate/inactivate T cell function depending on the redox state of the cells remains unknown.

1.6 Aims and objectives:

The aims of this thesis are to develop novel probes that can detect sulphenic acid formation and to apply it to detect sulphenic acid in T cells. Specific objectives are to;

- 1) Optimise conditions of sulphenic acid formation in the purified protein human serum albumin (HSA) using the commercially available sulphenic acid detection probe DCP-Bio1.
- 2) Establish a model for thiol oxidation using buthionine sulfoximine and activation of T cells.
- 3) Identify specific protein sulphenic acids formed during glutathione (GSH)-depletion in human proliferating and resting CD4+ T cells.
- 4) Synthesis of novel probes

Chapter 2.0 Materials and Methods

2.1 Materials:

All chemicals were purchased from Sigma-Aldrich (Poole, UK) and all solvents from Fisher Scientific (Loughborough, UK) unless stated otherwise. The Jurkat E6.1 T cells were from the European collection of cell cultures (ECACC-HPA cultures, Porton, Down, UK). Rosewell Park Memorial Park medium (RPMI) 1640 with stable L-glutamine, Foetal Bovine Serum (FBS) and Alexa Fluor 488C5 Maleimide were purchased from Life Technologies (Paisley, UK). Penicillin/Streptomycin 100x (containing 10,000 U penicillin and 10 mg/mL streptomycin) was purchased from PAA Laboratories (Pasching, Austria). Lymphoprep was purchased from Axis-Shield (Dundee, Scotland). Dynabead untouched human CD4 kit was purchased by Invitrogen (Paisley, UK). The recombinant human IL-2 ELISA development kit was purchased from Peprotech (London, UK). Protein Kaleidoscope markers were purchased from Bio-Rad (Hemel Hempstead, UK). Hydrobond-P transfer membrane and enhanced chemiluminescence (ECL) reagent were purchased from GE Healthcare (Piscataway, NJ, USA). Cell culture plastics and plastic ware and poly-L-lysine slides were from Thermo Scientific (Loughborough, UK). Needles and syringes were obtained from BD (Oxford, UK) and Vacuette blood collection tubes were from Greiner Bio-one (Gloucester, UK). Optilise was purchased from Beckman Coulter (High Wycombe, UK). DCP-Bio1 was purchased from Kerafast (Boston, USA). Mouse monoclonal (MEM-241) against CD4 conjugated to phycoerythrin (PE) (ab18282), mouse IgG1 isotype control conjugated to PE (ab81200) were purchased from Abcam (Cambridge, UK).

2.2 Methods:

2.2.1 Jurkat E6.1 T Cell culture:

Jurkat T cells are an immortalised line of the human T lymphocyte cells. The E6.1 T cell line is a sub clone derived from the original Jurkat T cell line taken from the peripheral blood of a patient with T cell leukaemia. Jurkat E6.1 T cells were from the European collection of cell cultures (ECACC-HPA cultures, Porton, Down, UK). Jurkat T cells were cultured in Rosewell Park Memorial Institute (RPMI) 1640 medium with L-glutamine (Gibco®, Life Technologies) supplemented with 10% heat inactivated foetal bovine serum (FBS) and 1% penicillin/streptomycin (P/S). Actively growing T cells were maintained between 2×10^5 - 5×10^5 cells per mL and passaged every three days. The cell cultures were maintained at 37 °C in a 5% CO₂/95% air-humidified atmosphere.

2.2.2 Trypan blue cell counting and cell viability:

Cells were collected by centrifugation and resuspended in RPMI media. The cell suspension was mixed with an equal volume of trypan blue solution and counted in a haemocytometer for determination of viable and non-viable cells.

Viability% = number of viable cells/number of total cells x 100

Total cells (number of viable and non-viable cells)

2.2.3 Sodium dodecyl sulphate polyacrylamide gel electrophoresis (SDS-PAGE):

2.2.3.1 Reagents:

Reagent	Description
1. Buffer 1 for the resolving gel	Tris-base (36.3 g) and SDS (0.8 g) were dissolved in 150 mL of water and the pH adjusted to 8.4. The solution was made up to 200 mL.
2. Buffer 2 for the stacking gel	Tris-base (6.05 g) and SDS (0.4 g) were dissolved in 80 mL water. The pH was adjusted to 6.8 and the solution made up to 100 mL
3. Ammonium persulphate (10 % w/v)	1.0 g APS was dissolved in 10 mL of water and was aliquoted to 200 μ L and frozen at -20 °C.
4. Running buffer	Tris-base (3 g), glycine (14.4 g) and SDS (1 g) were dissolved in 1 L of water.
5. Transfer buffer	Tris-base (4.5 g), glycine (21.6 g) was dissolved in 300 mL of methanol and 1200 mL of water
6. Acrylamide solution	Acrylamide/bis-Acrylamide 30% solution

7. TEMED	N,N,N',N'-tetramethylethylenamine
8. Tris buffered saline (TBS) buffer	NaCl (12 g), Tris-HCl (6 g) were dissolved in 900 mL water. pH was adjusted to 7.5 and the solution was made up to 1 L.
9. TTBS buffer	Tween20 (0.5 g) in 1 L of TBS buffer.

Table 2.1: Buffers and reagents used for SDS-PAGE

2.2.3.2 Gel Electrophoresis:

Resolving and stacking gels were prepared using the hand cast Bio-Rad Mini Protean III system (Bio Rad). The reagent concentrations for a 10% resolving and 3% stacking gel are described in **Table 2.2** below. Gels were left for 45 minutes to set at room temperature. Samples were mixed with 1:1 laemmli buffer (Sigma) or non-reducing buffer, boiled for 5 minutes at 95 °C. Varing sample volumes depending on the experiment were loaded into each well and electrophoresed at 115 V for 1 hour 45 minutes.

2.2.3.3 Reagents:

Reagent	Resolving (10%)	Stacking (3%)
Water	5 mL	4.87 mL
Buffer 1	3 mL	-
Buffer 2	-	1.87 mL
Acrylamide	4 mL	750 μ L
10% APS	100 μ L	100 μ L
TEMED	10 μ L	10 μ L

Table 2.2: Reagents required for the polyacrylamide gels

2.2.3.4. Western blot:

Proteins were separated by SDS-PAGE and were transferred on to polyvinylidene difluoride (PVDF) membrane (GE Healthcare, Amersham Hybond™) that was soaked in 100% methanol for 5 minutes and transfer buffer (Tris-base (4.5 g), glycine (21.6 g) was dissolved in 300 mL of methanol and 120 mL of water) for 5 minutes prior to use as shown in **Figure 2.1**.

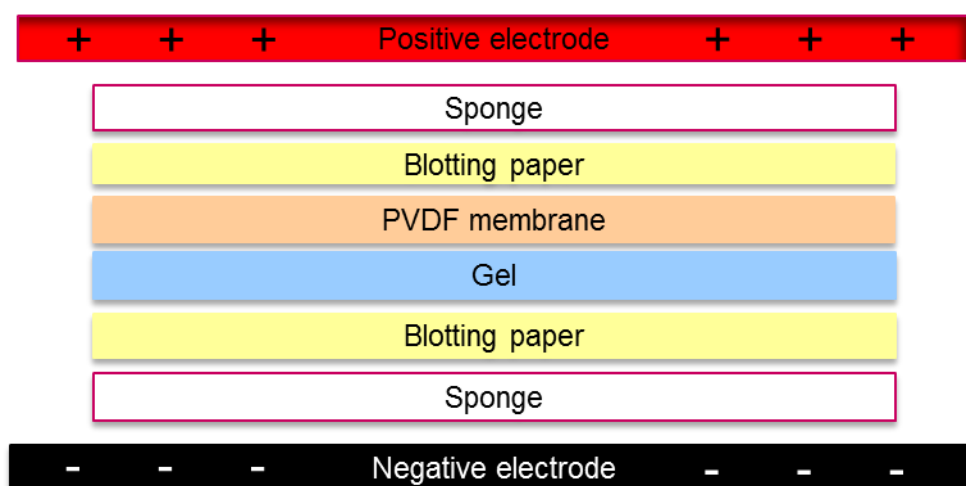


Figure 2.1: Schematic representation of protein transfer to PVDF membrane

The proteins were then transferred at 240 mA for 65 minutes in transfer buffer. After transfer the PVDF membrane was blocked with 3% BSA (bovine serum albumin) in Tris buffered saline Tween-20 (TBST) overnight at room temperature. The membrane was washed with TBST (6 x 15 minutes) then incubated with 1:20,000 HRP streptavidin (Sigma) for 2 hours at room temperature. The membrane was washed with TBST (6 x 5 minutes) and developed with Amersham ECL™ prime western blotting detection reagent (GE Healthcare). The membrane was visualised on the G box chemi XT4 (Syngene)

2.2.4 The bicinchoninic acid (BCA) assay:

The BCA assay was performed to determine the total protein concentrations of proteins and cell lysates after different treatments. The BCA method was adapted from Smith *et al* (115). Unknown protein concentrations were determined from a standard curve prepared fresh with each experiment. The protein standards were prepared by diluting stock solution of 1 mg/mL BSA in distilled water as described in **Table 2.3**

Protein concentration (mg/mL)	BSA (μ L)	Water (μ L)	Final volume (μ L)
0.0	0	10	10
0.2	2	8	10
0.4	4	6	10
0.6	6	4	10
0.8	8	2	10
1.0	10	0	10

Table 2.3: Combination of chemicals needed to prepare a standard curve to determine protein concentrations.

A standard curve was generated by plating BSA standards in triplicate wells of a 96 well plate with a final volume of 10 μ L. Samples (10 μ L) were also pipetted in triplicates onto the same plate. BCA reagent was prepared by adding bicinchoninic acid to copper II sulphate (50:1 v/v). 200 μ L of BCA reagent was pipetted into each well and the plate was incubated at 37 $^{\circ}$ C for 30 minutes and the absorbance was read at 570 nm on a micro plate reader (Biotek, UK).

2.2.5 Glutathione (GSH) assay:

2.2.5.1 Reagents:

Reagent	Description
Stock buffer	125 mM sodium phosphate, 6.3 mM EDTA adjusted to pH 7.5.
Daily buffer	3 mg of NADPH (reduced tetrasodium salt) in 10 mL of stock buffer.
DTNB solution	0.024g of 5,5'-dithiobis(2-nitrobenzoic acid) (DTNB) in 10 mL of stock buffer.
GSH solution	0.15 g of glutathione (GSH) in 5 mL of distilled water.
SSA	1 g of sulphosalicylic acid (SSA) in 1 mL of distilled water.
GSR	8 μ L (2U/mL) Glutathione reductase (GSR) in 1 mL of stock buffer.

Table 2.4: List of reagents required for the GSH assay

The total GSH levels were determined by a DTNB-GSR recycling procedure. Samples for the standard curve were prepared as described in **Table 2.5** below.

Concentration (μM)	GSH (μL)	SSA (μL)	Water (μL)
0	0	33.3	966
20	0.2	33.3	966
40	0.4	33.3	966
60	0.6	33.3	966
80	0.8	33.3	966

Table 2.5: Combination of reagents required for the standard curve to determine total GSH Level.

To a 96 well plate 25 μL of the standards and samples were added in triplicates followed by 150 μL of daily buffer and 50 μL of DTNB solution. The plate was incubated at 37 $^{\circ}\text{C}$ for 5 minutes. Finally 25 μL of GSR was added to each well and the plate was read at 405 nm at 0, 1, 2, 5 and 10 minutes on a spectrophotometric plate reader (Bio TeK).

2.2.6 Flow cytometry:

Flow cytometry was performed on a Cytomics™ FC500 flow cytometer with CXP software (Beckman-coulter, Miami, USA). It is equipped with 5 fluorescent channels, FL1 (525 nm), FL2 (575 nm) FL3 (620 nm) FL4 (660-690 nm) and FL5 (740-770 nm). It uses two lasers either the air-cooled argon ion laser at 488 nm or the red solid-state laser at 630 nm as excitation beams. It can measure and analyse multiple characteristics of single particles such as cells simultaneously. The cells that can be detected range from 0.5-40 µm in diameter. When a stained cell suspension is injected into the cytometer it is hydro-dynamically focused using sheath fluid to create a tiny stream of samples. The cells then pass the laser light one at a time. The different detectors capture the light scattered from the cells as they pass through the beam. Forward scatter (FS) is used as a relative measure of the particle size and side scatter (SC) represents relative granularity and internal complexity of the particles. Fluorescence detectors are used to detect the fluorescence emitted from the positively stained cells. The resulting scattering and fluorescent is collected and detected as electrical signals that can be processed and analysed by the computer. Specific antigens on the surface of the cells can be detected by labelling them with antibodies that are fluorescently tagged with fluorophores such as fluorescein isothiocyanate (FITC) or phycoerythrin (PE). Flow cytometry was used to compare and analyse CD4+ T cell purity and surface thiol levels as described later on in chapter 4.

Chapter 3.0 Detection of sulphenic acid in human serum albumin (HSA)

3.1 Preface:

This chapter describes optimisation of a method to detect sulphenic acid in human serum albumin (HSA) using the biotinylated probe, 3-(2,4-dioxocyclohexyl)propyl 5-((3aR,6S,6aS)-hexahydro-2-oxo-1H-thieno[3,4-d]imidazol-6-yl)pentanoate (DCP-Bio1). SDS-PAGE and western blotting techniques and mass spectrometry were used to detect the sulphenic acid modifications.

3.2 Introduction:

3.2.1 Thiol oxidation:

Proteins are preferential targets of oxidation and cysteine, because of its thiol group, is particularly susceptible to oxidation (116). When low molecular weight or protein thiols are oxidised typically disulphide bonds (RSSR) are formed. Disulphide bonds support extracellular proteins to fold correctly and to maintain structural stability. However, intracellular proteins usually contain mainly reduced cysteine due to the reducing environment inside the cellular compartment. Among the various other oxidation states that thiols can have, sulphenic acids (RSOH) are a key intermediate in thiol oxidation. Sulphenic acid has been identified to serve catalytic or regulatory functions in a number of redox-susceptible proteins (117).

3.2.2 Human serum albumin:

HSA is the most abundant protein in plasma and is a monomeric three-domain protein, which constitutes to about 60% of total plasma proteins (118). It contains 585 amino acids including 18 tyrosine, one tryptophan, six methionines, 17 disulphide bridges and one free reactive cysteine, Cys34 (64). Albumin is a 66 kDa globular protein, which is mainly synthesised in hepatocytes and accounts for about 10% of liver protein synthesis (119). It has a half-life of about 19 days and it is mostly degraded in muscle, skin, liver and kidney. Albumin that has been modified due to oxidative stress will be preferentially recognised over native protein by several receptors resulting in rapid internalization and degradation (120, 121). HSA due to its high number of negative charges at physiological pH plays an essential role in the maintenance of colloid osmotic pressure. It also binds and transports long chain fatty acids that are circulating in the plasma. In addition to fatty acids it can also bind to hormones and drugs as well as cations such as copper, zinc and gold (118). Albumin also functions as an antioxidant in the vascular compartment because of its ability to scavenge reactive oxygen species (ROS) and reactive nitrogen species (RNS) that are being

produced by various metabolic processes (122). This protective role is attributed to the free thiol of HSA, Cys34 that accounts for about 80% of free thiols in the plasma (64). Radi and co-workers have shown that reactive oxygen species such as hydrogen peroxide, superoxide and hydroxyl radicals, which are derived from the enzyme xanthine oxidase, are primarily scavenged by HSA-SH in the plasma and not by lipids or other biomolecules (123). Unlike other proteins that have thiols that are more reactive, such as peroxiredoxins and tyrosine phosphatases (124, 125, 126) the thiol HSA is not particularly reactive. It has a pK_{aSH} of 8.3-8.6, which is similar to those of cysteine (8.36) and glutathione (8.75) (127). Although the thiol is oxidised at slow rates, due to its high concentration in the plasma it still acts as a major scavenger. Recent work has shown that thiols reacting with ROS/RNS not only serve as scavengers but also serve as modulators in signalling mechanisms by changing protein function (128). In the plasma, HSA contains thiols that are in its reduced form and this accounts to about 70% of the total albumin, which is known as the mercaptalbumin. A main fraction of the non-mercaptalbumin contains mixed disulphides between the albumin thiol and other low molecular weight thiols. It forms mixed disulphides with cysteines, cysteinylglycine, homocysteine, γ -glutamylcysteine or glutathione. The remaining non-mercaptalbumin is further oxidised to non-reducible thiol reagents such as sulphinic and sulphonic acids (129, 130, 131). However, the balance between reduced and oxidised HSA can shift with intense exercise or during aging. An age dependent decrease in the amount of thiol per HSA molecule was observed, with is consistent with age-related oxidative damage (132, 133, 134). It has been reported that the oxidation of HSA-SH with hydrogen peroxide and peroxyxynitrite does not lead to the formation of disulphide bonded HSA dimers (135, 64). This could be due to the fact that the single free thiol is located in a crevice causing steric restrictions to hinder dimerisation. Therefore it is suggested that HSA-SH is oxidised to higher oxidation states such as sulphenic acid or further oxidised to sulphinic or sulphonic acids (116).

3.2.3 Sulphenic acid in human serum albumin:

The stabilisation of sulphenic acids in proteins is dependent on the local environment. The absence of other thiol groups close to the site of sulphenic acid formation is important as well as adequate hydrogen bond formation between molecules and limited solvent accessibility (116). Until recently it has been difficult to identify sulphenic acids because they are highly unstable and do not possess any unique absorbance or fluorescence properties that can be used for identification. The first evidence that sulphenic acid was formed in albumin came from its reaction with sodium arsenite. This reagent can reduce sulphenic acids back to its thiol form whereas disulphides would not be reduced (135). Other studies to detect sulphenic acid formation in albumin have used the electrophilic reagent 7-chloro-4-nitrobenz-2-oxa-1,3-diazole (NBD-Cl). The drawback of using this reagent is that it can also react with tyrosyl and amine groups especially at alkaline pH (136). Proof that albumin samples oxidised with hydrogen peroxide formed sulphenic acid was provided by mass spectrometry; the nucleophilic reagent 5,5-dimethyl-1,3-cyclohexanedione (dimedone) which was first discovered by Alison *et al* in 1974, has been used to show that sulphenic acid was formed at Cys34 of HSA (14).

The aim of this chapter is to develop a method to detect sulphenic acids in HSA, by optimising conditions in which sulphenic acid formation occurs and visualising them using the biotinylated probe, DCP-Bio1.

3.3 Materials and methods:

3.3.1 HSA sample preparation for dot blot and western blotting and mass spectrometry:

HSA (1.0 mM) (Sigma, UK) was incubated with 10 mM 2-mercaptoethanol at 4 °C, overnight. The protein samples were then cleaned up through a PD-10 desalting column (GE Healthcare, UK) to remove excess reducing agent and the final HSA concentrations were measured using a BCA assay. The concentration was adjusted to 0.5 mM HSA for subsequent experiments.

3.3.2 Glutathione preparation for mass spectrometry:

Glutathione (1.0 mM) samples (1 mL) were used as control or treated with 1 mM DCP-Bio1 and 2 mM hydrogen peroxide for 30 minutes on ice or treated with 1 mM DCP-Bio1 and 10 mM hydrogen peroxide for 30 minutes on ice. The samples were then cleaned up using a PD-10 column to get rid of excess DCP-Bio1. The final samples were prepared by adding formic acid to a final concentration of 0.1% to enhance ionisation and subjected to mass analysis by direct infusion at 1 μ L/min using a Finnigan LXQ linear ion trap mass spectrometer (Finnigan, Thermo Scientific, UK) equipped with a nano-electrospray ionisation (ESI) source operating in positive ionisation (PI) mode. The acceleration voltage was set to 2 KV. Data was collected as the average total scans and the scan range was set from 100-1000 m/z to search for glutathione and modifications. The data system was the Xcalibur® software version 2.0 SR2 (Thermo Scientific, UK).

3.3.3 Protein Enzyme Linked Sulphenyl Probe Assay (ELSPA):

3.3.3.1 Buffers:

Reagent	Description
PBS (Phosphate buffer saline)	NaCl (8.0 g), KCl (0.2 g) Na ₂ HPO ₄ (1.15 g), KH ₂ PO ₄ (0.2 g) were dissolved in 1 L of water.
Sodium carbonate coating buffer	Na ₂ CO ₃ (1.59 g), NaHCO ₃ (2.93 g) were dissolved in 900 mL of distilled water the pH was adjusted to 9.2 and the solution was made up to 1 L to a final concentration of 50 mM.
Washing buffer	To 1 L of PBS, Tween-20 was added to a final concentration of 0.05% v/v.
Blocking buffer	Tween-20 1% v/v in 1 L of PBS.
Citrate phosphate buffer	Citric acid (21.0 g) Na ₂ HPO ₄ (35.6 g) were dissolved in 900 mL of distilled water, the pH adjusted to 5.0 and solution was made up to 1 L with a final concentration of 0.15 M

Table 3.1: Reagents required for the ELSPA

HSA was dissolved in carbonate buffer to 20 µg/mL and added to a Nunc maxisorb 96 well plate in triplicate (50 µL) and incubated for 1 hour at 37 °C. The plate was then washed with 0.05% (v/v) Tween-20 containing PBS three times and blocked with 1% (v/v) Tween-20 in PBS overnight at 4 °C. The plate was washed again three times with washing buffer to remove excess blocking buffer and the different treatments in which the probe was added were performed. The plate was washed six times with washing buffer and incubated with 50 µL of streptavidin-HRP (1:10,000 in 1% BSA in PBS) for 1 hour at 37 °C. The plate was washed 3 times with washing buffer, then developed with 50 µL OPD substrate (10 mL citrate phosphate buffer, 20 mg of o-phenylenediamine tablet with 10 µL 8.8 M hydrogen peroxide) and incubated at 37 °C for 15 minutes in the dark. Adding 2 M H₂SO₄ stopped the reaction and the absorbance was read at 490 nm on the spectrometric plate reader (BioTek).

3.3.4 Dot blot for sulphenic acid on HSA:

HSA (0.5 mM) was either untreated or was treated with 1.0 mM hydrogen peroxide, 1.0 mM hydrogen peroxide and 1 mM DCP-Bio1 for 30 minutes on ice. The excess probe was removed using a PD-10 column and samples were kept on ice until they were ready for use. Meanwhile a PVDF membrane was soaked in methanol for 10 minutes and washed for 5 minutes in TTBS. 2 µL of the samples were dotted on to a small spot and left to dry. The membrane was then blocked overnight with 3% BSA in TTBS and washed 6 times at 15 minute intervals with 20 ml of TTBS. The blot was then incubated with streptavidin-HRP (1:20,000) in TTBS for 2 hours at room temperature. It was washed 6 times with 20 mL TTBS at 5 minute intervals and visualised with ECL reagent using a G-box Chemi XT4 transilluminator.

3.3.5 SDS-PAGE and western blotting for sulphenic acid on HSA:

HSA (0.5 mM) samples were prepared as described in 3.3.1 and either treated with varying concentrations of DCP-Bio1 or hydrogen peroxide or both. Samples were heated for 5 minutes at 95 °C in Laemmli buffer. Equal amounts (10 µg) of each sample were resolved on to a 10% polyacrylamide gel (SDS-PAGE) (see general methods 2.2.3) in running buffer and transferred onto a PVDF membrane in transfer buffer. The membrane was then blocked with 3% BSA in TTBS overnight and washed 6 times in 20 mL TTBS at 15 minute intervals. After washing the membrane was incubated with streptavidin-HRP (1:20,000) in TTBS for 2 hours at room temperature, washed again for 30 minutes at 5 minutes intervals with TTBS and visualised with ECL using a G-box transilluminator.

3.3.6 Coomassie staining:

SDS-PAGE gels were stained with coomassie blue staining solution [0.05% (w/v) coomassie brilliant blue R-250 was dissolved in 50% (v/v) methanol, 10% (v/v) acetic acid and 40% distilled water] for 1 hour on a rotator. Gels were then destained using destaining solution (5% methanol, 7% acetic acid and 88% distilled water) at least three times for one hour each to remove excess background stain.

3.3.7 HSA preparation for mass spectrometry:

HSA samples (0.5 mM) were used as a control or treated with 0.5 mM H₂O₂ with 0.5 mM DCP-Bio1 for 30 minutes on ice. The sample containing DCP-Bio1 was enriched using streptavidin-coupled Dynabeads (Life Technologies, UK) (100 µL) for 30 minutes. The magnetic bead-bound protein was boiled with Laemmli buffer (20 µL) and heated for 5 minutes at 95 °C and loaded on a 10% SDS-PAGE gel.

3.3.8 In-gel protein digestion for mass spectrometry:

In order to investigate protein sulphenic acid modifications, 20 μL albumin treated with peroxide and DCP Bio1 were separated by polyacrylamide gel electrophoresis and the major bands from the gels were digested. Bands were stained with coomassie staining as described previously. Using a clean razor blade, protein bands were carefully cut eliminating as much of the polyacrylamide as possible. The gel pieces were placed in clean 1.5 mL micro centrifuge tubes that were prewashed with 500 μL of 100 mM ammonium bicarbonate (NH_4HCO_3) for one hour on the shaker. After discarding the wash, the gel pieces were washed again with 500 μL of 50% acetonitrile (ACN) / 100 mM NH_4HCO_3 for one hour. Once the wash has been discarded 150 μL of 100 mM NH_4CO_3 and 10 μL of 45 mM dithiothreitol (DTT) was added to the sample and incubated for 30 minutes at 60 $^\circ\text{C}$ to reduce the protein. The sample was left to cool to room temperature followed by alkylation with 10 μL of 100 mM IAM for 30 minutes in the dark. After discarding the solvents the gel pieces were washed again with 500 μL of 50% ACN/100 mM NH_4HCO_3 for one hour. The gel slices were then dehydrated for 10 minutes at room temperature in 50 μL 100% ACN. At this point the slices were much smaller than their original size and were white or opaque in colour. The gel slices were then dried in a Speed Vac concentrator for 15 minutes at room temperature to remove all the solvent. The gel slices were pre-incubated in 20 μL of the trypsin gold solution (Trypsin gold was resuspended at 1 $\mu\text{g}/\mu\text{L}$ in 50 mM acetic acid, then diluted in 40 mM NH_4HCO_3 /10% ACN to 20 $\mu\text{g}/\text{mL}$) at room temperature not exceeding 30 $^\circ\text{C}$, for one hour. The gel slices rehydrated during this time. Another 20 μL of trypsin was added and incubated for another hour at room temperature if required. Enough digestion buffer (40 mM NH_4HCO_3 /10% ACN) was added to cover the gel slices completely and the tightly capped micro centrifuge tubes were incubated at 37 $^\circ\text{C}$ overnight. The gel slices were then diluted with 150 μL of MilliQ water for 10 minutes with frequent vortex mixing. The liquid was removed and transferred to new microcentrifuge tubes. Gel slice digests were

extracted twice with 50 μ L of 50% ACN/5% TFA with mixing for 60 minutes each time at room temperature. All the extracts including the wash with MilliQ water were pooled together. Extracts were dried in a Speed Vac concentrator at room temperature for 2-4 hours not exceeding 30 °C. The precipitate was dissolved in 100 μ L of 0.1% formic acid. Samples were analysed by mass spectrometry using a Thermo LTQ-Orbitrap Elite coupled to a Dionex Ultimate 3000 (RLSC). The samples were separated over a 56 minute gradient, 3.2-44% mobile phase (MP) B over 30 minutes (MP A = 0.1% formic acid in H₂O, MP B = 0.1% formic acid in ACN), then 90% MP B for 10 minutes before 16 minutes re-equilibrating at 3.2% B. The flow rate was set to 350 nL/min. The mass spectrometer operates in a data dependent mode where it performs a full MS scan at resolution 60,000 followed by CID of the 7 most abundant multiply charged ions. These are then entered into an exclusion list to ensure the ions are not analysed multiple times. The full scan followed by top seven then repeats. Proteome Discoverer version 1.4 was used to analyse the results and the data was searched against a human database (Uniprot) and the results were filtered to give a 1% false discovery rate.

3.3.9 Peptide sequencing using mass spectrometry:

Mass spectrometry is a technique that is used to sequence peptides after proteins have been tryptic digested. LC-MS involves the separation of peptides according to their hydrophobicity after which they can be ionised using one of several methods. Electrospray ionisation (ESI) is a popular technique where an electrospray is created by putting a high voltage on a flow of liquid, which is then directed to an opening in the vacuum system of the mass spectrometer where droplets are formed. When the high temperatures and voltage evaporates the droplets of solvent the ions are ejected from the droplets and accelerated into the mass analyser. It has an advantage over other techniques such as matrix-assisted laser desorption ionisation (MALDI) because of low flow rate of peptides to increase sensitivity. There are three main types on analyser: time of flight (TOF) where ions are accelerated

towards the analyser according to size with lighter ions arriving at the detector first. The second type is a quadrupole mass analyser where a radio frequency (RF) voltage is applied to 4 rods after which a direct current (DC) voltage is superimposed. This causes an oscillating electrical current in the analyser and the ions are filtered out according to their mass to charge (m/z). The third type is an ion trap where ions are separated according to their m/z resonance frequency. The Thermo LTQ Orbitrap Elite (Thermo Scientific) uses a linear-ion-trap quadrupole (LTQ) coupled to a mass analyser and is capable of tandem mass spectrometry (137, 138).

In tandem mass spectrometry a full scan is completed on a peak by the orbitrap from the liquid chromatograph to identify the parent ion. This is known as a full ms scan. A zoom scan is then done on this peak to identify the charge on the ion in order to determine the mass of the ion. The ion is then selected and fragmented further using collision induced fragmentation (CID). This results in spectra of b and y ions, which are fragments where the amide bonds have split during the collision. This is known as an ms/ms scan and the fragmentation into b and y ions are shown below (**Figure 3.1**) (137, 138)

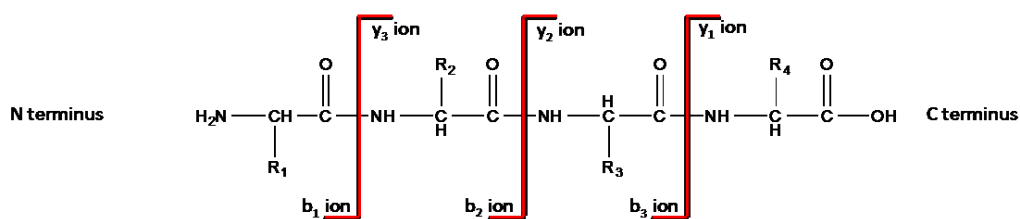


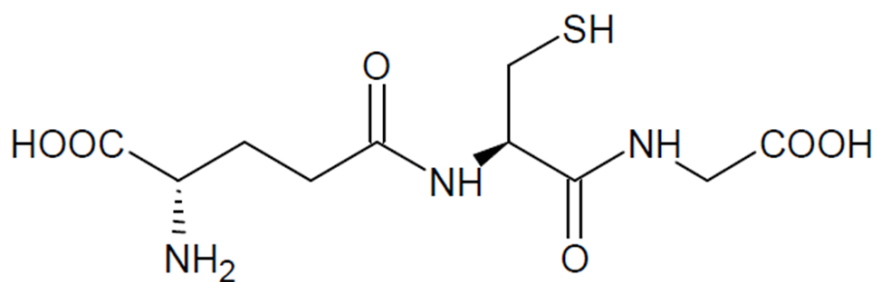
Figure 3.1: Schematic representation of b and y ions. During CID the amide bonds are split.

The sequence of the peptide can be determined from these ions. If a peptide had a sequence of $A_1B_1C_1D_1$ where each letter represents an amino acid the b ions would be calculated from the N terminus and b_1 ion would have a molecular weight equivalent to A_1 . The weight of the b_2 ion would be A_1+B_1 and so on. The y ions are calculated in the same way but start from the C terminus (137, 138).

3.4 Results:

3.4.1 Detection of glutathione (GSH) modifications by mass spectrometry:

In order to identify oxidative modifications of GSH (structure below), samples were treated with hydrogen peroxide as described in the materials and methods section above (3.3.2). The samples were subjected to mass analysis by direct infusion at 1 $\mu\text{L}/\text{min}$ using a Thermo LXQ tandem mass spectrometer. Three peaks were observed from GSH ($m/z = 308.17, 614.87, 921.13$) and hydrogen peroxide and DCP-bio1 ($m/z = 308.20, 614.91, 921.13$) treatment (**Figure 3.2**). There was no evidence of a DCP-bio1 conjugate with sulphenic acid on glutathione which has a predicted mass of 703.5 m/z in +ve ion mode when GSH is conjugated to DCP-bio1.



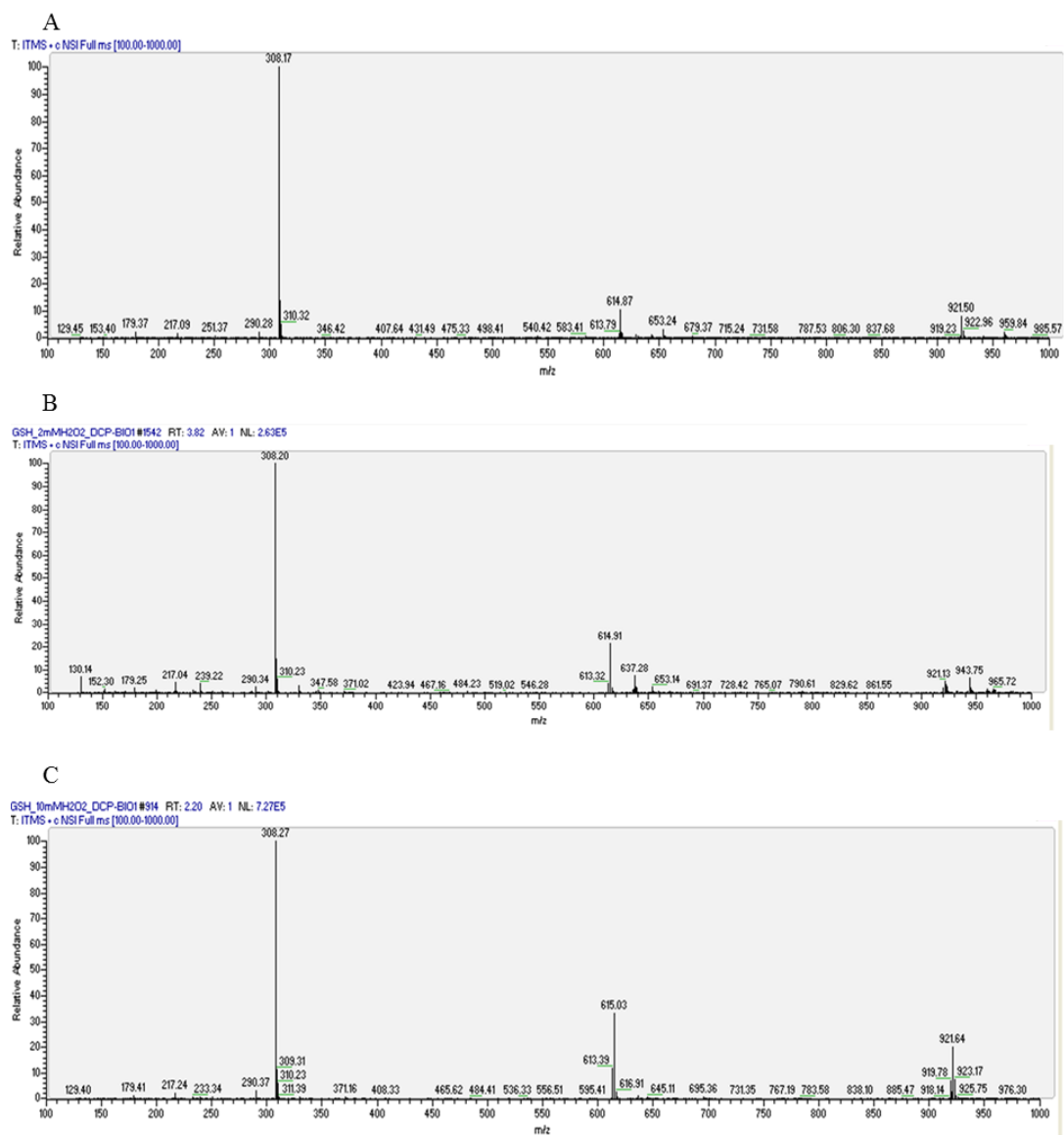


Figure 3.2: Disulphide bond formation in glutathione is increased by hydrogen peroxide.

A) 2 mM glutathione

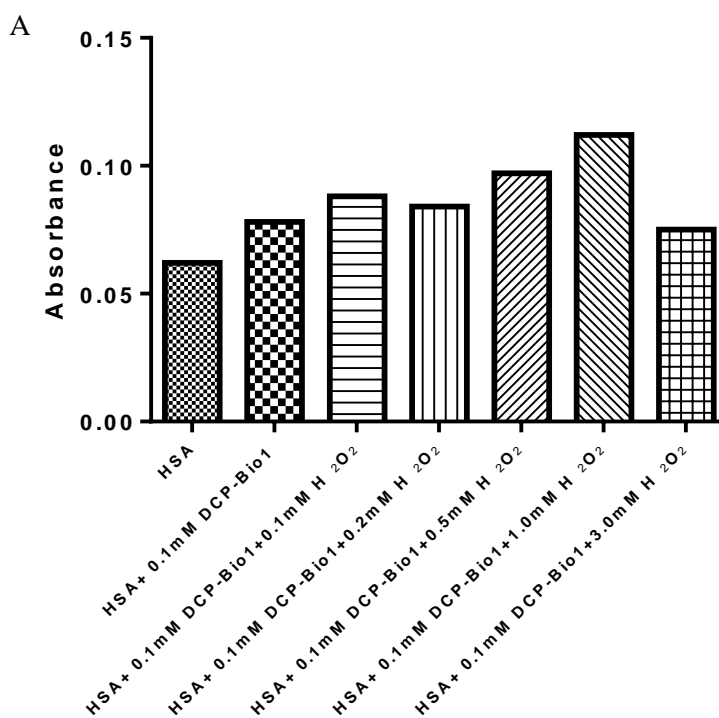
B) 2 mM glutathione treated with 2 mM H₂O₂ and 1 mM DCP-Bio1 for 30 minutes on ice

C) 2 mM glutathione treated with 10 mM H₂O₂ and 1 mM DCP-Bio1 for 30 minutes on ice.

Samples were injected at 1 μL/min and analysed using a Thermo LXQ tandem mass spectrometer. Data is representative of 2 independent experiments.

3.4.2 Optimisation of hydrogen peroxide concentrations for sulphenic acid formation determined by ELSPA:

To identify optimised conditions for formation of sulphenic acids under oxidising conditions an ELSPA was developed. HSA was dissolved in carbonate buffer to 20 $\mu\text{g/mL}$ and added to a Nunc maxisorb 96 well plate in triplicate (50 μL) and incubated for 1 hour at 37 $^{\circ}\text{C}$. After washing the plates the wells were either left untreated or treated with increasing amounts of hydrogen peroxide for 4 minutes washed 3 times and incubated with 0.1 mM DCP-Bio1 for 30 minutes on ice. There was an increase in absorbance until the addition of 1 mM hydrogen peroxide but further increase to 3 mM hydrogen peroxide resulted in less DCP-Bio1 bound than after 1 mM hydrogen peroxide treatment (**Figure 3.3**).



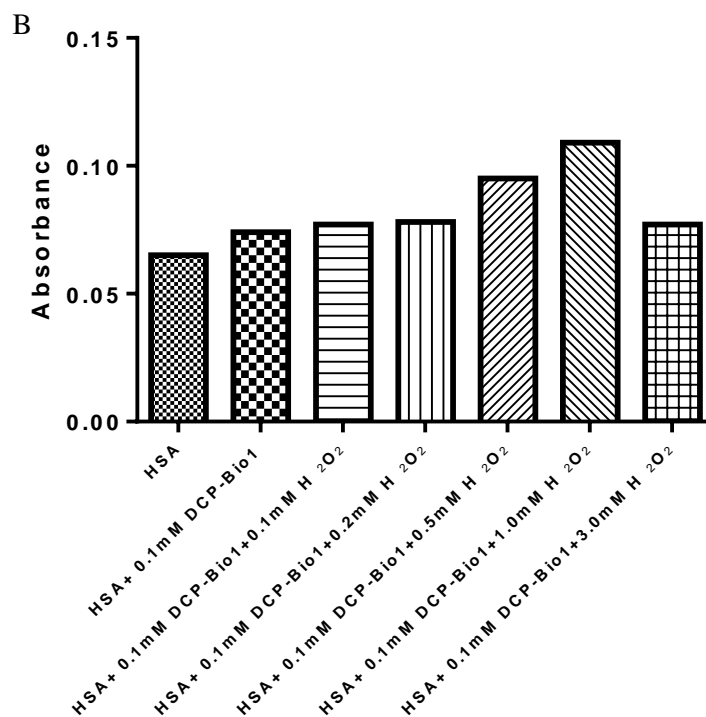


Figure 3.3: Increasing hydrogen peroxide concentration increases sulphenic acid modifications in HSA. HSA was treated with increasing concentrations of hydrogen peroxide while keeping the DCP-Bio1 concentration constant. The plates are washed 6 times with washing buffer to remove excess reagent and incubated with 50 μ L of streptavidin-HRP (1:10,000 in 1% BSA in PBS) for 1 hour at 37 $^{\circ}$ C. The plate was aspirated and washed 3 times with washing buffer and developed with 50 μ L OPD substrate (10 mL citrate phosphate buffer, 20 mg of o-phenylenediamine tablet with 10 μ L 8.8 M hydrogen peroxide) and incubated at 37 $^{\circ}$ C for 15 minutes in the dark. The reaction was stopped by adding 2 M H₂SO₄ and the absorbance was read at 490 nm on the spectrometric plate reader (BioTek). The experiment is representative from 2 independent experiments performed in triplicate.

To determine the effects of hydrogen peroxide further experiments were performed using two concentrations of DCP-Bio1 (0.1 mM and 1 mM) which yielded similar results. When HSA was incubated with just hydrogen peroxide or the probe on its own, there was no increase in the absorbance. However, when the protein was incubated with 1 mM hydrogen peroxide and 0.1 mM DCP-Bio1 as well as 1 mM DCP-Bio1 there was an increase in absorbance at 490 nm indicative of sulphenic acid formation in human serum albumin. When the HSA was oxidised with 3 mM hydrogen peroxide the absorbance was lower than with 1 mM hydrogen peroxide.(Figure 3.4).

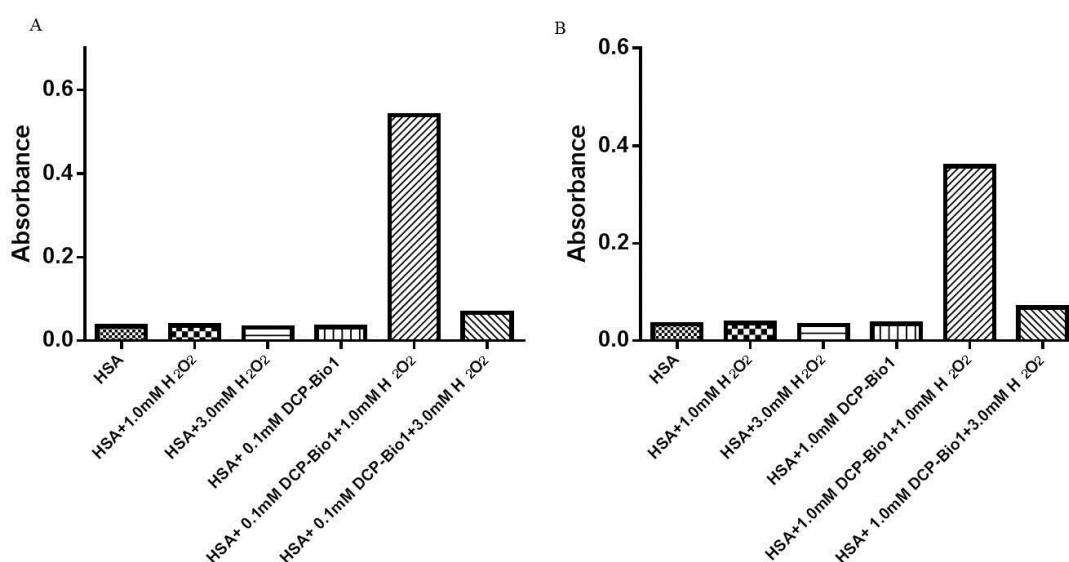


Figure 3.4: Effect of DCP-Bio1 concentration on detection of sulphenic acid formation in HSA with hydrogen peroxide. Detection with A) 0.1 mM DCP-Bio1, and B) with 1.0 mM DCP-Bio-1. Excess reagent was removed and incubated with 50 μ L of streptavidin-HRP (1:10,000 in 1% BSA in PBS) for 1 hour at 37 $^{\circ}$ C. Prior to developing with 50 μ L OPD substrate (10 mL citrate phosphate buffer, 20 mg of O-phenylenediamine tablet with 10 μ L 8.8 M hydrogen peroxide) and incubated at 37 $^{\circ}$ C for 15 minutes in the dark. The reaction was stopped by adding 2 M H₂SO₄ and the absorbance was read at 490 nm on the spectrometric plate reader (BioTek).The figure shows the results from one experiment performed in triplicate.

The effects of the order and timings of DCP-Bio1, H₂O₂ and catalase addition and the number of washing steps on sulphenic acid detection were examined. In the first experiment (**Figure 3.5**, bars 1-3) HSA was dissolved in carbonate buffer to 20 µg/mL, added to a Nunc maxisorb 96 well plate in triplicate (50 µL) and incubated for 1 hour at 37 °C. After washing, the plates were incubated with hydrogen peroxide for 4 minutes followed by the addition of the probe for 30 minutes on ice without further washing. In the second experiment (**Figure 3.5**, bars 4-6) the wells were treated as above with the addition of catalase for 1 minute before adding the probe, again without any washing steps. Experiment 7-9 (**Figure 3.5**) was carried out by adding the probe and hydrogen peroxide to HSA on the plate at the same time and incubating for 30 minutes on ice. The final experiment (**Figure 3.5**, 10-12) was done by adding hydrogen peroxide to HSA for 4 minutes, washing the plate 3 times and adding DCP-Bio1 for 30 minutes on ice. There is an increase in the absorbance after addition of hydrogen peroxide in all of the experiments with the highest absorbance in experiment 6 where catalase is present.

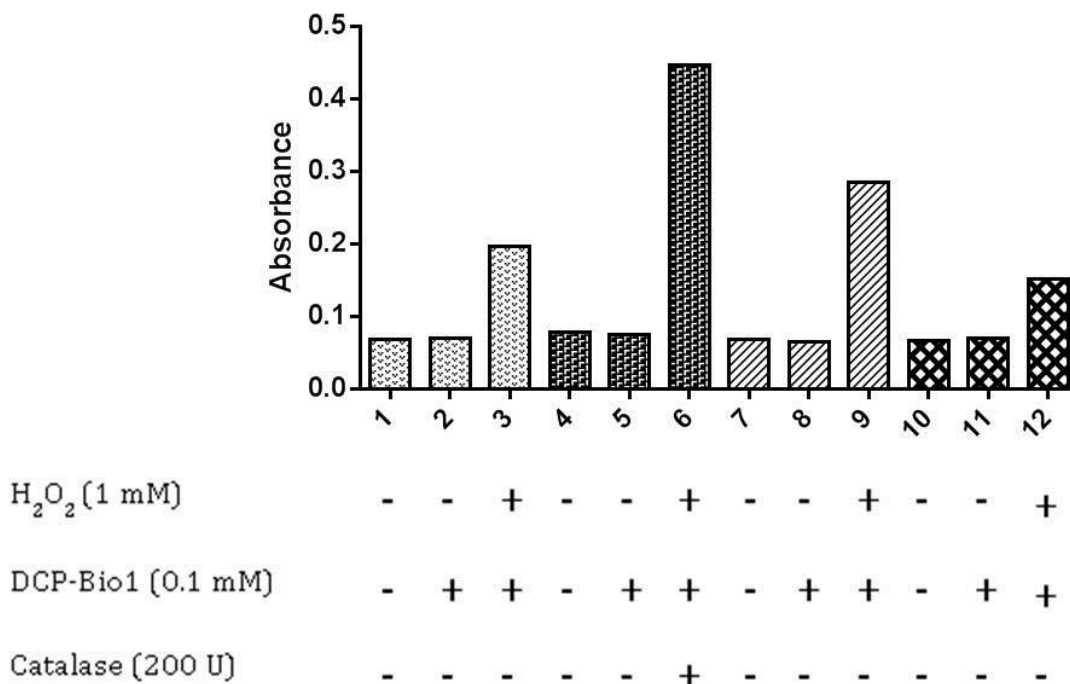


Figure 3.5: Treatment conditions affect the detection of sulphenic acids. HSA was either treated with 1.0 mM hydrogen peroxide for 4 minutes and 0.1 mM DCP-Bio1 for 30 minutes on ice without a wash step between the addition of reagents (1-3), treated with hydrogen peroxide for 4 minutes followed by the addition of catalase for 1 minute and addition of DCP-Bio1 without the wash step (4-6), addition of hydrogen peroxide and DCP-Bio1 at the same time and incubating for 30 minutes on ice (7-9) and addition of hydrogen peroxide for 4 minutes washing the plate 3 times followed by the addition of DCP-Bio1 for 30 minutes on ice. The plates are washed 6 times with washing buffer to remove excess reagent and incubated with 50 μ L of streptavidin-HRP (1:10,000 in 1% BSA in PBS) for 1 hour at 37 $^{\circ}$ C. The plate was aspirated and washed 3 times with washing buffer and developed with 50 μ L OPD substrate (10 mL citrate phosphate buffer, 20 mg of o-phenylenediamine tablet with 10 μ L 8.8 M hydrogen peroxide) and incubated at 37 $^{\circ}$ C for 15 minutes in the dark. The reaction was stopped by adding 2 M H₂SO₄ and the absorbance was read at 490 nm on the spectrometric plate reader (BioTek). The experiment is representative from one experiment performed in triplicate.

3.4.3 Visualisation of sulphenic acid formation on HSA by dot blot:

To determine if it is possible to visualise sulphenic acid modifications by western blotting a preliminary dot blot was performed using DCP-Bio1 that can detect sulphenic acid modifications. 0.5 mM HSA was untreated, treated with 1 mM hydrogen peroxide or 1 mM hydrogen peroxide and 1 mM DCP-Bio1 for 30 minutes on ice. The dot blot was performed as described in materials and methods (3.3.4) and visualised with ECL reagent on the G-box transilluminator. **Figure 3.6** shows a streptavidin peroxidase signal indicative of DCP-Bio1 binding to sulphenic acid in dot 3. Further experiments were done using SDS-PAGE and western blotting to optimise conditions for sulphenic acid formation.

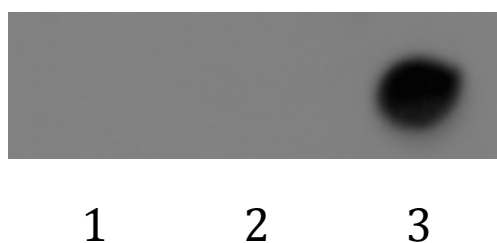
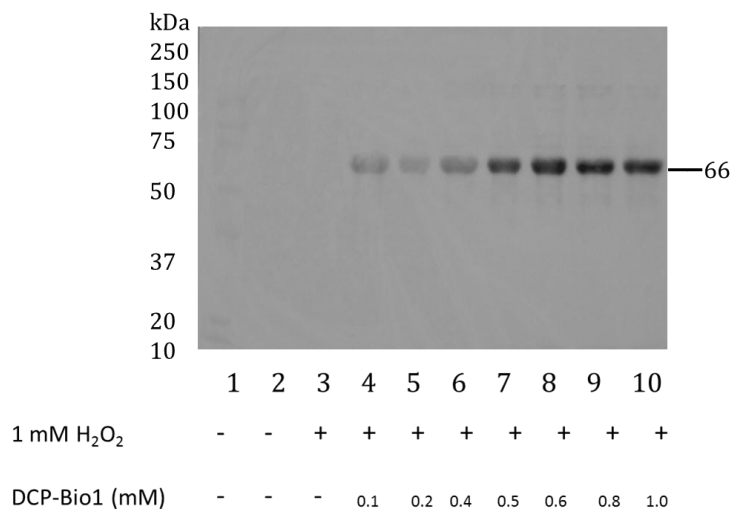


Figure 3.6: Sulphenic acid formation can be detected on dot blot. Protein spots were;
1-0.5 mM HSA
2-0.5 mM HSA+1.0 mM H₂O₂
3-0.5 mM HSA+1.0 mM H₂O₂ + 1.0 mM DCP-Bio1.
PVDF membrane was soaked in methanol for 10 minutes and washed for 5 minutes in TTBS. 2 μ L of the samples were spotted on to a small spot and left to dry. The membrane was then blocked overnight with 3% BSA in TTBS and washed 6 times at 15 minute intervals with 20 mL of TTBS. The blot was incubated with streptavidin-HRP (1:20,000) in TTBS for 2 hours at room temperature. It was washed 6 times with 20 mL TTBS at 5 minute intervals and visualised with ECL reagent. The blot is a representative of two independent experiments.

3.4.4 Effect of different concentrations of DCP-Bio1 on sulphenic acid formation in HSA:

As shown in **Figure 3.7A**, when incubating HSA with increasing concentrations of DCP-Bio1 (0.1 mM, 0.2 mM, 0.4 mM, 0.5 mM, 0.6 mM, 0.8 mM, 1.0 mM) the intensity of the bands increase until lane 7 (0.5 mM HSA + 1 mM H₂O₂ + 0.5 mM DCP-Bio1) after which the intensity of the bands remained the same. On the basis of these results 0.5 mM DCP-Bio1 was used for subsequent experiments.

A



B

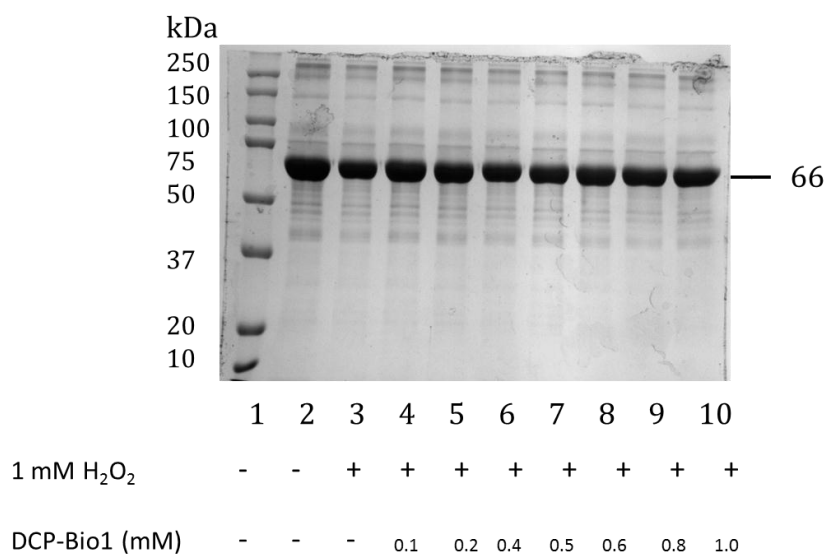
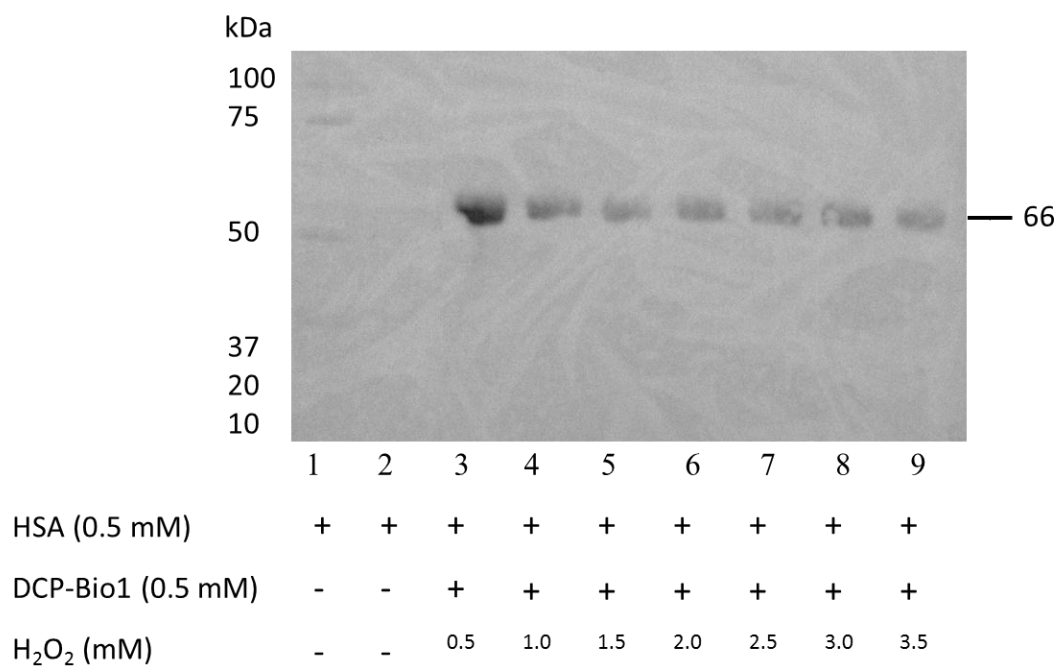


Figure 3.7: HSA sulphenic acid modifications with different concentrations of DCP-Bio1. The samples were resolved by 10% SDS-PAGE for western blot analysis with streptavidin-HRP against DCP-Bio1 detection as described in materials and methods. The blot is representative of 2 independent experiments. **A) Western blot B) Coomassie-stained gel for equal loading of the protein.**

3.4.5 HSA treatment with different concentrations of hydrogen peroxide:

HSA (0.5 mM) was either untreated or treated with increasing concentrations of hydrogen peroxide (0.5 mM, 1.0 mM, 1.5 mM, 2.0 mM, 2.5 mM, 3.0 mM, 3.5 mM) keeping the DCP-Bio1 concentrations constant at 0.5 mM. **Figure 3.8A** shows that the intensity of the bands has increased with 0.5 mM H₂O₂ compared to control. Band labelling was evident after treatment with concentrations of greater than 1 mM H₂O₂ but was lower than observed with 0.5 mM H₂O₂ treated HSA. Therefore further experiments were done with hydrogen peroxide concentrations ranging from 0.1 mM-0.8 mM. **Figure 3.8B** indicates that after treating HSA with 0.5 mM hydrogen peroxide and 0.5 mM DCP-Bio1 (lane 6) the band intensity does not increase. Therefore for subsequent experiments 0.5 mM hydrogen peroxide was used.

A



B

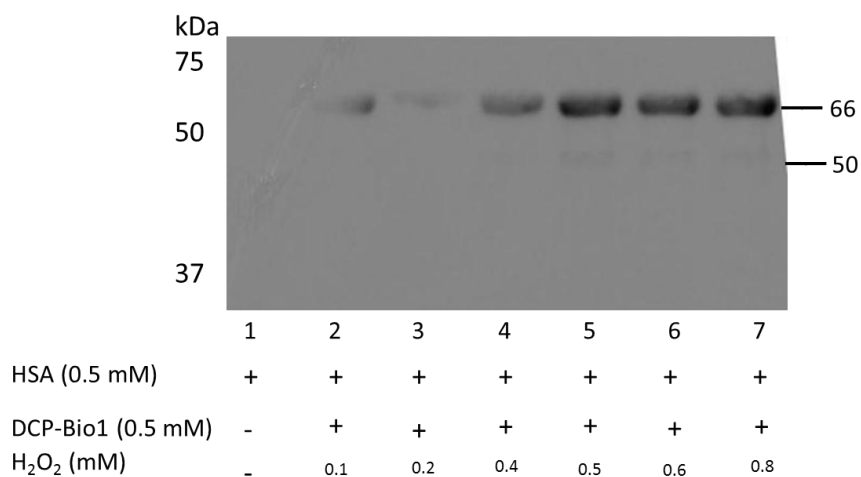


Figure 3.8: Increasing hydrogen peroxide concentrations increases sulphenic acid modifications in HSA. 0.5 mM HSA was either untreated or treated with different concentrations of hydrogen peroxide and 0.5 mM DCP-Bio1 and incubated on ice for 30 minutes. The samples were loaded onto 10% polyacrylamide gel and transferred onto a PVDF membrane as described before.

3.4.6 The effect of iodoacetamide on sulphenic acid formation in HSA:

To confirm the specificity of the probe, thiols in HSA were blocked to determine whether this would stop the recognition of sulphenic acid on HSA by DCP Bio1. HSA was prepared as described in materials and methods (3.3.1) and then either left untreated (**Figure 3.9**, lane 2) treated with 0.5 mM hydrogen peroxide (**Figure 3.9**, lane 3), HSA treated with 0.5 mM DCP-Bio1 (**Figure 3.9**, lane 4), HSA treated with 0.5 mM hydrogen peroxide and 0.5 mM DCP-Bio1 (**Figure 3.9**, lane 5), HSA treated with 10 mM iodoacetamide (**Figure 3.9**, lane 6), HSA treated with 0.5 mM hydrogen peroxide and 0.5 mM DCP-Bio1 on ice for 30 minutes and treated with 10 mM IAM on ice for 10 minutes to block thiols (**Figure 3.9**, lane 7) or treated with 10 mM IAM for 10 minutes on ice followed by 0.5 mM hydrogen peroxide and 0.5 mM DCP-Bio1 on ice for 30 minutes (**Figure 3.9**, lane 8). There are no bands visible for lane 2 or 3 as they both do not have the probe present. There is a prominent band in lane 4 indicative of sulphenic acid formation despite there being no addition of hydrogen peroxide. When IAM is added prior to the treatment of hydrogen peroxide and DCP-Bio1 there is no band visible, which suggests that there is no detection of sulphenic acid by DCP-Bio1 (**Figure 3.9**, lane 8). However when IAM is added after treating HSA with hydrogen peroxide, DCP-Bio1 binding is still observed, albeit to a lower level, which is visible in lane 7.

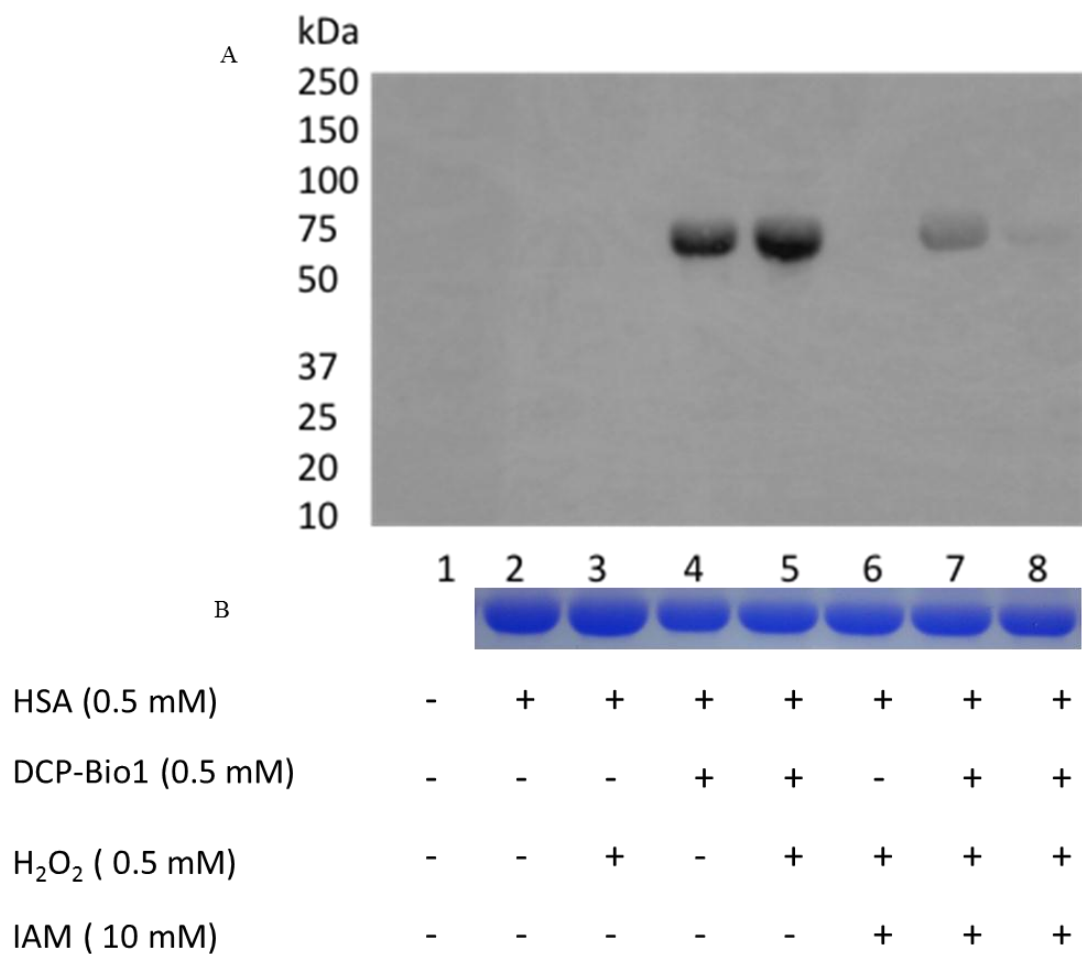


Figure 3.9: Sulphenic acid formation is prevented by the addition of iodoacetamide. A. Western Blot and **B.** coomassie stain for equal loading. Samples were prepared as described above and resolved on a 10% polyacrylamide gel and transferred on to a PVDF membrane. The membrane was probed with avidin-HRP (1:20,000) and developed with ECL reagent. The blot is a representative of 2 independent experiments.

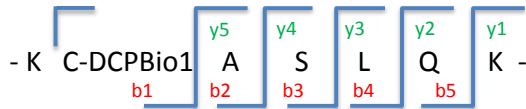
3.4.7 Detection of sulphenic acid modifications of HSA by mass spectrometry:

To identify oxidative modifications of HSA samples were treated with hydrogen peroxide and DCP-Bio1 as described in the materials and methods section above (3.3.7) followed by in gel tryptic digestion (3.3.8). The samples were subjected to mass analysis and two peaks observed ($m/z = 657.29, 770.38$) indicate the formation of adduct at the cysteine with DCP-Bio1. (**Figure 3.10**)

A

1	MKVVTFISLL	FLFSSAYSRG	VFRRDAHKSE	VAHRFKDLGE	ENFKALVLIA
51	FAQYLQQCPF	EDHVKLVNEV	TEFAKTCVAD	ESAENCDKSL	HTLFGDKLCT
101	VATLRETYGE	MADCCAQKQP	ERNECFLQHK	DDNPNLPRLV	RPEVDVMCTA
151	FHDNEETFLLK	KYLVEIARRH	PYFYAPPELLF	FAKRYKAAFT	ECCQAADKAA
201	CLLPKLDLRL	DEGKASSAKQ	RLK CASLQK F	GERAFKAWAV	ARLSQRFPKA
251	EFAEVSKLVT	DLTKVHTECC	HGDLLCADD	RADLAKYICE	NQDSISSKLLK
301	ECCEKPLLEK	SHCIAEVEND	EMPADLPSLA	ADFVESKDVC	KNYAEAKDVF
351	LGMFLYEYAR	RHPDYSVVLL	LRLAKTYETT	LEKCCAAADP	HECYAKVFDE
401	FKPLVEEPQN	LIKQNCLEFE	QLGEYKFNQA	LLVRYTKKVP	QVSTPTLVEV
451	SRNLGKVGSK	CCKHPEAKRM	PCAEDYLSVV	LNQLCLEHEK	TPVSDRVTKC
501	CTESLVNRRP	CFSALEVDET	YVPKEFNAET	FTFHADICTL	SEKERQIKKQ
551	TALVELVKHK	PKATKEQLKA	VMDDFAAFVE	KCKKADDKET	CFAEEGKKLV
601	AASQAALGL				

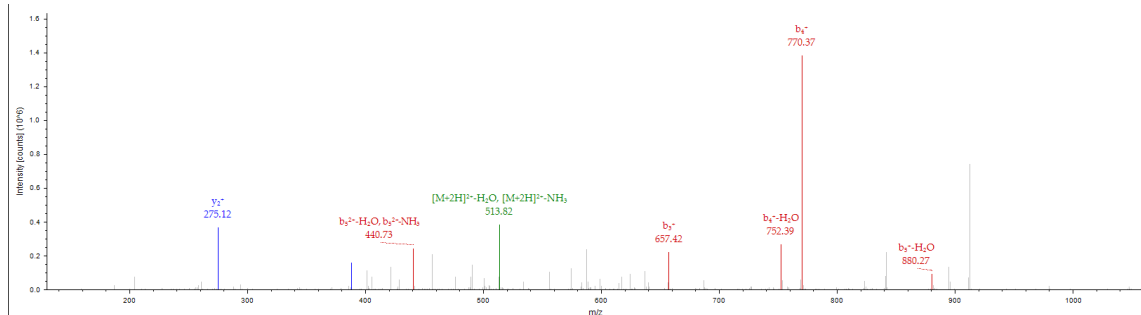
B



C

Fragment Matches						
Value Type: Theo. Mass [Da]						
Ion Series	Neutral Losses		Precursor Ions			
#1	b ⁺	b ²⁺	Seq.	y ⁺	y ²⁺	#2
1	499.22788	250.11758	C-DCP			6
2	570.26500	285.63614	A	546.32461	273.66594	5
3	657.29703	329.15215	S	475.28749	238.14738	4
4	770.38110	385.69419	L	388.25546	194.63137	3
5	898.43968	449.72348	Q	275.17139	138.08933	2
6			K	147.11281	74.06004	1

D



E

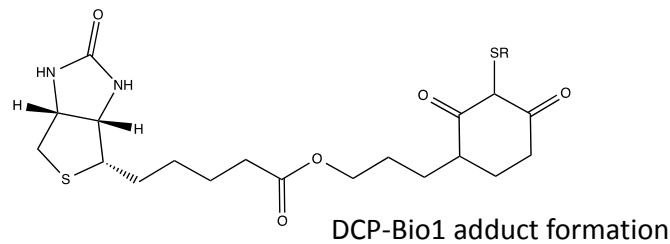


Figure 3.10: The formation of sulphenic acid detected by mass spectrometry. A) peptide sequence of HSA, B) peptide sequence with modified cysteine, C) fragment matches of modified sequence, D) ms/ms showing b and y ion peaks, E) DCP-Bio1 adduct formation with a thiol.

3.5 Discussion:

This chapter has described optimisation of a method for sulphenic acid formation in human serum albumin and of two methods for its detection using the biotinylated probe DCP-Bio1. Mass spectrometry experiments on glutathione showed that cysteine favours disulphide bond formation (m/z 614.87) in the presence of hydrogen peroxide and that sulphenic acid was not formed under the conditions shown here. This was also observed when performing dot blots using glutathione with DCP-Bio1, (data not shown) using similar conditions described for HSA in 3.4.3. Glutathione is a small thiol-containing molecule that is important in the regulation of cellular reducing environment. In the presence of oxidants such as hydrogen peroxide it will form glutathione disulphide (GSSG) with glutathione peroxidase as a substrate (139)

The results from the modified ELSPA with HSA could imply that there was an increase in sulphenic acid formation until the hydrogen peroxide concentration was increased to 1 mM and that the addition of more oxidant causes sulphenic acid to oxidise to its higher oxidation states such as sulphinic and sulphonic acids, which were not detectable by DCP-Bio1. When the concentration of the DCP-Bio1 was increased to 1 mM a similar result was observed. Results from the ELSPA also show that simultaneous addition of DCP-Bio1 with H_2O_2 resulted in more sulphenic acid detection; the absorbance was higher than that of the experiment where a wash step was introduced. This protocol was adopted for future HSA oxidation experiments. Addition of catalase to stop the oxidation of HSA gave the highest absorbance value. Although a lower absorbance was expected, as fewer sulphenic acids would be formed, this could be due to the fact that catalase also contains cysteines some of which could have been oxidised to form sulphenic acids.

Before performing SDS-PAGE and western blotting a simple dot blot experiment was performed on HSA to determine whether sulphenic acid modifications would be detectable. When 0.5 mM HSA was treated with hydrogen peroxide and 1.0 mM DCP-Bio1 a spot was observed which is indicative of sulphenic acid formation. Next, experiments were performed

to investigate the concentration of DCP-Bio1 needed to capture all the modified sulphenic acids in 0.5 mM HSA. With increasing concentrations of the probe the band intensity increased until 0.5 mM of the probe was added after which the intensity remained the same. This could be an indication that all the sulphenic acid modified HSA has been detected by the DCP-Bio1. To determine the concentrations of hydrogen peroxide needed to modify cysteine residues to sulphenic acids using 0.5 mM DCP-Bio1, increasing amounts of hydrogen peroxide were added to 0.5 mM HSA keeping all other conditions the same. The band intensity decreased when the concentrations were increased further than 0.5 mM H₂O₂. These observations imply that between 0.5 mM-1 mM hydrogen peroxide was needed to oxidise sulphenic acids of HSA and at higher concentrations it will over oxidise. 0.5 mM hydrogen peroxide was needed to oxidise all of the thiols to sulphenic acids as the band intensity did not increase after adding higher concentrations of H₂O₂. When increasing concentrations of hydrogen peroxide was used to oxidise HSA the intensity of the bands on the western blots increased until hydrogen peroxide and HSA were at a 1:1 ratio. Over-oxidation of HSA led to a decrease in absorption in the ELSPA as well as a decrease in band intensity on the western blots. Previous studies done by Carballal and co-workers suggest that the reaction between hydrogen peroxide and HSA proceeds with a 1:1 stoichiometry (64). They performed experiments using 0.5 mM HSA and adding hydrogen peroxide at increasing concentrations and quantifying the thiols after the reaction was completed. The advantage of the method used here over NBD-Cl used previously is that DCP-Bio1 is specific towards sulphenic acids and also the fact that because of its biotin tag it can be visualised by western blotting. Using different concentrations of the probe led to the conclusion that in order to capture all the sulphenic acids formed 0.5 mM DCP-Bio1 had to be used with 0.5 mM HSA in an equimolar ratio. Therefore it can be concluded that HSA sulphenic acid is formed and DCP-Bio1 reacts to a 1:1 ratio. To determine the effects of alkylating agents such as IAM on the formation of sulphenic acid experiments were done adding excess of IAM before the treatment of HSA with hydrogen peroxide or DCP-Bio1. The absence of a band is indicative that the thiol has been blocked by IAM preventing it

from being oxidised to the sulphenic acid. Noting the liability of HSA thiol groups to oxidation, although there was no H_2O_2 present a DCP-Bio1 bound band was observed which could be due to oxidation of HSA by air. It is also interesting to note that the sulphenic acid and probe adduct formation is stable even in the presence of reducing agents such as 2-mercaptoethanol which is present in the Laemmli buffer used to load samples on to the gels. Work by Allison has demonstrated that the covalent bond between dimedone and sulphenic acid cannot be broken by reducing agents (140). As DCP-Bio1 is a biotinylated dimedone-like molecule, it is not surprising that the same trend is observed.

Previously, others have trapped the sulphenic acid with the nucleophilic reagent dimedone and after mass spectral analyses have confirmed that the site of modification is Cys34, which is the redox active thiol of human serum albumin (118). Although sulphenic acids are considered to be unstable and intermediates to higher oxidation states such as sulphinic and sulphonic acids, the microenvironment plays an important role in the stabilisation of sulphenic acids. Nevertheless, research by Carballal *et al* suggests that HSA-SOH is remarkably stable. The three-dimensional structure of HSA provided by X-ray diffraction confirms that the Cys34 is situated in a hydrophobic crevice, which is partially protected against solvents. The fact that there are no other thiols adjacent to Cys34 and side chains of Pro35 and Val77 help in preserving the oxidised HSA (110). Finally, the imidazole ring from His39, the hydroxyl group of Tyr84 and the carboxylate group of Asp38 could also help in the stabilisation of sulphenic acid at Cys34 with hydrogen bond and electrostatic interactions (141, 142, 143).

Mass spectrometry also suggests that sulphenic acid modifications occur at the cysteines of albumin. Although the expected modification is at the Cys34 the observed modification here was at cysteine 200. This cysteine usually takes part in intramolecular disulphide formation. A possible explanation for finding this modification could be that when the albumin is reduced with 2-ME and desalted using a spin column, some of the reducing agent remained in the sample while the H_2O_2 was added leading to some of the disulphide bonds not

reforming but instead becoming available, oxidised to sulphenic acids by peroxide and then reacting with DCP-Bio1.

In conclusion HSA reacts with hydrogen peroxide and DCP-Bio1 in a 1:1:1 ratio indicating that sulphenic acid formation occurs at one cysteine. If high concentrations of hydrogen peroxide are present, sulphenic acids may over oxidise and not be detectable by the probe. The sulphenic acid of human serum albumin could be a central intermediate in thiol oxidation pathways and further work needs to be done to understand properties and reactivity of biological sulphenic acid.

Chapter 4.0 Protein sulphenic acid formation in Jurkat T cells and human CD4+ T cells

4.1 Preface:

The purpose of this chapter was to investigate protein sulphenic acid modifications in Jurkat T cells and human CD4⁺ T cells under oxidative and activating conditions. Previous studies have demonstrated that intra- and extra-cellular antioxidant concentration can play a key role in T cell thiol content. To investigate this buthionine sulfoximine (BSO) has been used to manipulate the endogenous antioxidant glutathione (GSH) in human CD4⁺ T cells and surface protein sulphenic acid and thiol levels (using flow cytometry and DTNB assay) have been examined. T cells were treated with BSO and activated by lectins such as the lectin phytohaemagglutinin-L (PHA-L). Any effect on sulphenic acid formation of proteins was investigated using the commercially available probe, DCP-Bio1 that specifically interacts with sulphenic acids. Techniques such as SDS-PAGE, western blotting and confocal microscopy were used to identify T cell protein modification.

4.2 Introduction:

If the balance between the production of ROS and the removal is disrupted, cells are said to be under oxidative stress, which can lead to irreversible changes in bio molecules (144). For cells to function properly a redox balance needs to be maintained within the cellular environment (145). The redox balance in cells is maintained through three major redox couples; NAD^+ -NADH; NADP^+ -NADPH and GSH-GSSG (150). GSH, which is a cysteine containing tripeptide, is the most abundant non-protein thiol. GSH and its oxidised dimer, GSSG play an important role in the maintenance of the redox state and the thiol groups in cells. GSH reacts with some ROS such as hydrogen peroxide and is converted to its oxidised GSSG. It is ultimately reduced back to GSH by GSH reductase and NADPH to maintain cellular GSH levels. The ratio of GSH/GSSG is very important to cell survival and is a sensitive indicator to oxidative stress (146). GSH synthesis is dependent on the enzyme gamma-glutamyl cysteinyl ligase (GCL) and cysteine availability. A decrease in protein thiols, due to oxidation leads to an Nrf-2 mediated transcriptional increase in the synthesis of GSH to restore the redox balance (147).

The main role of T cells is to recognise foreign matter and promote efficient removal of them and therefore they play a key role in the effective adaptive immune response (107). The functions of T cells are greatly influenced by alterations in the redox balance. Lymphocytes require a reducing environment for optimal activation and proliferation which relies on the expression and secretion of IL-2 to affect T cell surface CD25 in an autocrine manner (148, 149). It has been shown that an increase of cell surface thiols increases T cell activation and proliferation in vitro and in vivo. Therefore the presence of ROS can have an inhibitory effect on T cell activity (149). However if APCs are present that produce GSH, ROS can help mediate T cell activation, thus maintaining the redox balance (144). Membrane proteins that reside on the cell surface of T cells contain many cysteine (Cys) residues that can be oxidised if there is an increase of ROS production, if there is a lack of free thiols on proteins or peptides such as albumin, GSH and thioredoxin, or if there is insufficient enzyme activity to

reduce the oxidised GSSG or thioredoxin back to the reduced forms (108). Therefore changes in the redox balance of extracellular proteins can result in modifications not only in proteins that act as redox sensors but also in receptors and can affect cell activation by ligands (150,151). Therefore, a decrease in the function of NADPH oxidase will lead to a decrease in the production of ROS. This results in changes in the redox balance of immune cells and could lead to defective immune regulation (152).

Although ROS can modify proteins and other macromolecules irreversibly, reversible modifications of cysteine play important roles in events such as cell signalling. Phosphatases such as PTEN (phosphatase and tensin homologue deleted on chromosome 10) and SHP-2 (Scr homology 2 domain-containing phosphatase) and transcription factors such as AP-1 and NF- κ B undergo reversible cysteine oxidation that regulates their function (153, 154, 155, 156). Therefore it is important to understand the role of sulphenic acid modification in T cells, and how these protein modifications change under oxidative stress and activation.

The aims of this chapter are as follows:

1. To optimise conditions to detect protein sulphenic acid modifications in Jurkat T cells
2. To investigate the effect of BSO on GSH levels, surface thiols and sulphenic acid modifications of human CD4⁺ T cells.
3. To explore activation of T cells using phytohaemagglutinin-L (PHA-L) at different concentrations.
4. To examine the effect of PHA-L on sulphenic acid formation in primary CD4⁺ T cells.

4.3 Materials and Methods:

4.3.1 Isolation of peripheral blood mononuclear cells (PBMC):

Venous blood (20 mL) from consenting volunteers was collected into Vacuette blood collection tubes (Greiner Bio-one) containing EDTA. The blood was then transferred to a 50 mL centrifuge tube and 30 mL of PBS containing 0.1% BSA was added. The above solution (25 mL) was layered carefully over 11 mL of Lymphoprep (Beckman Coulter). The blood was separated by centrifugation at $160 \times g$ for 20 minutes at 20°C . A typical separation is shown in **Figure 4.1**. The top layer of plasma (~10 mL) was removed and discarded and the samples were centrifuged at $381 \times g$ for 20 minutes at 20°C . The PBMCs were removed from two tubes using a sterile pasteur pipette and transferred to a 50 mL centrifuge tube. PBS containing 0.1% BSA was added to create a cell suspension with a final volume of until 50 mL and centrifuged at $500 \times g$ for 10 minutes at 20°C to wash the cells. The supernatant was discarded and the pellet was resuspended in 10 mL PBS containing 0.1% BSA and transferred into a 15 mL centrifuge tube for a final wash. The cells were diluted ten times for cell counting using a haemocytometer.

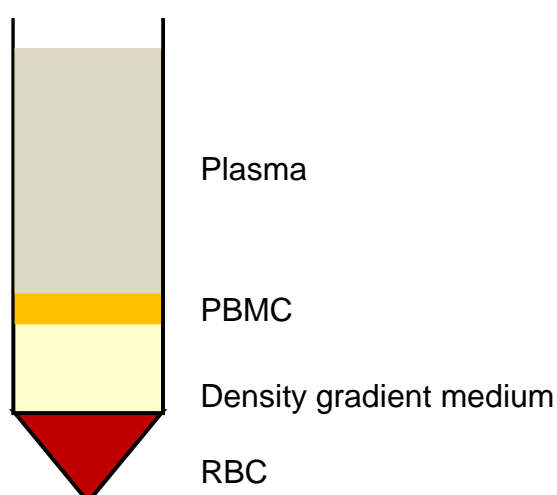


Figure 4.1: Schematic representation of centrifuged whole blood in lymphoprep® density gradient with Red blood cells (RBC), peripheral blood mononuclear cells (PBMC)

4.3.2 Negative isolation of human CD4+ T cells:

4.3.2.1 Reagents:

Reagent	Description	Volume per 1×10^7 PBMC
1. Isolation buffer	Ca ²⁺ Mg ²⁺ free PBS supplemented with 0.1% BSA and 2 mM EDTA	100 μ L
2. Antibody mix (Human CD4+ T Cells)		20 μ L
3. FBS		20 μ L
4. Depletion Dynabeads		100 μ L

Table 4.1: Reagents and quantities used for isolation of CD4+ T cells

Isolated PBMCs were resuspended at 1×10^7 cells in isolation buffer (100 μ L). FBS (20 μ L) and antibody mix (20 μ L) (Dynabeads untouched human CD4 T cells kit, Invitrogen) was added and incubated for 20 minutes at 4 °C. The cells were washed by adding isolation buffer (2 mL), mixed and then centrifuged at 300 x g for 8 minutes at 4 °C. The supernatant was discarded and the cells were resuspended in isolation buffer (100 μ L). Meanwhile MyOne Dynabeads (Dynabeads untouched human CD4 T cells, Invitrogen; 100 μ L) were washed by resuspending in 1mL of isolation buffer. The supernatant was discarded after placing the sample in a magnet. The washed beads were resuspended in isolation buffer (100 μ L) and added to the cells and incubated for 15 minutes at room temperature with gentle tilting and rotation. Isolation buffer (2 mL) was added and the bead bound cells were resuspended by thoroughly pipetting 10 times using a pipette with a narrow tip opening.

After placing the micro centrifuge tubes in the magnet for 2 minutes the supernatant containing the untouched human CD4+ T cells were isolated. The bead-bound cells were resuspended in isolation buffer (2 mL) and the supernatant was again collected and combined with the previously isolated untouched T cells and counted on the haemocytometer prior to further experiments.

4.3.3 Flow cytometric assay for cell surface CD4+ analysis:

Human CD4+ T cells were washed twice with PBS (500 μ L) and resuspended to 1×10^6 cells/mL in RPMI-1640 media supplemented with 10% FBS and 1% penicillin/streptomycin for 30 minutes on ice. Phycoerythrin (PE) labelled anti-CD4 monoclonal antibody (1 μ L, Abcam) or negative isotype control (2 μ L, Abcam) were added to 100 μ L of cell suspension and incubated on ice in the dark for 30 minutes. The samples were analysed on the Cytomics TM FC500 flow cytometer (Beckman-Coulter, Miami, USA). Cells were gated based on the forward scatter (FS)/side scatter (SS) and applying FL2 positive gate. The data was collected for 10000 events against forward scatter (FS).

4.3.4 Modulation of cellular CD4+ T cell thiol levels:

CD4+ T cells (1×10^6 cells/mL) were treated with 25 μ M buthionine sulfoximine (BSO) for 24 hours to investigate whether decreasing GSH levels intracellularly has any effect on surface thiol levels and sulphenic acid modifications.

4.3.5 Preparation of cells for flow cytometry to detect surface thiols:

0.5×10^6 BSO-treated and control cells were collected into independent 1.5 mL microcentrifuge tubes and were centrifuged for 2 minutes at 400 x g in the microcentrifuge (Eppendorf Centrifuge 5415D). The supernatants were removed and the cell pellet was washed twice with PBS (500 μ L) by centrifugation at 400 x g for 2 minutes. The cells were resuspended in PBS (500 μ L). Maleimide (1 mM, 9 μ L) and maleimide Alexafluor-488C5 (1 mM, 1 μ L) was added to each tube and incubated at 37 $^{\circ}$ C for 30 minutes in the dark. The samples were centrifuged at 400 x g for 2 minutes and washed three times with PBS (500 μ L) each. The pellet was resuspended in PBS (500 μ L) and the samples were analysed on the Cytomics TM FC500 flow cytometer ((Beckman-coulter, Miami, USA). Cells were gated

based on the FS/SS using FL1 and results and data was collected for 5000 events against forward scatter (FS).

4.3.6 Effect of BSO on surface thiols using 5,5'-dithiobis(2-nitrobenzoic acid) (DTNB) assay:

DTNB is a water-soluble non-cell permeable compound that is used to quantify sulphhydryl groups. DTNB reacts with a free sulphhydryl group to yield a mixed disulphide and 2-nitro-5-benzoic acid (TNB⁻), which is a measurable yellow coloured product (**Figure 4.2**).

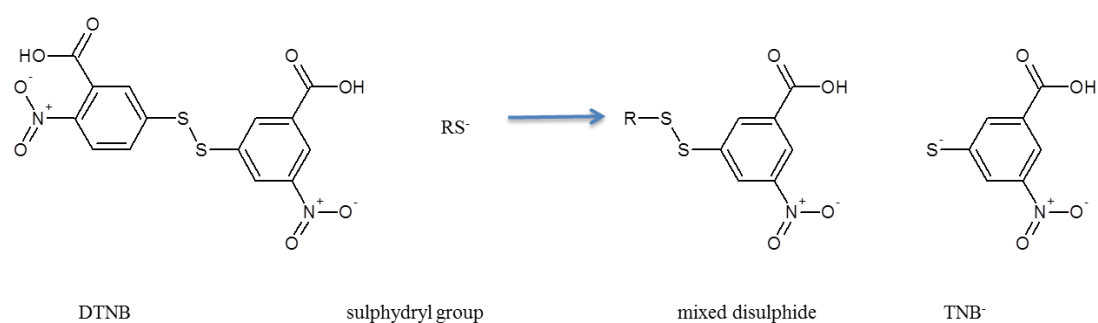


Figure 4.2: The reaction between a thiol and 5,5'-dithiobis(2-nitrobenzoic) acid. In the presence of a free sulphhydryl group the DTNB reacts to yield the yellow TNB⁻

DTNB is used to determine the cell surface thiol levels. The method was adapted from the method described by Laragione *et al* (157). CD4⁺T cells (1×10^6 cells/ mL) were either treated with or without 25 μ M buthionine sulfoximine (BSO) for 24 hours. The cells were washed twice in PBS (1 mL), centrifuged at 1200 x g for 5 minutes in the microcentrifuge (Eppendorf centrifuge 5415D) and resuspended in 1 mL of PBS. The cells (1.5×10^5 cells) were then incubated in a 96 well plate with DTNB (200 μ M) for 20 minutes in the dark at room temperature. All the samples were centrifuged at 1200 x g for 5 minutes and the supernatants were collected after the incubation time and the absorbance read at 405 nm using a spectrophotometric plate reader (BioTek). The results were calculated from a standard curve using freshly prepared N-acetyl cysteine (NAC) where concentrations of the calibration curve ranged from 0-100 μ M.

4.3.7 Cell lysate preparation for GSH assay:

Cells (2×10^6 cells/mL) were collected in 1.5 mL micro centrifuge tubes and centrifuged at $6600 \times g$ (Eppendorf Centrifuge 5415D) for 1.5 minutes. The supernatants were removed and PBS (0.5 mL) was added to resuspend the pellet. The tubes were centrifuged at $6600 \times g$ for 1.5 minutes and the PBS was removed making sure that the pellet was completely dry. SSA (3.33 μ L) was then added to the micro centrifuge tubes to precipitate the proteins and immediately centrifuged at $13000 \times g$ for 1.5 minutes. Stock buffer (96.6 μ L) was added and the tubes were vortexed and centrifuged as above. The supernatants were transferred into new micro centrifuge tubes and samples were analysed for GSH as described in chapter 2 and total protein content (BCA assay) or frozen at $-80 \text{ }^\circ\text{C}$.

4.3.8 Activation of T cells by PHA-L and PHA-P:

CD4⁺ T cells (1×10^6 cells/mL) were either untreated or treated with 1 μ g/mL PHA-L, 5 μ g/mL PHA-L, 1 μ g/mL PHA-P and 5 μ g/mL PHA-P for 24 hours in at $37 \text{ }^\circ\text{C}$ in a 5% CO₂/95% air humidified atmosphere. The cells were collected to 1.5 mL microcentrifuge tubes and centrifuged $400 \times g$ for 2 minutes. The supernatants were collected and analysed for interleukin-2 (IL-2) secretion. The cells were resuspended in 1 mL of Optilyse® C lysing solution (Beckman Coulter, France) to be used for flow cytometry experiments.

4.3.9 Quantification of interleukin-2 (IL-2):

The supernatants that were collected from activated and control T cells were analysed by a standard enzyme linked immunosorbent assay (ELISA). The IL-2 detection and quantification was performed according to manufacturer's instructions (Peprotech, UK) with some modifications. A monoclonal goat anti-IL-2 capture antibody was diluted with PBS for a final concentration of 2 μ g/mL and coated onto a NUNC 96 well plate overnight at room temperature. The plate was washed 4 times with 300 μ L of wash buffer per well and blocked

for 1 hour with 1% (w/v) BSA in PBS (300 μ L). Triplicates of IL-2 standards (0.0-4.0 ng/mL) and supernatants from treated and untreated cells were added to the plate and incubated for 2 hours at room temperature. A biotinylated polyclonal anti IL-2 antibody was diluted in diluent (0.05% Tween-20, 0.1% (w/v) BSA in PBS) to a final concentration of 0.25 μ g/mL and added to the plate for 2 hours at room temperature. Avidin horseradish peroxidase (HRP) conjugate (1:2000) was then added and incubated for 30 minutes at room temperature. The amount of bound avidin was measured using o-phenylenediamine dihydrochloride (OPD), which was added to each well (100 μ L) and incubated for 15 minutes in the dark. The reaction was stopped using 2 M sulphuric acid (H_2SO_4) and the absorbance was read at 490 nm using a spectrophotometric plate reader (Biotek, USA).

4.3.10 Flow cytometry for the detection of T cell activation:

Activated and control cells (1×10^6 cells/mL) were collected into 1.5 mL microcentrifuge tubes and were centrifuged for 2 minutes at 400 x g in the microcentrifuge (Eppendorf Centrifuge 5415D). The supernatants were removed and the cell pellet was washed twice with PBS (500 μ L) by centrifugation at 400 x g for 2 minutes. Cells were resuspended in RPMI-1640 media and left on ice for 30 minutes for blocking. Cells (2.5×10^5) were then either treated with allophycocyanin (APC) conjugated mouse monoclonal antibody to IL-2 receptor alpha (CD25; 1.25 μ L), or APC-conjugated isotype control (1.25 μ L) in the dark and were kept on ice for 30 minutes. The samples were analysed on the Cytomics TM FC500 flow cytometer (Beckman-Coulter, Miami, USA). Cells were gated based on the FS/SS using FL4 and results and data was collected for 10000 events against forward scatter (FS).

4.3.11 Protein sulphenic acid extraction in Jurkat T cells and human CD4+ T cells:

Jurkat T cells or CD4+ T cells (1×10^6 cells/mL) were either left untreated or treated with 25 μ M BSO, 5 μ g/mL PHA-L or a combination of both for 24 hours. The cells were washed three times with ice cold PBS (1 mL) and centrifuged at 1200 x g for 5 minutes in the microcentrifuge (Eppendorf centrifuge 5415D) each time. The cells were resuspended in PBS (90 μ L) and 10 mM DCP-Bio1 (10 μ L) (Kerafast, USA) the biotinylated probe that detects acid modifications, was added and the cells were incubated for 30 minutes on ice. The principles for the separation and major steps are illustrated in **Figure 4.3**.

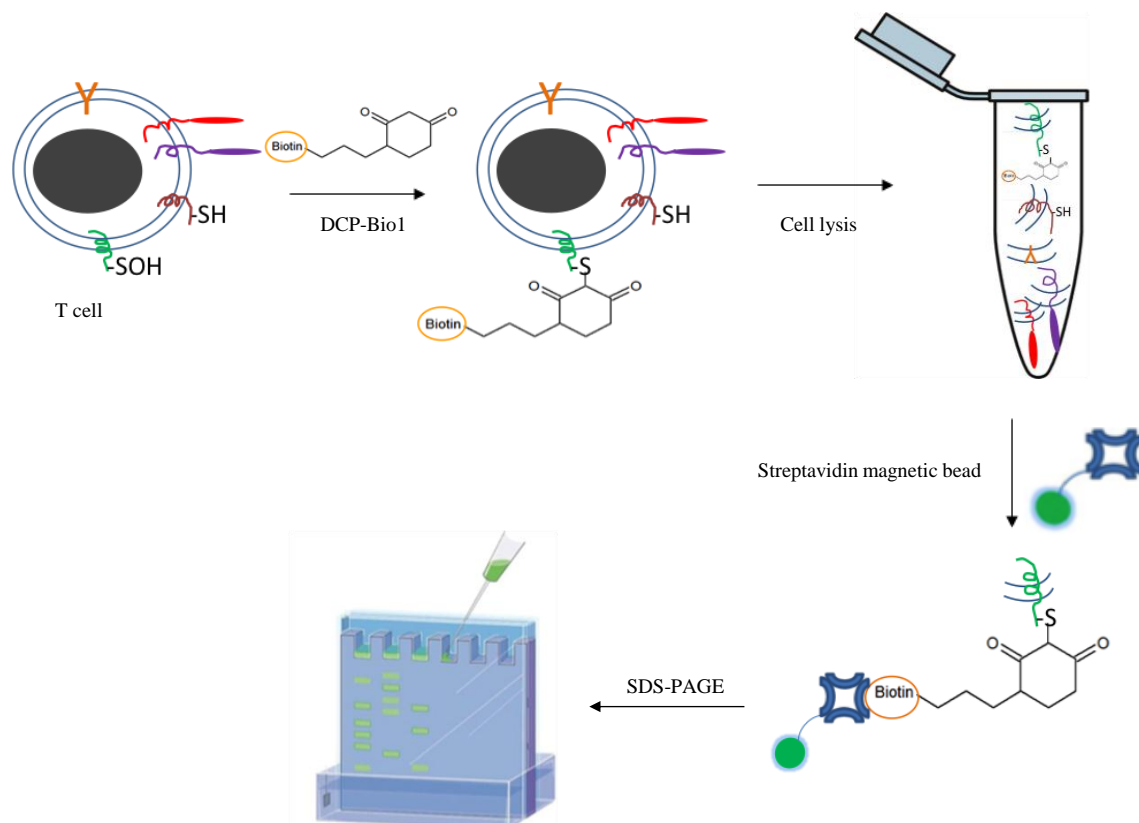


Figure 4.3: Schematic representation of the approach for isolation of sulphenic acid modified proteins. After incubating with 10 mM iodoacetamide (IAM) for 10 minutes on ice, the samples were washed three times with ice cold PBS (1 mL) and centrifuged at 1200 x g for 5 minutes to remove excess DCP-Bio1 and IAM. The cells were resuspended in ice cold MNE lysis buffer (100 μ L, 150 mM NaCl, 2 mM EDTA, 25 mM MES, 1 mM Na_3VO_4 , 1% Triton X-100 and 0.1% protease inhibitor cocktail) for 30 minutes on ice and sheared with a 21G needle (BD, UK) to lyse the cells. Meanwhile, streptavidin magnetic beads (200 μ L) were washed 3 times in PBS (1mL) and the supernatants were removed with the use of magnet. The beads were then resuspended in PBS (200 μ L) and added to the cell lysates and incubated for 30 minutes at room temperature with gentle tilting and rotation. The proteins that have sulphenic acid modifications are bound to the streptavidin magnetic bead through biotin-streptavidin covalent binding. The magnetic bead bound proteins were then captured and resuspended in Laemmli sample buffer (40 μ L), heated for five minutes at 95 $^\circ\text{C}$ to elute the modified proteins off the bead. Samples were analysed by SDS-PAGE and western blotting.

4.3.12 Method development for protein sulphenic acid extraction using Jurkat T cell line:

4.3.12.1 Determination of DCP-Bio1 concentration:

To determine the concentration of probe needed for the capture of sulphenic acid-modified proteins Jurkat T cells (1×10^6 cells/mL) were harvested. The cells were washed three times with ice cold PBS (1 mL) and centrifuged at $1200 \times g$ for 5 minutes in the microcentrifuge (Eppendorf centrifuge 5415D) each time. The cells were resuspended in four different conditions; PBS (99 μ L) and 10 mM DCP-Bio1 (1 μ L) **1**; PBS (95 μ L) and 10 mM DCP-Bio1 (5 μ L) **2**; PBS (90 μ L) and 10 mM DCP-Bio1 (10 μ L) **3**; or PBS (80 μ L) and 10 mM DCP-Bio1 (20 μ L) **4** to give final concentrations of DCP-Bio1 of 0.1 mM, 0.5 mM, 1.0 mM and 2.0 mM respectively. The cells were incubated for 30 minutes on ice and washed three times with ice cold PBS (1 mL) and centrifuged at $1200 \times g$ for 5 minutes to remove excess DCP-Bio1. The cells were lysed and streptavidin magnetic beads (200 μ L) were added to the cell lysates and incubated for 30 minutes at room temperature with gentle tilting and rotation. The proteins that have sulphenic acid modifications are bound via DCP-Bio1 to the streptavidin magnetic bead through biotin-streptavidin covalent binding. The magnetic bead-bound proteins were then captured and resuspended in Laemmli sample buffer (40 μ L), heated for five minutes at 95°C to elute the modified proteins off the bead. Samples were analysed by SDS-PAGE and western blotting as shown on **Figure 4.4**. At low concentration of the probe, a band is visible at 65 kDa. When the concentration is at 1 mM of DCP-Bio1 two bands are visible which can be seen when the DCP-Bio1 concentration is increased further. Since at 1 mM DCP-Bio1 concentration bands were observed with high intensity, this concentration was used for subsequent experiments.

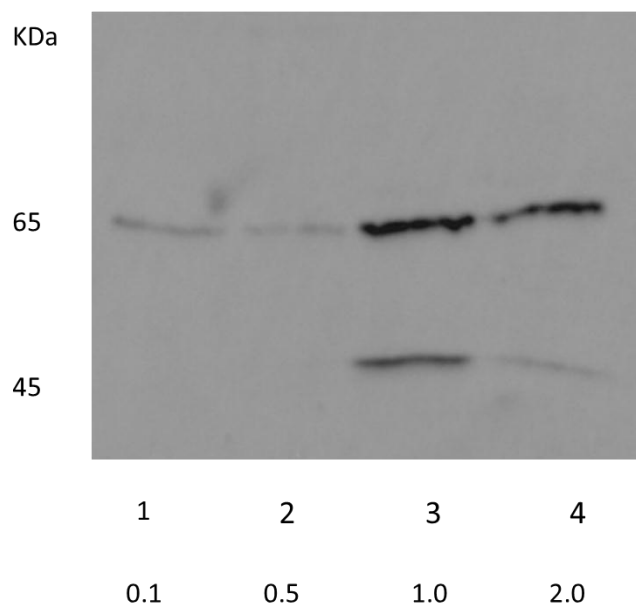


Figure 4.4: Determination of DCP-Bio1 concentration required for sulphenic acid detection in Jurkat T cells. Jurkat T cells (1×10^6 cells/mL) were harvested, washed three times with ice cold PBS (1 mL) and resuspended in PBS as described in methods 4.3.12.1 to achieve final concentrations of DCP-Bio1 of 0.1 mM (1), 0.5 mM (2), 1.0 mM (3) and 2.0 mM (4) respectively. The probe was incubated on ice for 30 minutes and washed 3 times with PBS (1 mL) to remove excess reagent. The cells were lysed and streptavidin magnetic beads (200 μ L) were added to the cell lysate and incubated for 30 minutes. The magnetic bound proteins were captured and loaded onto a 10% polyacrylamide gels and analysed by western blotting using HRP-conjugated streptavidin for biotinylated probe detection.

4.3.13 T cell sample preparation for mass spectrometry:

In order to identify the proteins which have sulphenic modifications, spots removed from PVDF membranes were used for mass spectrometric analysis using a method adapted from Klarskov *et al* (158). After stripping the membrane by leaving it in stripping buffer for 15 minutes the membranes were washed with TTBS at 15-minute intervals 6 times. Protein bands were excised from the PVDF membrane after staining with Ponceau red for 10 minutes to visualise the bands. Bands of the same molecular weight were cut into small pieces, pooled together and washed with TTBS 3 times every 15 minutes to remove the staining. The bands were then reduced in 10 μL of 100 mM NH_4HCO_3 containing 5 mg/mL DTT for 45 minutes at 37 °C. After the sample had cooled to room temperature alkylation was performed in the dark in 20 μL of 200 mM NH_4HCO_3 containing 25 $\mu\text{g}/\mu\text{L}$ of IAM for 30 minutes. After discarding the solvents the membrane pieces were washed 4 times with 400 μL 50 mM NH_4HCO_3 containing 10% ACN each at 15 minute intervals on the shaker. Digestion was performed at 37 °C for 3.5 hours in 8 μL of 50 mM NH_4HCO_3 containing 20 ng/ μL of trypsin with 50% DMF. The samples were centrifuged every half an hour to prevent the membranes from drying out. The samples were then sonicated for 2 minutes and 30 μL 5% formic acid was added to them. The samples were concentrated with Millipore[®] ZipTip C18 (Sigma, UK) according to the manufacturer's instructions. Extracts were dried in a Speed Vac concentrator at room temperature for 2-4 hours and the precipitate was dissolved in 100 μL 0.1% formic acid. Samples were analysed by mass spectrometry using a Thermo LTQ-Orbitrap Elite coupled to a Dionex Ultimate 3000 (RLSC). The samples were separated over a 56 minute gradient, 3.2-44% mobile phase (MP) B over 30 minutes (A = 0.1% formic acid in H_2O , B = 0.1% formic acid in ACN), then 90% MP B for 10 minutes before 16 minutes re-equilibrating at 3.2% B. The flow rate was set to 350 nL/min. The mass spectrometer operates in a data-dependent mode where it performs a full MS scan at resolution 60,000 followed by CID of the 7 most abundant multiply charged ions. These are then entered into an exclusion list to ensure the ions are not analysed multiple times. The full scan followed by top seven then

repeats. Proteome Discoverer version 1.4 was used to analyze the results and the data was searched against a human database (Uniprot) and the results were filtered to give a 1% false discovery rate. Haemoglobin and keratin identifications were discounted as contaminants. Successful identification of other proteins was based on the protein band being of expected mass, having at least two distinct peptides and >10% coverage.

4.3.14 Confocal microscopy:

Isolated CD4⁺ T cells (1×10^6 cells/mL) were washed three times with PBS (1 mL) and allowed to adhere to poly-L-lysine coated microscope slides (Thermo Scientific, UK) for 20 minutes. Cells were fixed with 70% ice-cold methanol for 5 minutes and washed three times with PBS (1 mL). The fixed cells were then either treated with 1 mM DCP-Bio1 for 30 minutes on ice, 1 mM maleimide (9 μ L) and 1 mM maleimide Alexafluor-488C5 (1 μ L) for 30 minutes at 37 °C in the dark or a combination of all the reagents. The slides were then blocked with 1% (w/v) PBS for 30 minutes at 4 °C and rinsed three times with PBS. On the slides where DCP-Bio1 was present, streptavidin-PE (Sigma, UK) was used in 1:100 dilution in PBS and incubated for 30 minutes at 4 °C in the dark. Cells were rinsed three times with PBS mounted with 4',6-diamidino-2-phenylindole (DAPI) containing mounting media and visualised using Leica Confocal microscopy (Leica, UK).

4.3.15 Data analysis:

Unless specified all data is presented as the mean \pm standard error of the mean (SEM) of at least 3 independent experiments performed in triplicates. Statistical analysis was done using a paired student's t-test when comparing the differences between two group means. When comparing means of columns from more than two samples the one-way analysis of variance (one way ANOVA) followed by Dunnett's multiple comparison tests was used. A $P \leq 0.05$ was considered to be significant and a 95% confidence interval was used for the difference between all selected pairs of means in the t-test. Statistical analysis was performed using the Graphpad Prism version 5.0 software.

4.4 Results:

4.4.1 Isolation of PBMCs and CD4+ T cells from 20 mL of blood:

To investigate the number of PBMCs and CD4+ T cells isolated, 20 mL of blood was taken and isolated as described in the methods 4.3.1 and 4.3.2. From 20 mL of blood, $22 \times 10^6 \pm 1.53$ PBMCs (mean \pm SEM, n=3) were recovered while $5.4 \times 10^6 \pm 0.31$ CD4+ T cells (mean \pm SEM) were negatively isolated (**Figure 4.5**).

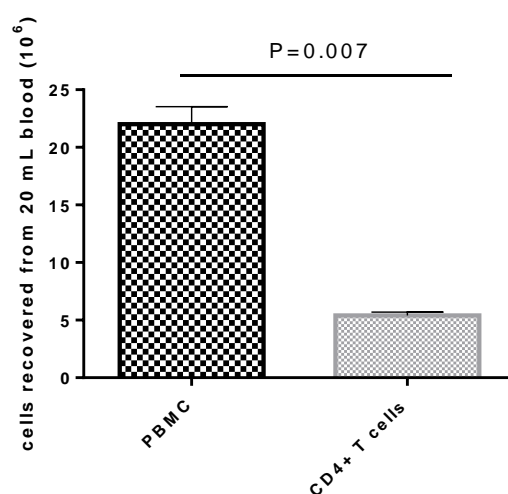


Figure 4.5: PBMC and CD4+ T cells recovered from 20 mL of blood. Blood (20 mL) was mixed with 30 mL of 0.1% BSA in PBS and layered onto 11 mL of lymphoprep. The blood was separated by centrifugation at 160 x g for 20 minutes followed by 381 g for 20 minutes. The PBMCs were recovered as described in methods 4.3.1. From the isolated PBMCs, CD4+ T cells were negatively isolated using the Dynabeads untouched CD4 T cells kit as described in methods 4.3.2. Cells (20 μ L) were transferred into a micro centrifuge tube with an equal volume of trypan blue and transferred onto a haemocytometer for cell counting. Mean values are shown with standard error of mean for three independent experiments. Statistical analysis was done using two tailed paired students t test.

4.4.2 Purity of negatively isolated human CD4+ T cells using flow cytometry:

To determine the purity of the negatively isolated CD4+ T cells, cells were either stained with phycoerythrin (PE)-labelled anti-CD4 monoclonal antibody on ice, in the dark or labelled with PE-labelled isotype control antibody. The purity of the CD4+ T cell gated population was 95% (**Figure 4.6**).

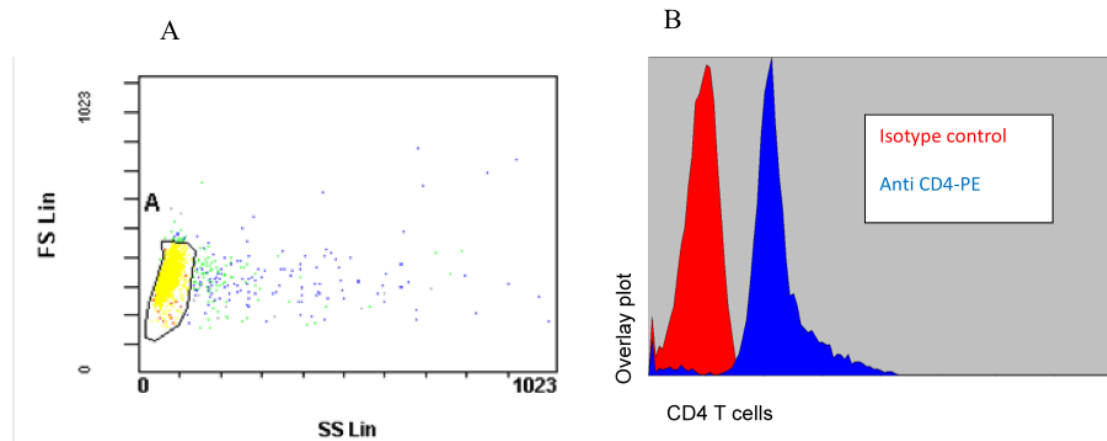


Figure 4.6: Purity of negatively isolated CD4+ T cells. CD4+ T cells were isolated as described previously and stained with PE-labelled anti-CD4 or PE-labelled isotype control antibody and analysed by flow cytometry. CD4+ positive cells were gated and data was collected for 10000 events. (A) Forward and side scatter (FS and SS respectively) of the whole T cell population. (B) Overlay plot of isotype control antibody and anti-CD4-PE stained T cell population.

4.4.3 The effect of GSH synthetase inhibitor, buthionine sulphoximine (BSO) on CD4+ T cell viability:

To investigate if depletion of the intracellular GSH level by BSO affects cell viability, the human CD4+ T cells were treated with 25 μ M BSO, which is an inhibitor of GSH synthesis, for 24 hours. Cells were counted before and after the 24-hour treatment and measured using trypan blue exclusion method (**Figure 4.7**). The cell viability of the BSO treated cells (95.6 ± 0.30 ; mean \pm SEM) was the same as the untreated cells (97.5 ± 0.88) after 24 hours.

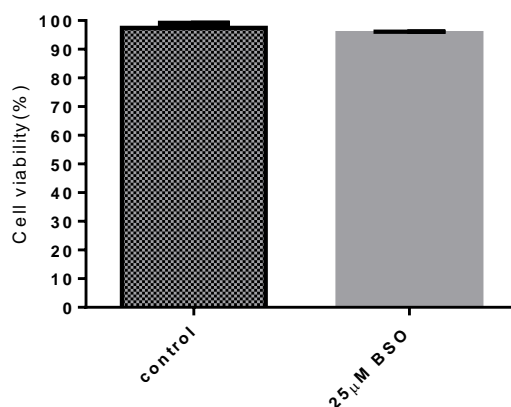


Figure 4.7: Buthionine sulphoximine (BSO) treatment of CD4+ T cells does not affect cell viability. Cells (20 μ L) were transferred into a micro centrifuge tube with an equal amount of trypan blue. The contents were mixed gently and transferred onto a haemocytometer for cell counting. Mean values are shown with standard error of mean for 3 independent experiments.

4.4.4 Effect of buthionine sulphoximine on CD4+ T cell total GSH level:

To confirm that treatment of CD4+ T cells with BSO has an effect on the intracellular GSH levels, cells (1×10^6 cells/mL) were incubated for 24 hours with 25 μ M BSO. After 24 hours the GSH and BCA assays were performed to determine the intracellular GSH levels. The GSH levels have decreased significantly ($P=0.042$) after 24 hours of BSO treatment 8.80 ± 0.87 nmol GSH/total protein (mean \pm SEM), compared to the control samples 10.07 ± 1.03 nmol GSH/total protein were detected (**Figure 4.8**).

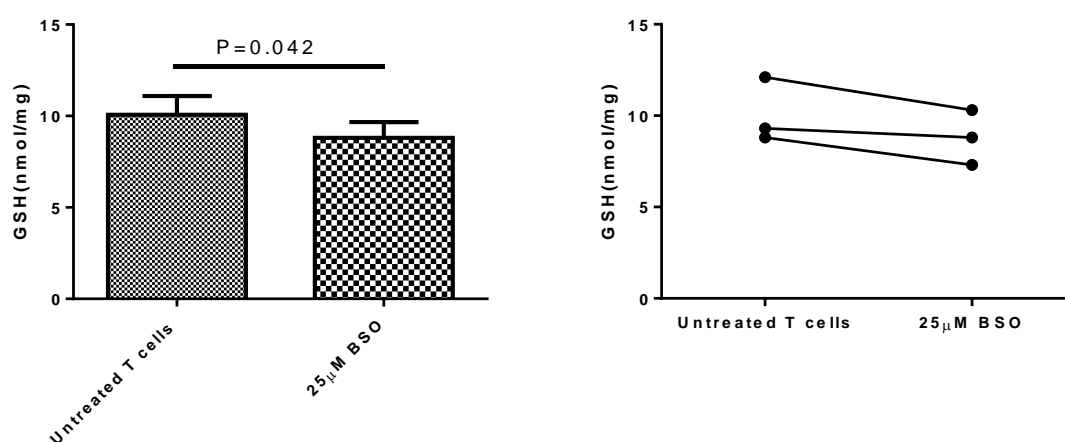
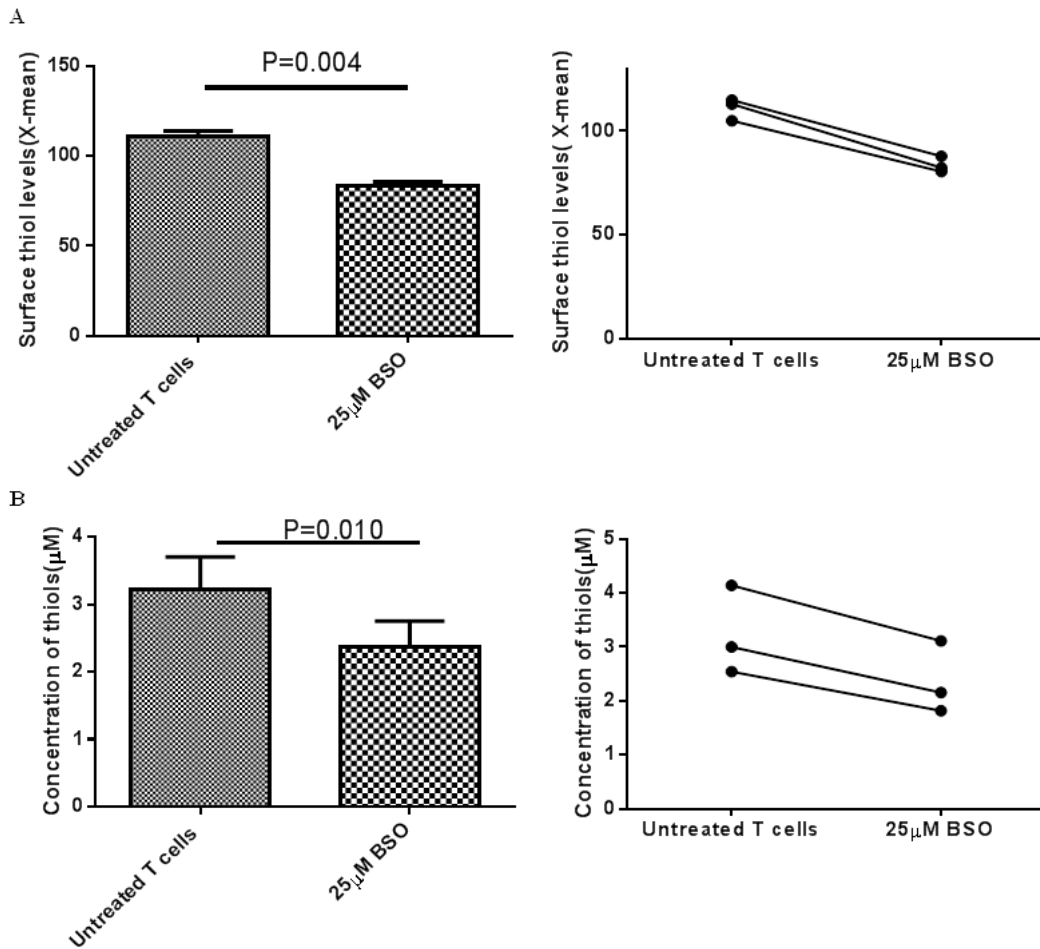


Figure 4.8: Pre-incubation with buthionine sulphoximine (BSO) affects the total glutathione (GSH) levels in CD4+ T cells. CD4+ T cells (1×10^6 cells/mL) were treated with BSO (25 μ M) for 24 hours then harvested and analysed for total GSH as described in the methods. Significant differences were calculated with one tailed, paired student's t-test. The results are for 3 independent experiments done in triplicates.

4.4.5 Effect of BSO on surface thiols of CD4+T cells:

In order to investigate the cell surface thiol levels under normal and oxidatively stressed conditions, such as GSH depletion, CD4+ T cells were treated with 25 μ M BSO for 24 hours. Surface thiols were measured using DTNB assay and flow cytometry and the results are displayed in **Figure 4.9**. Cells treated with BSO for 24 hours show a significant decrease in surface thiols levels (2.36 ± 0.38 μ M; mean \pm SEM) compared to untreated cells (3.23 ± 0.47 μ M) when measured by the DTNB assay ($P=0.01$). Flow cytometry data show similar results with treated cells (83.6 ± 2.22 X-mean) showing a significant decrease in maleimide Alexafluor-488C5 binding ($P=0.004$) compared to control sample (111.0 ± 3.05 X-mean)



C

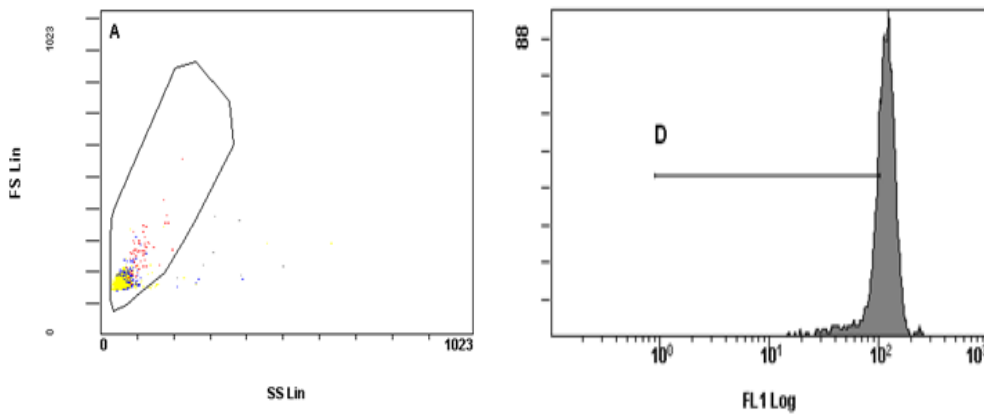


Figure 4.9: Buthionine sulphoximine (BSO) pre-incubation with CD4⁺ T cells reduces surface thiol levels. 1×10^6 cells/mL were treated with 25 μ M BSO for 24 hours. A) 0.5×10^6 cells either treated or untreated were washed twice with PBS to remove media and excess BSO. Cells were resuspended in PBS and thiols were labelled with 1 mM maleimide Alexafluor-488C5 then analysed by flow cytometry. Mean peak staining intensity for thiols is displayed with standard error of the mean from 3 independent experiments. Statistical analysis was done using two tailed paired students t test. B) Cells were washed twice with PBS and resuspended in PBS. CD4⁺ T cells (1.5×10^5) were added to 96 well plates and DTNB was added to a final concentration of 200 μ M for 20 minutes in the dark at room temperature. Supernatants were collected and absorbance read at 405 nm and the free thiols calculated. Data represent three independent experiments of three replicates. Significant differences were calculated using two tailed, paired student's t test. C) Forward and side scatter (FS and SS respectively) of the whole T cell population and histogram of T cell population without BSO treatment

4.4.6 Effect of PHA-L and PHA-P on cell viability:

Phytohemagglutinin (PHA) is a lectin derived from *Phaseolus vulgaris*. It consists of two related proteins, leukoagglutinin (PHA-L), which has a high mitogen activity to T lymphocytes and erythroagglutinin (PHA-E), which has low mitogenic activity but high erythroagglutinin activity. PHA-P is the protein form of lectin prior to the purification to PHA-L and PHA-E. To study their effects on T cell activation 1 µg/mL PHA-L, 5 µg/mL PHA-L, 1 µg/mL PHA-P and 5 µg/mL PHA-P were studied over 24 hours. T cell viability was assessed by the trypan blue exclusion method. **Figure 4.10** shows that when increasing the concentration of PHA-L there is a decrease in cell viability from 88.2±7.8% (mean±SEM) for 1µg/mL PHA-L to 72.1±23.9% with 5µg/mL PHA-L. The decrease in cell viability is similar when using 1µg/mL PHA-P (84.7±11.23%) and 5 µg/mL PHA-P (76.6±19.2%) (P< 0.05) at 5 µg/ml for both lectins compared to untreated controls.

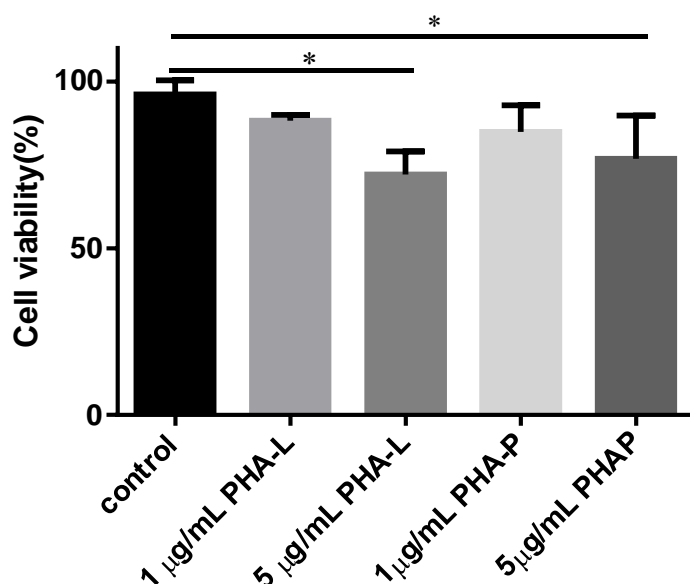


Figure 4.10: PHA-L and PHA-P treatment decreases cell viability. Cells (1×10^6 cells/mL) were treated with lectins for 24 hours then an aliquot was transferred into a micro centrifuge tube with an equal amount of trypan blue. The contents were mixed gently and transferred onto a haemocytometer for cell counting. Mean values are shown with standard error of mean for 3 independent experiments. Significant differences were calculated (* P< 0.05) with one-way ANOVA analysis followed by Dunnett's multiple comparison tests.

4.4.7 Effect of PHA-L and PHA-P on CD4 + T cell activation:

To investigate the effect of 1 µg/mL PHA-L, 5 µg/mL PHA-L, 1 µg/mL PHA-P and 5 µg/mL PHA-P on the activation of T cells after 24 hours of treatment, flow cytometry was used to determine the amount of cells expressing CD25 at the cell surface. Results show a PHA-concentration dependent increase in the amount of activated cells for both PHA-L and PHA-P. In untreated T cells, 24.0% were positive for CD25 and after 5 µg/mL PHA-L treatment, 64.5% of cells were CD25 positive (**Figure 4.11**).

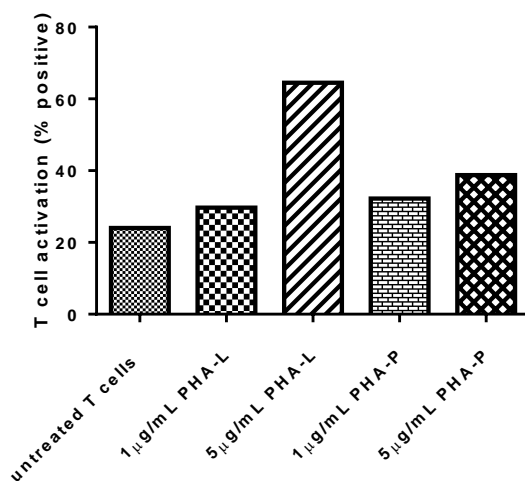


Figure 4.11: T cell activation markers are increased by increasing concentrations of PHA-L and PHA-P. Isolated CD4⁺ T cells (1×10^6 cells/mL) were activated with 1 µg/mL PHA-L, 5 µg/mL PHA-L, 1 µg/mL PHA-P and 5 µg/mL PHA-P for 24 hours or left untreated. Samples were collected to 1.5 mL microcentrifuge tubes, washed in PBS then resuspended in RPMI-1640 media for blocking. Cells (2.5×10^5) were then either treated with allophycocyanin (APC)-conjugated mouse monoclonal antibody to IL-2 receptor alpha (CD25; 1.25 µL), or APC-conjugated isotype control antibody (1.25 µL) in the dark and were kept on ice for 30 minutes. The samples were analysed on the Cytomics TM FC500 flow cytometer (Beckman-Coulter, USA). Cells were gated based on the forward scatter (FS)/side scatter (SS) using FL4 and results and data was collected for 10000 events against FS. The results shown are from one experiment.

4.4.8 Effect of PHA-P and PHA-L on T cells using IL-2 ELISA:

The CD4⁺ T cell response to activation with 1 µg/mL PHA-L, 5 µg/mL PHA-L, 1 µg/mL PHA-P and 5 µg/mL PHA-P after 24 hour treatment was assessed by measuring the levels of the interleukin-2 (IL-2) secreted into the supernatant. IL-2 is a cytokine that is mainly produced by activated CD4⁺ T cells in response to TCR and CD28 signalling (42). **Figure 4.12** shows that there is an increase in IL-2 secretion when PHA-L concentration was increased to 5 µg/mL (0.29 ng/mL).

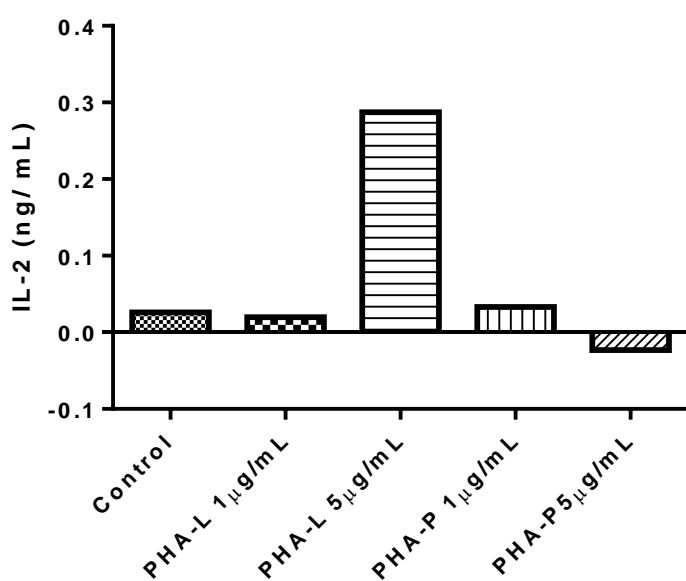


Figure 4.12: PHA-L increases IL-2 secretion. Isolated CD4⁺ T cells (1×10^6 cells/mL) were activated with 1 µg/mL PHA-L, 5 µg/mL PHA-L, 1 µg/mL PHA-P and 5 µg/mL PHA-P for 24 hours or left untreated. Samples were collected to 1.5 mL microcentrifuge tubes and centrifuged at 400 x g for 2 minutes. The supernatants were collected and analysed for IL-2 using a human IL-2 ELISA as described in the methods. Data is from one experiment.

4.4.9 Protein sulphenic acid modifications in Jurkat E6.1 T cells:

To investigate protein sulphenic acid modifications in T cells, a cultured Jurkat E6.1 T cell line was used. The biotinylated dimedone based probe, 3-(2,4-dioxocyclohexyl)propyl 5-((3aR,6S,6aS)-hexahydro-2-oxo-1H-thieno[3,4-d]imidazol-6-yl)pentanoate (DCP-Bio1, Kerafast) was used to capture sulphenic acid modified proteins. Jurkat T cells (1×10^6 cells/mL) were washed three times with ice cold PBS and treated with 1 mM DCP-Bio1 for 30 minutes on ice. The free thiols were blocked with 10 mM IAM for 10 minutes. Cells were incubated in MNE lysis buffer for 30 minutes on ice. Excess reagent was washed off and the cells were lysed and proteins separated by SDS-PAGE. The gels were then transferred on to a PVDF membrane and probed with HRP-conjugated streptavidin. Gels were run under reducing and non-reducing conditions and showed similar band patterns (**Figure 4.14**). Lane **4** where cells have been treated with DCP-Bio1 and IAM show two prominent bands at around 65 kDa and 45 kDa respectively. Lane **2** (total cell lysate) and lane **3** where cells were first treated with 10 mM IAM to block free thiols and then treated with DCP-Bio1 show weaker bands at around 65 kDa.

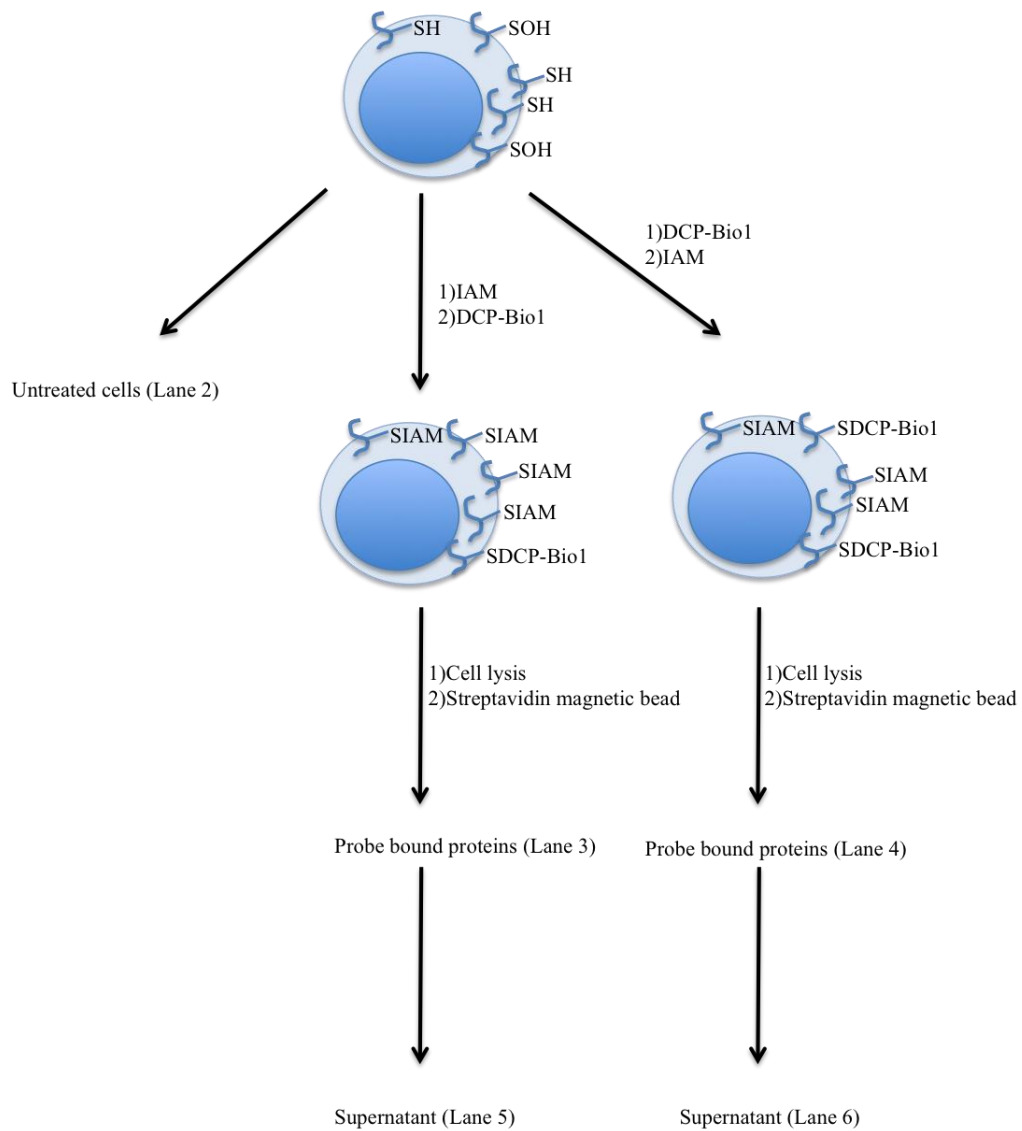


Figure 4.13: Schematic presentation of isolation of sulphenic acid modified proteins.

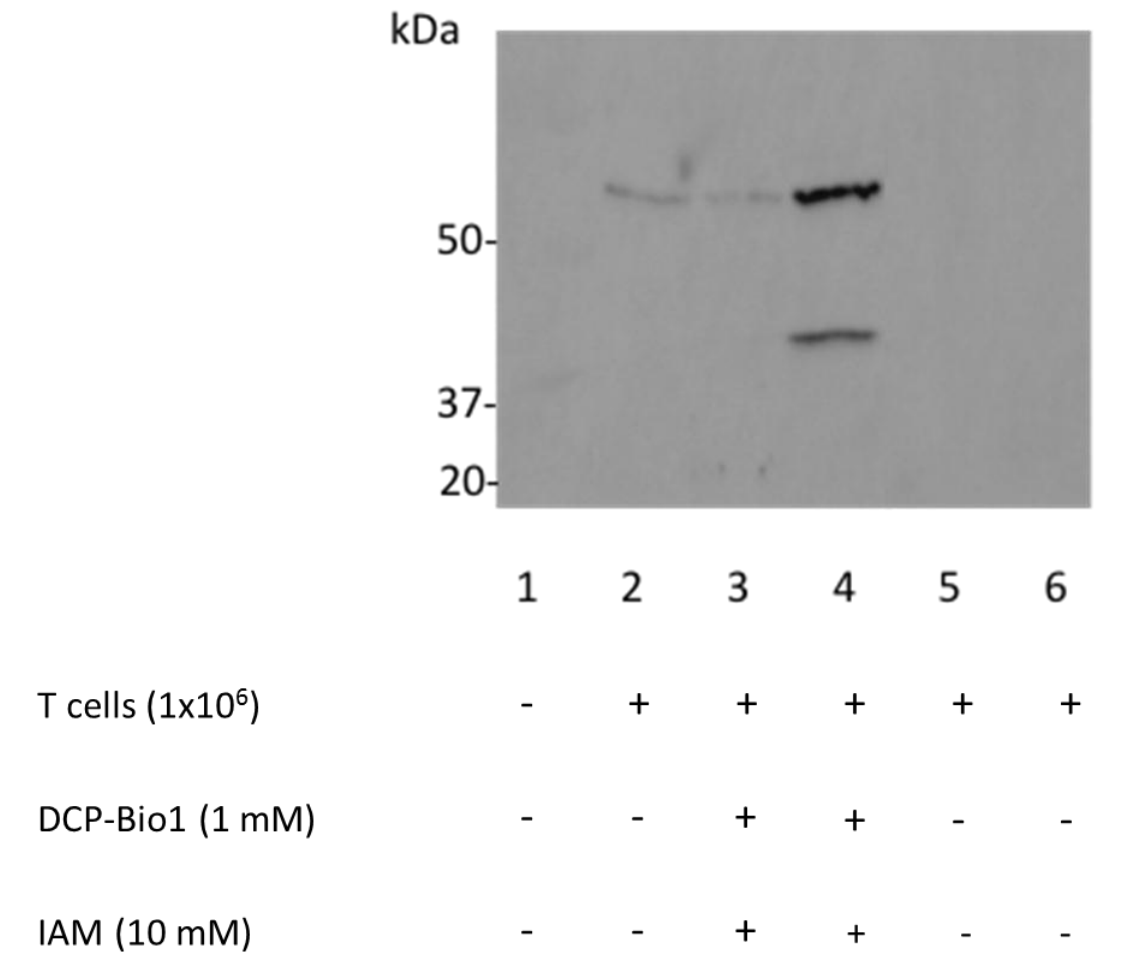


Figure 4.14: Protein sulphenic acid modifications in Jurkat E6.1 T cells. Jurkat T cells (1×10^6 cells/mL) were washed three times ice cold PBS (1 mL) and treated as follows prior to SDS-PAGE and western blotting with HRP-streptavidin.

1-Protein marker

2-Untreated T cells

3-Cells treated with 10 mM IAM for 10 minutes followed by 1 mM DCP-Bio1 for 30 minutes on ice

4-Cells treated with 1 mM DCP-Bio1 for 30 minutes on ice followed by 10 mM IAM,

5- Supernatant of 2 after protein removal by streptavidin magnetic beads,

6- Supernatant of 3 after protein removal by streptavidin magnetic beads.

The gel is representative of 3 independent experiments.

4.4.10 CD4+ T cell protein sulphenic acid modifications:

To investigate protein sulphenic acid modifications in primary cells, CD4+ T cells were isolated from blood. T cells (1×10^6 cells/mL) were either left untreated (**Figure 4.15**, lane 2), treated with 10 mM IAM for 10 minutes followed by 1 mM DCP-Bio1 for 30 minutes on ice (**Figure 4.15**, lane 3) or treated with 1mM DCP-Bio1 for 30 minutes on ice followed by 10 mM IAM treatment for 10 minutes (**Figure 4.15**, lane 4). The cells were washed with ice cold PBS three times to get rid of any excess chemicals and incubated with MNE lysis buffer for 30 minutes on ice and lysed with a 21 G needle. Samples were run on a 10% SDS-PAGE to separate the proteins. After transfer to a PVDF membrane, they were probed with HRP-conjugated streptavidin. When treated with DCP-Bio1 prior to IAM treatment 3 bands are visible around 65 kDa, 45 kDa and 25 kDa (**Figure 4.15**). The band at 65 kDa is also visible in both total cell lysate (lane 2) and treatment with IAM followed by treatment with DCP-Bio1 (lane 3).

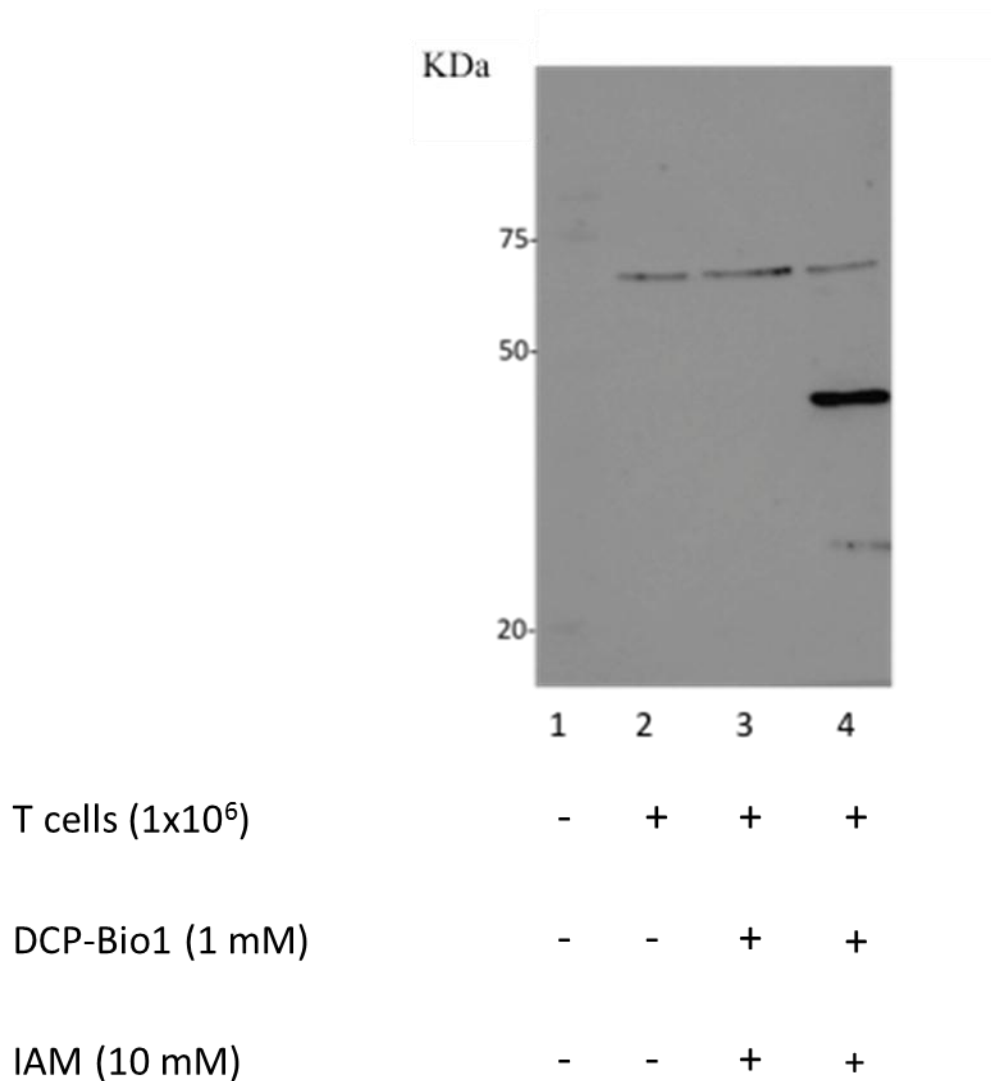
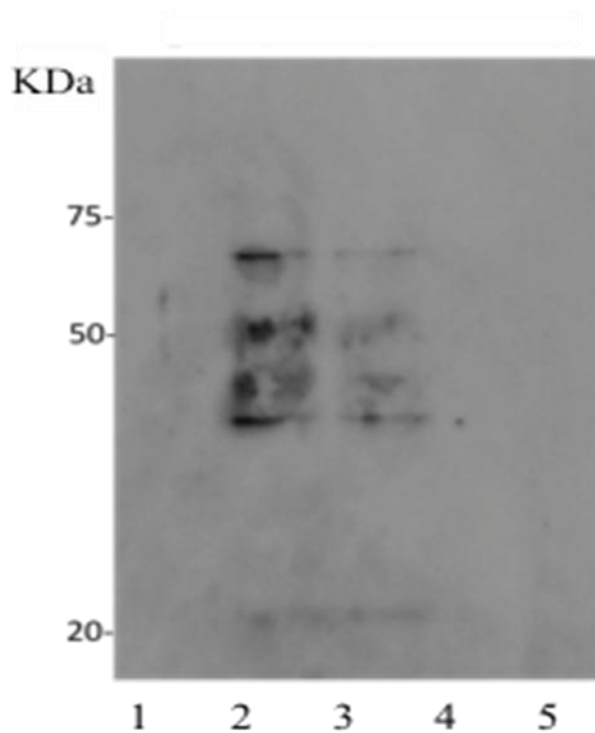


Figure 4.15: Protein sulphenic acid modifications in resting CD4+T cells. CD4+ T cells (1×10^6 cells/mL) were washed three times with ice cold PBS. Cells were either untreated (2), treated with 10 mM IAM for 10 minutes followed by 1 mM DCP-Bio1 for 30 minutes on ice (3) or treated with DCP-Bio1 for 30 minutes on ice followed by 10 mM IAM for 10 minutes (4). Cells were lysed and loaded onto 10% polyacrylamide gels and analysed by western blotting using HRP conjugated streptavidin for biotinylated probe detection. The blot is representative of 3 independent experiments.

4.4.11 BSO treated CD4+ T cell protein sulphenic acid modifications:

To explore the formation of protein sulphenic acid modifications under oxidatively stressed conditions, CD4+ T cells (1×10^6 cells/mL) were treated with 25 μ M BSO for 24 hours. The cells were either left untreated, treated with 10 mM IAM for 10 minutes followed by 1 mM DCP-Bio1 treatment for 30 minutes on ice or vice versa. An increased number of bands at 65 kDa, 50 kDa, 45 kDa, 40 kDa and 25 kDa, are visible in **Figure 4.16** compared to resting cells shown in **Figure 4.15**. Lane **3** where the cells have been treated with excess IAM followed by 1 mM DCP-Bio1 show similar banding patterns although bands are less prominent.



T cells (1×10^6)	+	+	+	+	+
DCP-Bio1 (1 mM)	-	+	+	-	-
IAM (10 mM)	-	+	+	-	-

Figure 4.16: Sulphenic acid modifications in buthionine sulphoximine (BSO) treated T cells. CD4⁺ T cells (1×10^6 cells/mL) were washed three times with ice cold PBS. Cells were either untreated (1), treated with DCP-Bio1 for 30 minutes on ice followed by 10 mM IAM for 10 minutes (2) or treated with 10 mM iodoacetamide (IAM) for 10 minutes followed by 1 mM DCP-Bio1 for 30 minutes on ice (3) Cells were lysed and loaded onto 10% polyacrylamide gels and analysed by western blotting using HRP conjugated streptavidin for biotinylated probe detection.

4.4.12 BSO and PHA-L treated CD4+ T cell protein sulphenic acid modifications:

To investigate the effects of oxidative stress and T cell activation on the formation of protein sulphenic acid modifications, T cells (1×10^6 cells/mL) were treated with 25 μ M BSO and 5 μ g/mL PHA-L for 24 hours. Western blot results show 4 bands at 65 kDa, 50 kDa, 45 kDa and 40 kDa (**Figure 4.17**, lane 2) where cells have been treated with 1 mM DCP-Bio1 followed by 10 mM IAM. Similar less intense bands are observed in lane 3 where cells were first treated with IAM followed by DCP-Bio1 treatment. Although there is an increase in the number of bands compared with untreated T cells (**Figure 4.15**) there is one band missing (25 kDa) compared to the BSO-treated T cells (**Figure 4.16**).

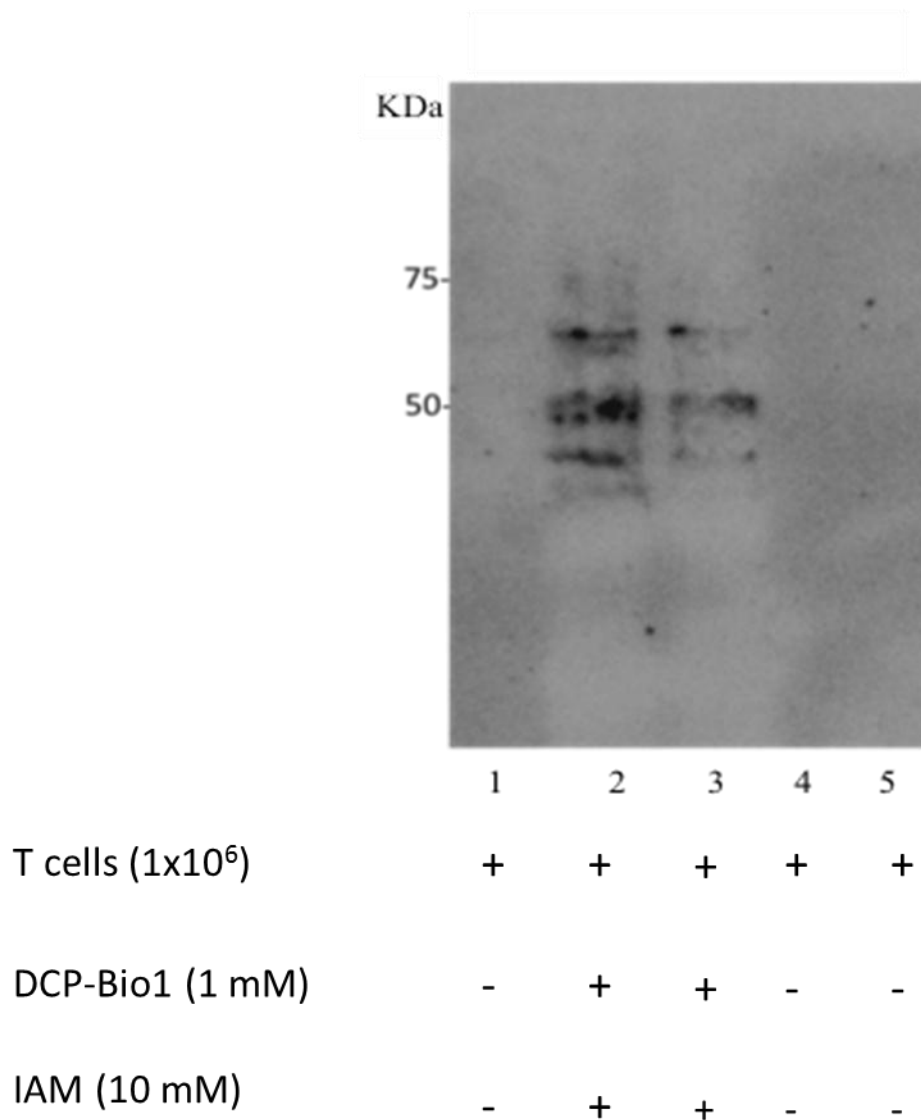


Figure 4.17: Protein sulphenic acid modifications with BSO and PHA-L treated T cells. CD4⁺ T cells (1×10^6 cells/mL) were washed three times with ice cold PBS. Cells were either untreated (1), treated with DCP-Bio1 for 30 minutes on ice followed by 10 mM IAM for 10 minutes (2) or treated with 10 mM iodoacetamide (IAM) for 10 minutes followed by 1 mM DCP-Bio1 for 30 minutes on ice (3). Cells were lysed and biotinylated proteins were captured with streptavidin magnetic beads. The proteins were eluted with sample buffer and proteins and supernatants of sample 2 (lane 4) and sample 3 (lane 5) were loaded onto 10% polyacrylamide gels and analysed by western blotting using HRP conjugated streptavidin for biotinylated probe detection.

4.4.13 PHA-L treated CD4+ T cell protein sulphenic acid modifications:

To investigate the effects of T cell activation on the formation of sulphenic acid modifications, CD4+ T cells (1×10^6 cells/mL) were treated with 5 μ g/mL PHA-L for 24 hours. After activation, cells that were treated with DCP-Bio1 for 30 minutes, followed by excess IAM, show bands at 65 kDa and 25 kDa (**Figure 4.18**, lane 3). Lane 2 where cells were treated with 10 mM IAM followed by 1 mM DCP-Bio1 treatment also show a similar, but less intense, banding pattern. There is a decrease in the number of bands present in **Figure 4.18** compared with untreated, BSO treated and BSO and PHA-L treated T cells.

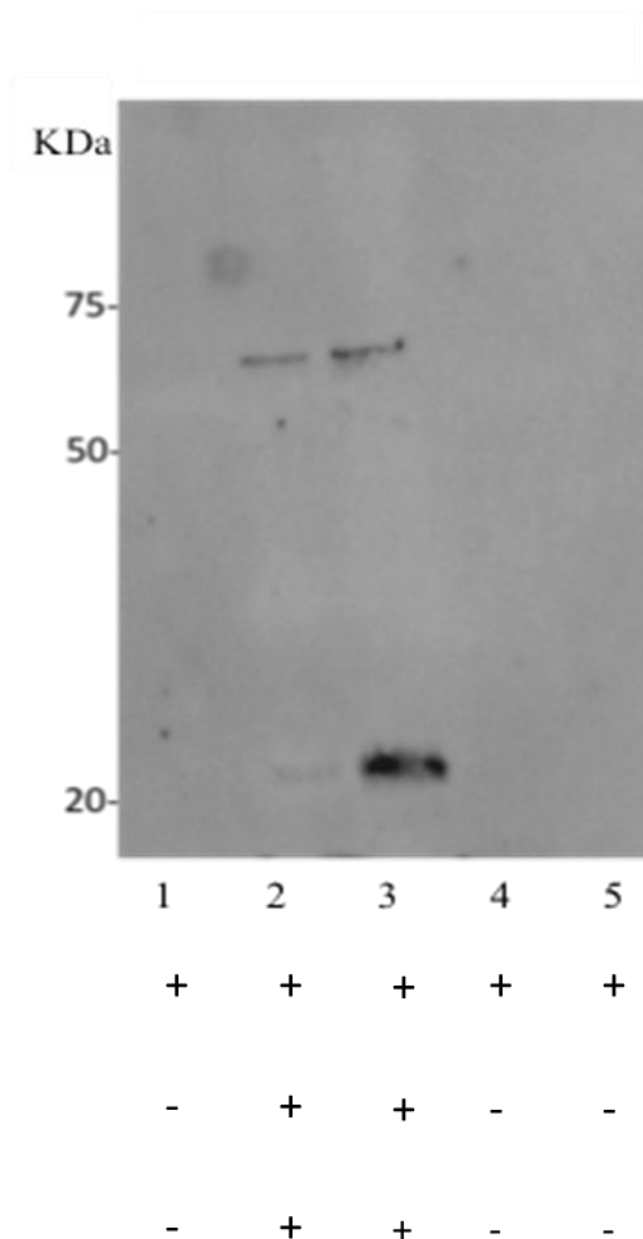


Figure 4.18: Protein sulphenic acid modifications after 5 $\mu\text{g}/\text{mL}$ PHA-L for 24 hours. CD4⁺ T cells (1×10^6 cells/mL) were treated with 5 $\mu\text{g}/\text{mL}$ PHA-L for 24 hours. The cells were washed 3 times with ice cold PBS to remove excess reagent and either untreated (**1**), treated with 10 mM iodoacetamide (IAM) for 10 minutes followed by 1 mM DCP-Bio1 for 30 minutes on ice (**2**) or treated with 1 mM DCP-Bio1 for 30 minutes followed by incubation of 10 mM iodoacetamide for 10 minutes (**3**). Cells were lysed in MNE lysis buffer and proteins separated on a 10% polyacrylamide gel. Proteins were transferred on to a PVDF membrane and probed with HRP-conjugated streptavidin for visualisation.

4.4.14 Mass spectrometry identification of protein bands containing sulphenic acid modifications:

In order to identify proteins that contained sulphenic acid modifications, bands were cut out from PVDF membranes as described in the methods section above (4.3.13). The samples were subjected to mass analysis and the proteins that met inclusion criteria for each band excluding keratin and haemoglobin are listed in **Table 4.2-6** below.

Accession	Protein	Function	Unique peptides	MW (KDa)	Coverage
P02768	Serum albumin	Maintaining osmotic pressure. Transportation of molecules	3	69.3	11.66
P30043	Flavin reductase (NADPH)	Catalyses the NADPH-dependent reduction of a variety of flavins. Can also reduce the complexed Fe(3+) iron to Fe(2+) in the presence of FMN and NADPH	1	22.1	14.56
P81605	Dermcidin	Antimicrobial, limits skin infection	1	11.3	22.73

Table 4.2: Results of protein identifications for the 25 kDa band. The Accession is the unique identifier used for the sequence. The coverage indicates the percentage of the protein sequence that has been covered by the identified protein. The number of unique peptides displays the number of peptides matching the protein identified. The proteins highlighted in red are closest matched to the MW of the band identified.

Accession	Protein	Function	Unique Peptides	MW (KDa)	Coverage
P81605	Dermcidin	Antimicrobial. Limits skin infection	4	11.3	35.45
P04406	Glyceraldehyde-3-phosphate dehydrogenase	Plays a role in glycolysis and nuclear function	6	36.0	24.78
P60709	Actin, cytoplasmic 1	Internalisation of TCR and activation of calcium signalling	5	41.7	18.40
Q9NZT1	Calmodulin like protein 5	Plays a role in calcium binding	2	15.9	21.23
Q06830	Peroxiredoxin-1	Involved in redox regulation of the cell and reduces peroxides through the thioredoxin system	3	22.1	16.58
P07355	Annexin A2	Calcium and phospholipid binding protein	3	38.6	12.09
P05089	Arginase-1	Synthesis of polyamines such as putrescine, spermidine and spermine	3	34.7	10.56

Table 4.3: Results of protein identifications for 40 kDa band. The Accession is the unique identifier used for the sequence. The coverage indicates the percentage of the protein sequence that has been covered by the identified protein. The number of unique peptides displays the number of peptides matching the protein identified. The proteins highlighted in red are closest matched to the MW of the band identified.

Accession	Protein	Function	Unique peptides	MW(KDa)	Coverage
P30043	Flavin reductase (NADPH)	Catalyses the NADPH dependent reduction of a variety of flavins. Can also reduce the complexed Fe(3+) to Fe(2+) in the presence of FMN and NADPH	1	22.1	14.45
P02768	Serum albumin	Maintains osmotic pressure. Transportation of molecules	3	69.3	10.18

Table 4.4: Results of protein identifications for 45 kDa band. The Accession is the unique identifier used for the sequence. The coverage indicates the percentage of the protein sequence that has been covered by the identified protein. The number of unique peptides displays the number of peptides matching the protein identified.

Accession	Protein	Function	Unique peptides	MW(KDa)	Coverage
P81605	Dermcidin	Antimicrobial. Limits skin infection	3	11.3	35.45
P05109	Protein s100-A8	Functions as a calcium and zinc binding protein and has a prominent role in the regulation of immune response	2	10.8	19.35
P47929	Galectin-7	A Pro-apoptotic protein that functions intracellularly upstream of JNK activation and cytochrome release	2	15.1	18.38
P02656	Apolipoprotein C-III	Plays a role in triglyceride homeostasis	1	10.8	16.16
P30043	Flavin reductase (NADPH)	Catalyses the NADPH dependent reduction of a variety of flavins. Can also reduce complexed Fe (3+) iron to Fe(2+) in the presence of FMN and NADPH	1	22.1	14.56
P02768	Serum albumin	Regulates osmotic pressure and plays a role in the transport of molecules	3	69.3	13.46
P31151	Protein S100-A7	May function in calcium and zinc binding	1	11.5	10.89

Table 4.5: Results of protein identifications for 50 kDa band. The Accession is the unique identifier used for the sequence. The coverage indicates the percentage of the protein sequence that has been covered by the identified protein. The number of unique peptides displays the number of peptides matching the protein identified.

Accession	Protein	Function	Unique peptides	MW(KDa)	Coverage
J3QL26	Serine/threonine-protein phosphatase 4 regulatory subunit 1	May be involved with regulation of cell division in renal glomeruli	1	15.5	21.48
P02768	Serum albumin	Functions as a transporter molecule and in maintaining osmotic pressure	4	69.3	16.91
P02656	Apolipoprotein C-III	Plays a role in triglyceride homeostasis	1	10.8	16.16
P30043	Flavin reductase (NADPH)	Catalyses the NADPH dependent reduction of a variety of flavins. Can also reduce complexed Fe(3+) iron to Fe(2+) in the presence of FMN and NADPH	1	22.1	14.56

Table 4.6: Results of protein identifications for 65 kDa band. The Accession is the unique identifier used for the sequence. The coverage indicates the percentage of the protein sequence that has been covered by the identified protein. The number of unique peptides displays the number of peptides matching the protein identified. The proteins highlighted in red are closest matched to the MW of the band identified.

4.4.15 Cell imaging:

To investigate the labelling of thiols as well as to examine if DCP-Bio1 labelling of protein sulphenic acids was extracellular, intracellular or both, CD4⁺ T cells (1×10^6 cells/mL) were either stained with maleimide/maleimide Alexafluor488C5, DCP-Bio1 followed by streptavidin-PE or a combination of all of the reagents above. The nucleus was stained with DAPI (4',6-diamino-2-phenylindole) and visualised by confocal microscopy (Leica, UK). **Figure 4.19** shows the nucleus of the T cells stained in blue, DCP-Bio1 (red) appears to be cell permeable and is able to detect protein sulphenic acid modifications on the membrane as well as in the cytosol of T cells. T Cells stained with maleimide/maleimide Alexafluor 488C5 (green) show extensive surface thiols (**Figure 4.19B**). When cells are stained for sulphenic acids and surface thiols, yellow patches are observed in the nucleus, which are areas where both sulphenic acids and thiols are present. In some cells blebbing could also be observed (**Figure 4.19D**).

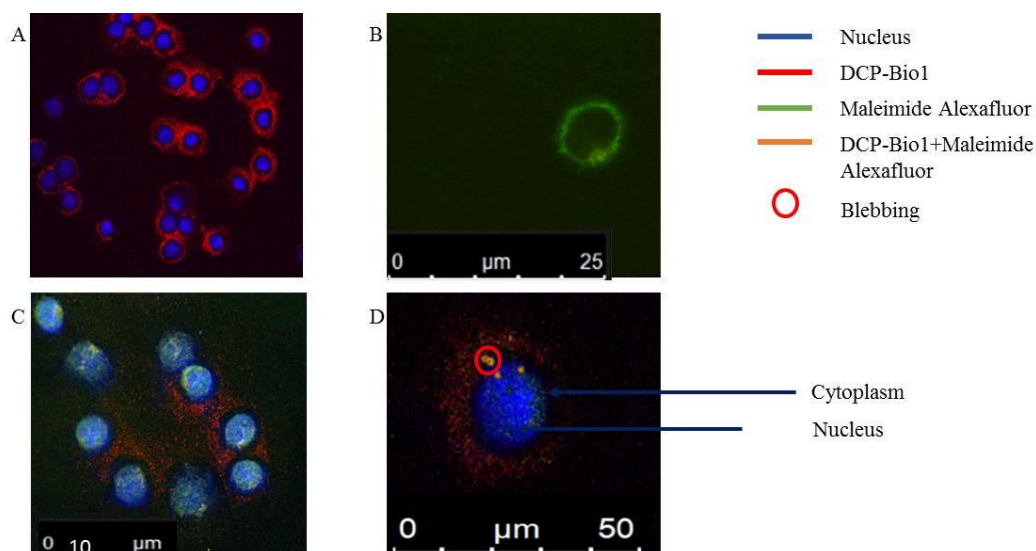


Figure 4.19: Detection of protein thiols and sulphenic acids in CD4+ T cells. CD4+ T cells (1×10^6 cells/mL) were adhered onto poly-L-lysine microscopy slides for 20 minutes at room temperature (Thermo Scientific, UK). Cells were fixed with 70% ice-cold methanol for 5 minutes and washed three times with PBS (1 mL). The fixed cells were then either A) treated with 1 mM DCP-Bio1 for 30 minutes on ice, B) 1 mM maleimide (9 μ L) and 1 mM maleimide Alexafluor-488C5 (1 μ L) for 30 minutes at 37 $^{\circ}$ C in the dark C) a combination of all the reagents. D) presence of blebs when both DCP-Bio1 and maleimide are present. The slides were then blocked with 1% (w/v) PBS for 30 minutes at 4 $^{\circ}$ C and rinsed three times with PBS. On the slides where DCP-Bio1 was present streptavidin-PE (Sigma, UK) was used in 1:100 dilution in PBS and incubated for 30 minutes at 4 $^{\circ}$ C in the dark. Cells were rinsed three times with PBS, nucleus stained with DAPI and visualised using Leica Confocal microscopy (Leica, UK).

4.5 Discussion:

This chapter has described the identification of sulphenic acids on proteins in primary human T cells for the first time and has shown that activation and oxidative stress can affect the presence of sulphenic acids discretely and independently. A method was optimised in which sulphenic acid modified proteins could be captured using the biotin tagged probe DCP-Bio1. Incubation of the probe at increasing concentrations showed that 1mM DCP-Bio1 was optimised for western blot experiments, as the band intensity did not increase further after the addition of 1 mM DCP-Bio1. Iodoacetamide (IAM), which is an alkylating agent, was used to block thiols to reduce non-physiological cysteine oxidation that could occur during lysis of cells. Although it is important to block thiols using alkylating agents such as IAM or N-ethylmaleimide (NEM) Reisz *et al* (159) have demonstrated that these reagents themselves could react with sulphenic acids thus competing with the probes that are used to detect the modifications. This could be a possible explanation as to why there are faint bands visible when adding IAM before treatment of DCP-Bio1 in T cells.

Under normal conditions cells maintain a reducing intracellular environment. A major factor influencing the redox status in the cytosol is the concentration of the cysteine containing tripeptide, GSH (160). BSO has been widely used to deplete GSH in T cells. BSO is preferred as a GSH depleting agent in cell culture and in primary cells since it does not appear to have any toxic effects (161). This was confirmed when cell viability was assessed after treatment of CD4+ T cells with BSO for 24 hours. CD4+ T cells exposed to BSO for 24 hours showed lower level of cellular GSH compared to untreated cells. Unreported experiments using lower concentrations of BSO (12.5 μ M) did not show a decrease in the total GSH levels. This decrease in GSH suggested that the cell was in a more oxidised environment. This would lead to more thiols being oxidised not only inside the cell but also potentially on the cell surface. Previous work from our lab has shown that BSO elicited a change in surface T cell Trx (108) Intracellular oxidative stress did affect the amount of surface thiols on the cell surface, after

being depleted of GSH by treatment of BSO for 24 hours, as shown by both DTNB assay and flow cytometry.

Thiol containing proteins undergo oxidation when cells are under oxidative stress. Among the various oxidation states of cysteine, cysteine sulphenic acid modifications are important as it is a reversible modification and has been implicated as a molecular switch to activate or deactivate protein function (42). Therefore the effects of GSH depletion on the formation of cysteine sulphenic acids was investigated and compared to T cells under normal conditions. To investigate sulphenic acid formation in T cells a method was developed using the biotin tagged dimedone based probe, DCP-Bio1. This probe specifically reacts with sulphenic acids either by a Michael addition or a nucleophilic substitution reaction (7). Once the probe was bound to the modified proteins, they were pulled out of the total cell lysate using streptavidin bound magnetic beads. When the proteins were eluted off the beads they were easily detected. The modified proteins will carry the biotin tag, which allows their detection via western blot methods and cellular localisation by fluorescence microscopy.

Following western blotting of T cell lysates, an increase in the number of sulphenated protein bands were present when cells are treated with BSO. A non-specific band was detected in all cell lysates following labelling with streptavidin peroxidase. Others have also reported this observation and it is suggested to be an endogenously biotinylated protein (1). Its mass was greater than any other band that could be specifically detected using DCP-Bio1 hence it is unlikely to interfere with other experiments that were designed to identify specifically sulphenated proteins. This suggests that when GSH levels were lower in the cells and the redox state of the T cell were disrupted, more proteins undergo cysteine oxidation and form stable sulphenic acids that can be captured and isolated.

In order to visualise the location of sulphenic acid formation, microscopy of the DCP-Bio1 and maleimide-labelled T cells was undertaken. It was anticipated that the membranes only would be labelled by maleimide Alexafluor due to its hydrophilicity but the data gathered here suggest that DCP-Bio1 may label intra and extra-cellular proteins. Although larger, DCP-Bio1 is a much more hydrophobic structure and at a molecular mass of 396.5 is

predicted to be membrane permeable. Microscopy confirmed that maleimide-Alexafluor labelled the cell membranes only. However, in the presence of DCP bio1, the membrane labelling was lost and instead co-localised staining of the nucleus was observed. In some images, there was apparent labelling of blebs with DCP bio1. These findings suggest that under the conditions used here, DCP bio1 is exerting some toxicity and this may limit its use in real time studies of sulphenic acid formation.

Reactive oxygen species are generated in response to mitogen-induced activation of naïve T cells (58). Therefore the hypothesis was that when T cells were activated the formation of protein sulphenic acid modifications would increase. To investigate the effects of activation, cells were treated with lectins, PHA-L or P. Increasing the concentrations of PHA-L and PHA-P reduced the percentage of viable cells. The cell viability and levels of CD25 expressed at the cell surface was measured after 24-hour treatment. CD25 expression is a key marker of T cell activation (70). When naïve CD4⁺ T cells become activated through the presentation of antigen by APCs, IL-2 secretion and IL-2R expression is stimulated. The interaction between IL-2 and IL-2R induces cell growth and differentiation (162). IL-2 secretion was measured by using IL-2 ELISA and CD25 expression was measured by flow cytometry. In both cases data showed that there was an increase in IL-2 secretion and CD25 expression with activation of T cells using 5 µg/mL PHA-L. Therefore for further experiments where cells were activated to detect protein sulphenic acid modifications, this concentration was used. When T cells were activated to look at sulphenic acid modifications, although an increase in the number of protein bands was expected, only two bands could be observed. However, when cells were activated under oxidative stress, the number of bands increased. Subsequent experiments by mass spectrometry analysis have identified several interesting proteins for the band at ~40 kDa. Peroxiredoxin-1 belongs to the 2-cys peroxiredoxins, which are responsible in the reduction of peroxides such as H₂O₂ through cysteine sulphenic acid formation at the active site and subsequently forming disulphide bonds with a second resolving cysteine (163). Experiments conducted by Morais *et al* (164) have demonstrated that pH changes can determine the formation of dimers or decamers of

peroxiredoxin-1. They have demonstrated that at physiological pH peroxiredoxins remain as dimers but with small changes to pH (8.0) the decamer is formed (164). The formation of a dimer which as a molecular mass of ~44 kDa fits well with the data and with the fact that under oxidative stress conditions sulphenic acids are formed. Another possibility for this protein is Arginase 1. Iyamu *et al* (165) have recently reported that oxidation of thiols leads to increased arginase activity in the cells and increases the levels of arginase 1 being produced. Aurothiomalate (ATM) a gold analogue forms a thiol gold adduct with cysteine thiols and prevents the thiols being oxidised. As expected, the enzyme activity decreased thereby proving the importance of cysteine oxidation (165). Since this protein band appears when T cells are treated with BSO whereby a more oxidised environment is present it is plausible that this could be the protein of interest. Furthermore studies by Ckless *et al* (166) have demonstrated that reduction of arginase activity leads to an increase in nitric oxide concentrations in cells, which results in a decrease in NF κ B activity. Therefore arginase 1 dependent nitric oxide regulation could have an influence in inflammatory diseases that are regulated by the transcription factor NF κ B (166). Actin is a main component of the cytoskeleton, which is involved, in many cellular functions including cell adhesion, growth and cytokinesis (167). Cell adhesion is important in various biological processes including inflammation and wound healing. In β -actin six cysteine residues are present but only one of them the Cys374 is exposed on the molecular surface, which makes it susceptible to oxidation. Recent studies by Sobierajska *et al* (168) have demonstrated that protein disulphide isomerase (PDI), which is a member of the thiol disulphide oxidoreductase family, interacts with β -actin to form disulphide bonds during cell adhesion to mediate cytoskeletal rearrangement (168). Perhaps the oxidation of actin Cys374 to form disulphide bonds occur via sulphenic acid formation as this was one of the proteins identified ~40 kDa protein band. The peptide sequences of these proteins do not cover any cysteine residues and therefore it is not possible to detect the DCP-Bio1 modification in any of the proteins. Perhaps different ionisation methods need to be employed in order to detect more modified peptides. Although

several proteins hits were obtained for bands 45 kDa and 50 kDa none of the proteins identified matched the molecular mass of the proteins and therefore were disregarded. A possibility for the proteins at ~65 kDa could be human serum albumin which has a mass around ~66 kDa and has been shown in chapter 3 to have a sulphenic acid that can be detected by DCP-Bio1.

T cell inactivation has been suggested to be due to oxidation of surface thiols. In models of rheumatoid arthritis (RA) a specific defect in ROS production led to more aggressive disease (109). Phillips *et al* (106) have shown that RA patients, who have hyperactive T cells, have lower ROS production. The model developed here, using BSO to deplete intracellular GSH, has simulated conditions of older adults without RA, who have lower intracellular GSH and refractory T cells. By identifying the proteins that are sulphenated in conditions of low GSH, in the future it will be possible to explore whether these proteins are differentially affected by RA and ageing.

Chapter 5.0 Synthesis of novel compounds for the detection of cysteine sulphenic acids

5.1 Preface:

This chapter describes the synthesis of two novel probes that have the potential to be targets for the detection of sulphenic acid modifications.

5.2 Introduction:

Sulphenic acids are highly unstable molecules that are difficult to isolate from biological systems. Therefore scientists have spent a significant amount of time synthesising sulphenic acids that could be used as a model system to better understand these moieties in a biological system (7). The first stable sulphenic acid, which was an anthraquinone-1-sulphenic acid, was reported by Fries in 1912. The formation of a hydrogen bond with the neighbouring carbonyl group gives this structure its stability (169). This and the synthesis of two other compounds, 1-methyluracil-4-sulphenic acid (170) and 1,3,6-trimethyluracil-7-sulphenic acid (171) which show similar stability due to hydrogen bonding lead to the conclusion that sulphenic acids in biological systems could be stabilised if hydrogen bonds could be formed (171). To explore the influence of steric hindrance in the stabilisation of sulphenic acids Yoshimura *et al* (172) synthesised a molecule, trans-decalin-9-sulphenic acid containing a trans-9-decalyl group with four axial protons. This molecule proved to be stable at room temperature for about 30 minutes before it was either converted to its disulphide or further oxidised to the sulphonic acid. When two molecules with the sulphenic groups come into close proximity the four axial protons causes a steric hindrance, which is attributed to the stability of the molecule (172). Another important contribution in finding out what contributes to the stability of sulphenic acids in a protein was done by Goto and co-workers in 1997 (173). They synthesised a bowl shaped cyclophane framework abbreviated as Bmt (4-tert-butyl-2,6-bis[(2,2'',6,6''-tetramethyl-m-terphenyl-2'-yl)methyl]phenyl) bearing a thiol which under mild oxidation could be oxidised to the corresponding sulphenic acid. The sulphenic acid proved to be stable towards self-condensation even after weeks of exposure to air because of its location inside the cavity. When reactions were carried out with reducing agents such as DTT it was reduced back to the thiol form. This Bmt framework mimics the environment of crevices often present in protein with sulphenic acid modifications. It has been suggested that the position of the cysteine on proteins are very important in the stable formation of sulphenic acids (173). Therefore these molecules give important information on why only some

sulphenic acids can be captured in a biological system. Apart from hydrogen bonding and limited solvent access as well as an apolar protein environment the absence of adjacent thiols is the major factor in the formation of sulphenic acids. This has been demonstrated by work done by Miller and co-workers using the enzyme glutathione reductase (GR) (174). The reduced form of GR has two cysteine thiols; Cys58 and Cys63. When Cys58 was reacted with small molecules like GSH formed mixed disulphides and became inactive. When this inactive form was oxidised further, sulphenic acid modification was detected at Cys63, which were not present when the active form was oxidised. Therefore elimination of the neighbouring cysteine stabilised the formation of Cys-SOH (174).

Although there was growing interest to understand the biological significance sulphenic acid formation, the initial evidence was indirect because there were no direct detection techniques. One of the most common methods used was stoichiometry and proving that the oxidation of some protein thiols was consistent with formation of sulphenic acids and not disulphide bonds. As an example, work done by Fraenkel-Conrat (175) indicated that in the tobacco mosaic virus (TMV) under certain conditions, when treated with iodine reacted to form sulphenyl iodine groups, which was based on the stoichiometry of the reaction (175). Over the years several elegant methods have been introduced to detect sulphenic acid formation directly in proteins as well as in cells in physiological conditions. While probes like DCP-Bio1 which is a biotinylated probe has been used in the identification of sulphenic acids in a number of proteins like GAPDH, papain and even in cell lysates the drawback of these probes are that because of their bulky nature they could have limitations on cell permeability and that they can cause steric hindrance and obstruct protein target labelling. To address these issues Carroll *et al* synthesised small molecules while still retaining the dimedone “warhead” added an azide or alkyne functional group to make dimedone analogues DAz-1, DAz-2, DYn-1 and DYn-2(1, 10, 66). The same group in 2009 developed a method using antibodies to detect protein sulphenic acid modifications. A synthetic hapten, which consists of the dimedone moiety on a cysteamine backbone with a five-carbon linker to keyhole limpet hemocyanin (KLH) was synthesized and was used to extract rabbit α -hapten-Ig gamma (IgG) (176).

Although much progress has been made over the recent years in the development of tools to detect SOH there is still scope for novel probes. As an example when DCP-Bio1 was used to identify SOH in primary T cells a possible toxic effect was observed. With this in mind the aim of this chapter was to synthesise a novel fluorescent probe that would be smaller than the existing probes to make them cell permeable and also reduce bulk steric hindrance and be able to monitor sulphenic acid formation in real time. The synthesis of the novel magnetic probe could be used to pull modified proteins directly from a cell lysate and then be cleaved off to detect the protein using methods such as mass spectrometry.

5.2.1 Strategy for the synthesis of fluorescent probe:

The aim of this work was to synthesise a new fluorescent probe for the detection of sulphenic acids. The general structure of the probe is described in **Figure 5.1**. Based on this general structure, compound 1 has been proposed as a potential probe.

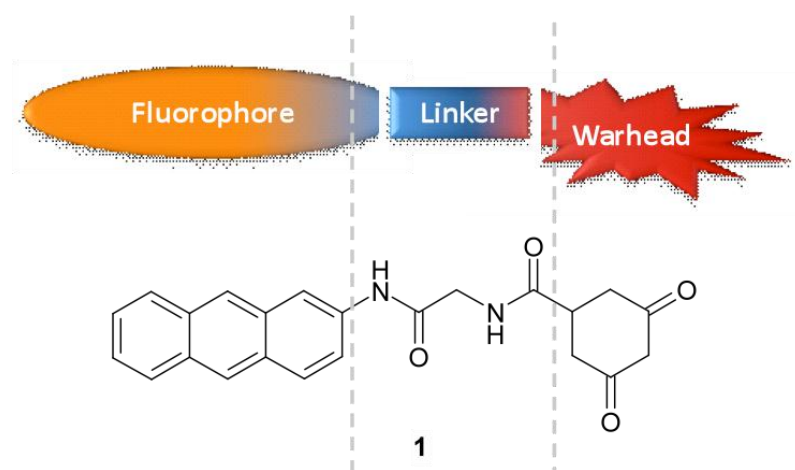


Figure 5.1: General structure of the fluorescent probe.

The diketocyclohexane ring was chosen as a warhead, as it is a dimedone like molecule and can act as a nucleophile to attack the sulphur atom of the cysteine sulphenic acid. The anthracene group will be used as a fluorophore. Both moieties will be connected through a glycine linker, which is relatively short, but will still bring flexibility to the molecule to enhance targeting of sulphenic acids.

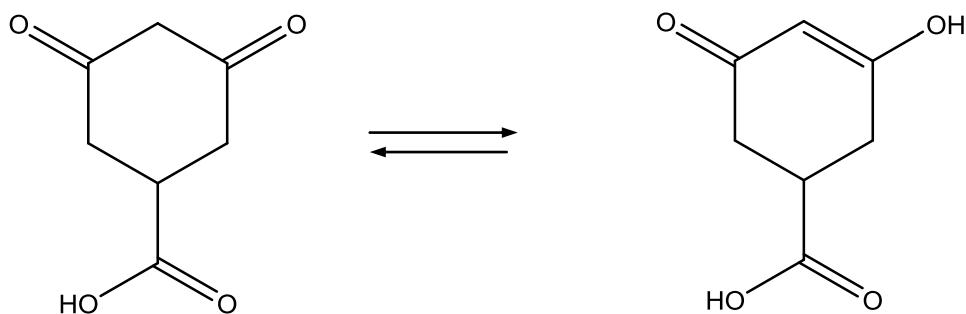
5.3 Materials and methods:

5.3.1 Materials:

Unless otherwise noted all reactions were performed in oven dried glassware. Chemicals unless stated, were obtained from Sigma (Sigma-Aldrich, UK) or Fisher (Fisher Scientific, UK) without further purification. Magnabind amine linked magnetic beads were from Invitrogen (Invitrogen, Sweden). All work was carried out at Aston University in the medicinal chemistry laboratory, NMR and instrumentation suits. All experiments were COSHH assessed using the standard practices in the medicinal chemistry laboratory. Thin layer chromatography (TLC) was carried out using Millipore 60 F₂₅₄ silica gel sheets. TLC plates were visualised using a combination of UV, ninhydrin, vanillin and potassium permanganate staining. Flash chromatography was performed using silica gel (40-63 µm pore size) from Millipore. Dry column chromatography was performed using Kieselgel 60G (Merck, Germany). NMR spectra were obtained using a Bruker AC250 (250 MHz for ¹H; 62.9 MHz for ¹³C) spectrometer. ¹H and ¹³C NMR chemical shifts are reported as parts per million (ppm) relative to TMS (0.00 ppm) with its solvent peak used as an internal reference. Infra-red (IR) spectra were obtained with samples made of KBr discs on a Mattson 3000 FT spectrometer or Thermo Scientific Nicolet is5 with iD5 ATR attachment as a solid sample. Melting points were obtained using a Reichert-Jung Thermo Galen hot stage microscope. Fluorescence spectrometry was done on Spectramax GeminiXS using softmax proV5 software for analysis. Mass spectrometry was performed on a Waters 2795 LC/MS using Mass lynx software.

5.3.2 Methods:

5.3.2.1 Synthesis of 3,5-diketohexahydrobenzoic acid:



Using a method adapted by Hildahl *et al* (61) 3,5-dihydroxybenzoic acid (15.4 g, 0.1 mol), sodium hydroxide (8.8 g, 0.22 mol) and Raney nickel (0.1 g) was mixed with water (45 mL) and added to the hydrogenator. The hydrogenation was carried out overnight at 50 °C, 42 bars with continuous stirring. The solution was cooled in an ice bath; the Raney nickel filtered off and acidified using concentrated hydrochloric acid (30 mL). The solution was kept at 4 °C overnight to give white crystals which were vacuum dried to give white crystals with a yield of 9.6 g (61.4%)

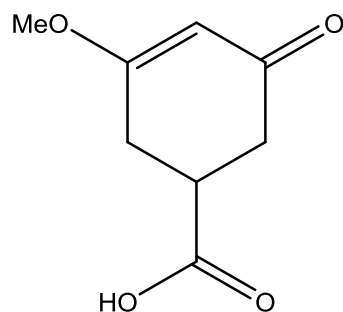
R_f (Methanol: ethyl acetate: acetic acid 1:1:0.1): 0.44

Melting point: 178.2-179.0 °C (reference (61) 178.0-178.7 °C)

IR (KBr): 844, 1133, 1266, 1197, 1312, 1600, 1687, 1947, 3200 cm^{-1}

Mass spectrum (TOF MS ES+) ($M+\text{Na}^+$) m/z : = 179.01 expected: 179.12

5.3.2.2 Synthesis of 3-methoxy-5-oxocyclohex-3-ene-1-carboxylic acid:



3,5-diketohexahydrobenzoic acid (0.2 g, 1.34 mmol), p-toluenesulphonic acid (PTSA) (0.013 g, 0.067 mmol) was added to methanol (10 mL) in a round bottom flask purged with argon and stirred at room temperature for 10 minutes. The reaction mixture was concentrated on the rotary evaporator. The white solid was purified by silica gel chromatography eluting with 9:1 ethyl acetate: methanol to give a white solid in a yield of 0.207 g (91%).

R_f (Ethyl acetate: methanol 1:1) : 0.55

Melting point: 196.3-199.6 °C

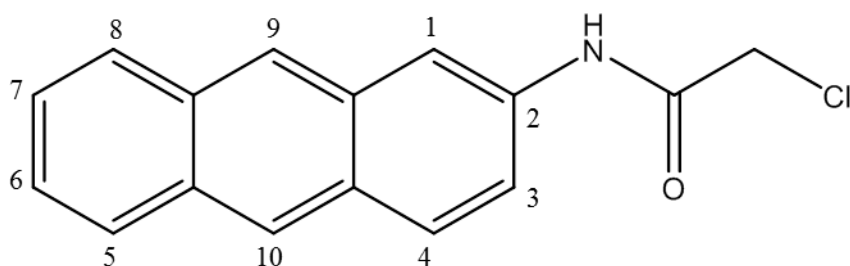
^1H NMR DMSO (250 MHz) δ : 2.45 (d, 2H) ppm, 2.64-2.61 (m, 2H), 2.99-3.07 (m, 1H), 3.68 (s, 3H), 5.36 (s, 1H) ppm

^{13}C NMR DMSO (63 MHz) δ : 30.73 (C2), 37.53 (C1), 38.38 (C6), 55.84 (CH₃), 101.42 (C4), 174.18 (C=OCH₃), 176.32 (C=OOH), 195.89 (C=O) ppm

IR: 3206.91, 2916.92, 2507.53, 1931.81, 1684.47, 1556.53, 1415.80 cm^{-1}

Mass spectrum (TOF MSES+) ($\text{M}+\text{Na}^+$) m/z : 193.03 expected: C₈H₉O₄Na: 193.16

5.3.2.3 Synthesis of N-(anthracen-2-yl)-2-chloroacetamide:



Chloroacetyl chloride (0.41 mL, 5.2 mmol) was added drop wise to a solution of 2-aminoanthracene (0.1 g, 0.52 mmol) in 5 mL DCM and TEA (0.72 mL, 5.2 mmol). The reaction was refluxed at for 2 hours and monitored by TLC. Upon completion the solvents were evaporated and the solid was washed with water and the light brown precipitate was vacuum filtered and dried under vacuum to give a light brown powder in a final yield of 1.30 g (93%).

R_f (Methanol: ethyl acetate 1:1) : 0.88

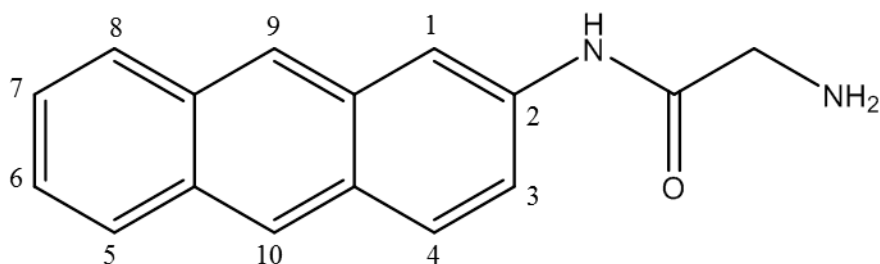
Melting point: 233.4-235.6 °C

^1H NMR DMSO (250 MHz) δ : 10.5 (s, 1H, NH), 8.5 (m, 3H, CH), 8.0 (m, 3H, CH), 7.5 (m, 1H, CH), 7.4 (m, 2H, CH), 4.3 (s, 2H, CH₂) ppm

^{13}C NMR DMSO (63MHz) δ : 165.0 (C=O), 135.41 (C2), 133.68 (C9C1), 131.69 (C8C9), 131.37 (C10C5), 130.53 (C4), 129.04 (C8), 128.59 (C5), 128.05 (C4C10), 127.70 (C7), 125.89 (C6), 125.71 (C10), 125.22 (C9), 125.10 (C3), 120.67 (C1), 43.64 (CH₂Cl) ppm

IR: 3262.78, 3044.31, 2367.66, 1921.61, 1657.62, 1569.63 cm⁻¹

5.3.2.4 Synthesis of 2-amino-N-(anthracen-2-yl) acetamide:



N-(anthracen-1-yl)-2-chloroacetamide (0.25 g, 0.92 mmol) and urotropine (0.26 g, 1.84 mmol) was dissolved in THF (10 mL) and water (0.1 mL) and refluxed overnight. The precipitate was filtered off vacuum dried and dissolved in methanol (20 mL) and HCl (2 M, 1 mL) and refluxed for 2 hours while monitoring by TLC. The solvent was evaporated and the precipitate was re-dissolved in acetone (10 mL) and stirred at room temperature for 10 minutes. The precipitate was vacuum filtered to give a yellow product with a yield of 0.087 g (38%).

R_f (Petroleum ether: ethyl acetate 1:1): 0.2

Melting point: 231.6-235.5 °C

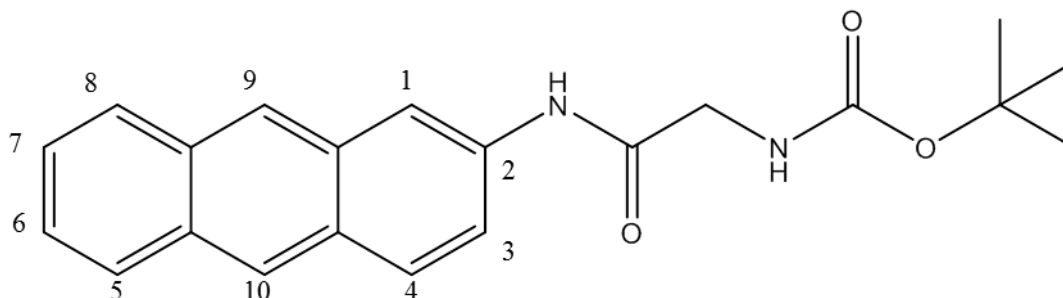
¹H NMR DMSO (250 MHz) δ : 10.72 (s, 1H, NH), 8.54 (m, 3H, CH), 8.22 (NH₂), 8.05 (m, 3H, CH), 7.60 (m, 1H, CH), 7.52 (m, 2H, CH), 3.90 (s, 2H, CH₂) ppm

¹³C NMR DMSO (63 MHz) δ : 165.16 (C=O), 135.31 (C2), 131.69 (C9C1), 131.38 (C8C9), 130.51 (C10C5), 129.09 (C4), 128.56 (C8), 128.05 (C5), 127.66 (C4C10), 125.94 (C7), 125.73 (C6), 125.15 (C10), 125.11 (C9), 120.51 (C3), 114.16 (C1), 41.10 (CH₂NH₂) ppm

IR: 3378.84, 2629.93, 2358.15, 1708.90, 1669.64, 1630.39 cm⁻¹

Mass spectrum (TOF MS ES+) m/z: 251.16 expected C₁₆H₁₄N₂O 250.29

5.3.2.5 Synthesis of tert-butyl [2-(anthracen-2-ylamino)-2-oxoethyl]carbamate:



To a cold solution (ice bath) of N-Boc-glycine (168 mg, 0.96 mmol) in dry THF (8.0 mL), triethylamine (148 μ L, 1.06 mmol) and ethyl chloroformate (91 μ L, 0.96 mmol) were added dropwise. The mixture was stirred for 30 minutes in the ice bath before adding a solution of 2-aminoanthracene (185 mg, 0.96 mmol) in 12 mL of dry THF. The reaction mixture was stirred at room temperature overnight and monitored with TLC. The compound was extracted 3 times with ethyl acetate (20 mL) and washed with saturated sodium bicarbonate (3 x 30 mL) and 0.1 M hydrochloric acid (3 x 30 mL). The solvent was evaporated and purified with dry column chromatography to give the final product in a yield of 0.302 g (90%) as a light yellow powder.

R_f (Petroleum ether: ethyl acetate 1: 1): 0.50

Melting point = 186.3 -187.8 $^{\circ}$ C

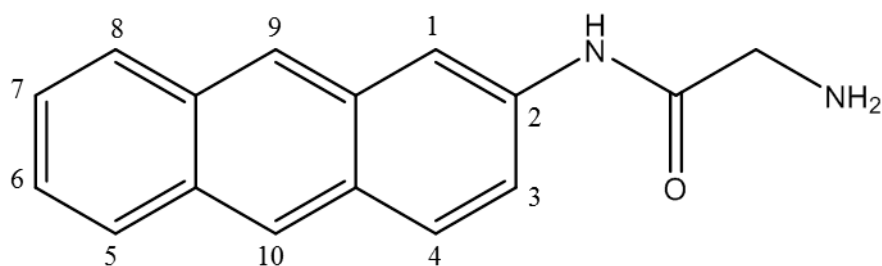
^1H NMR DMSO (250 MHz) δ : 10.12 (s, 1H, NH), 8.53 (m, 3H, CH), 8.06 (m, 3H, CH), 7.64 (m, 1H, CH), 7.47 (m, 2H, CH), 3.82 (d, 2H, CH_2), 1.44 (s, 9H, CH_3) ppm

^{13}C NMR DMSO (63 MHz) δ : 168.64 (C=O), 156.04 (OC=O), 135.89 (C2), 131.68 (C9CC1), 131.58 (C8CC9), 130.36 (C10CC5), 128.84 (C4), 128.46 (C8), 128.03 (C5), 127.66 (C4CC10), 125.81 (C7), 125.59 (C6), 124.91(C10), 120.85 (C9), 119.02 (C3), 113.79 (C1), 78.15 (C(CH₃)₃), 43.88 (CH₂), 28.2 (3C, C(CH₃)₃) ppm

IR: 3312.40, 3273.15, 2974.19, 2358.15, 1690.78, 1657.56, 1361.62 cm^{-1}

Mass spectrum (TOF MS ES-) m/z: 349.1314 Expected C₂₁H₂₂N₂O₃: 350.42

5.3.2.6 Synthesis of 2-amino-N-(anthracen-2-yl) acetamide by removal of Boc protection:



tert-Butyl [2-(anthracen-2-ylamino)-2-oxoethyl]carbamate (0.3 g, 0.85 mmol) was dissolved in 35 mL of DCM at room temperature and trifluoroacetic acid (TFA) (8.5 mL) was added to it. The reaction was left to stir for 10 minutes and monitored by TLC. The solvents were evaporated under reduced pressure and the residue was dissolved in ethanol 2 times and evaporated to remove any TFA residue to afford the title compound in 85% yield (0.18 g) as a yellow powder.

R_f (Petroleum ether: ethyl acetate 1:1): 0.20

Melting point: 231.6-235.5 °C

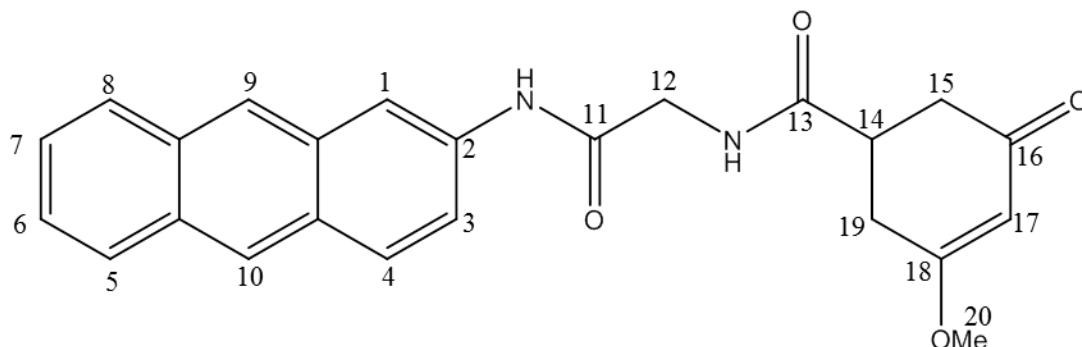
¹H NMR DMSO (250 MHz) δ : 10.72 (s, 1H, NH), 8.54 (m, 3H, CH), 8.22 (NH₂), 8.05 (m, 3H, CH), 7.60 (m, 1H, CH), 7.52 (m, 2H, CH), 3.90 (s, 2H, CH₂) ppm

¹³C NMR DMSO (63MHz) δ : 165.16 (C=O), 135.31 (C2), 131.69 (C9C1), 131.38 (C8C9), 130.51 (C10C5), 129.09 (C4), 128.56 (C8), 128.05 (C5), 127.66 (C4C10), 125.94 (C7), 125.73 (C6), 125.15(C10), 125.11 (C9), 120.51 (C3), 114.16 (C1), 41.10 (CH₂NH₂) ppm

IR: 3378.84, 2629.93, 2358.15, 1708.90, 1669.64, 1630.39 cm⁻¹

Mass spectrum (TOF MS ES+) m/z: 251.16 expected C₁₆H₁₄N₂O 250.29

5.3.2.7 Synthesis of N-[(2-anthracen-2-ylamino)-2-oxoethyl]-3-methoxy-5-oxocyclohex-3-ene-1-carboxamide:



To a cold solution (ice bath) of 3-methoxy-5-oxocyclohex-3-ene-1-carboxylic acid (168 mg, 0.96 mmol) in dry DMF (8.0 mL), triethylamine (148 μ L, 1.06 mmol) and ethyl chloroformate (91 μ L, 0.96 mmol) were added drop wise over 5 minutes. The mixture was stirred for 30 minutes in the ice bath before adding a solution of 2-amino-N-(anthracen-2-yl)acetamide (240 mg, 0.96 mmol) in 12 mL of dry DMF and TEA (148 μ L, 1.06 mmol). The reaction mixture was stirred at room temperature overnight and monitored by TLC. The solvent was evaporated and purified with dry column chromatography eluting with ethyl acetate: methanol 9:1 to give the final product in 43% (0.165 g) yield as a pale yellow powder.

R_f (Ethyl acetate: methanol 1:1): 0.88

Melting point: 245.4-247.8 $^{\circ}$ C

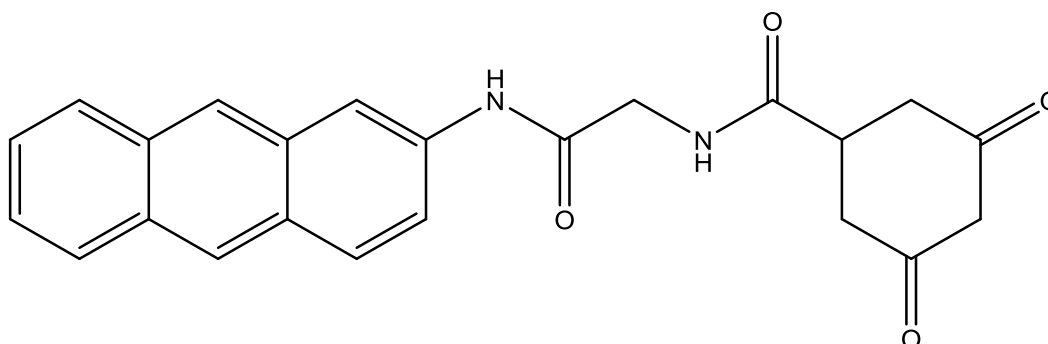
^1H NMR DMSO (250 MHz) δ : 10.25 (s, 1H,NH), 8.51 (m, 3H,CH), 8.05 (m, 3H,CH), 7.60 (m, 1H,CH), 7.52 (m, 2H,CH), 5.36 (s, 1H), 4.01 (s, 2H,CH₂), 3.72 (s, 3H,CH₃), 3.03-3.12(m, 1H), 2.74 (s, 1H), 2.67(s, 1H), 2.44 (d, 2H) ppm

^{13}C NMR DMSO (63 MHz) δ : 196.29(C16), 176.56 (C13), 172.63 (C11), 168.01 (C18), 135.79 (C2), 131.67 (C9CC1), 131.56 (C8CC9), 130.39 (C10CC5), 128.85 (C4), 128.48 (C8), 128.09 (C5), 128.03 (C4CC10), 127.65 (C7), 125.83 (C6), 125.61 (C10), 124.94 (C9), 120.87 (C3), 113.92 (C1), 101.48 (C17), 55.98 (C20), 42.79 (C12), 31.00 (C19) ppm

IR: 3274.92, 2944.18, 2364.62, 2161.32, 2161.32, 1697.07, 1630.31 cm^{-1}

Mass spectrum (TOF MS ES+) (M+CN⁻) m/z: 429.39 expected: C₂₅H₂₂N₃O₄: 429.45

5.3.2.8 Synthesis of N-[2-(anthracen-2-ylamino)-2-oxoethyl]-3,5-dioxocyclohexanecarboxamide:



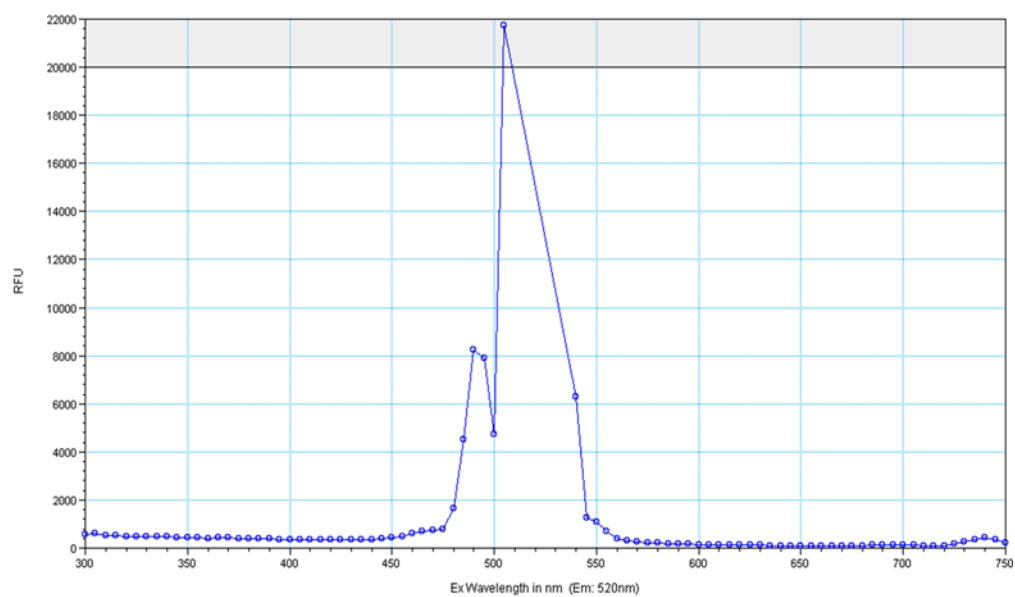
N-[(2-anthracen-2-ylamino)-2-oxoethyl]-3-methoxy-5-oxocyclohex-3-ene-1-carboxamide (0.03 g, 0.074 mmol) was dissolved in DMF (5 mL) and 1 M HCl (2 mL) was added to it and stirred at room temperature for 1 hour. The reaction was monitored by TLC and the solvent was evaporated to get the crude product of light brown powder in 23% (0.006 g) yield.

R_f (Methanol: ethyl acetate 1:1): 0.55

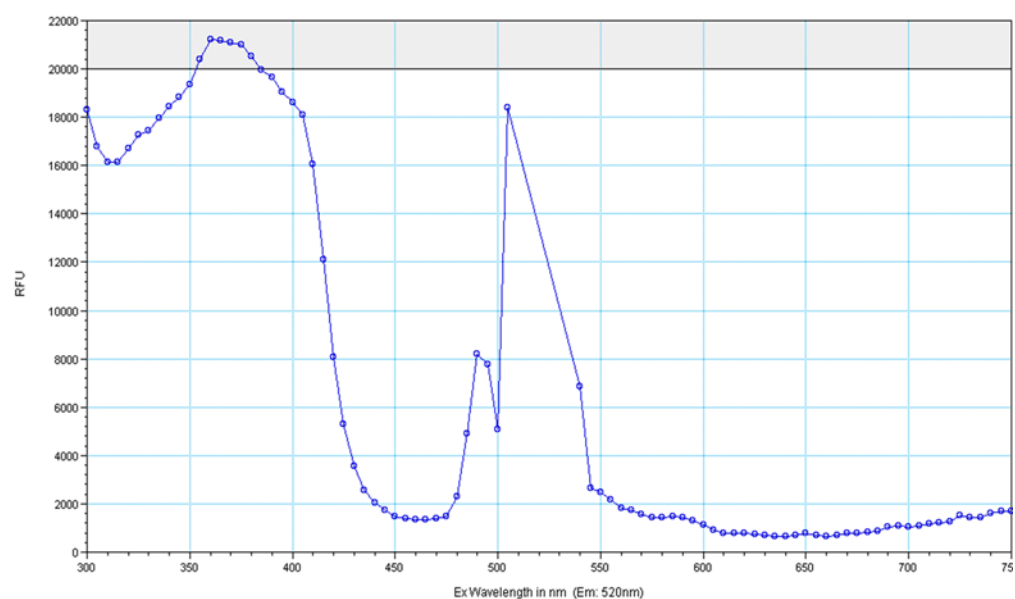
¹H NMR DMSO (250 MHz) δ : 10.43 (s, 1H,NH), 8.50 (m, 3H,CH), 8.07 (m, 3H,CH), 7.65 (m, 1H,CH), 7.52 (m, 2H,CH), 5.29 (s, 1H), 4.02 (s, 2H,CH₂), 2.98-3.07 (m, 1H), 2.62(s, 1H), 2.42 (d, 2H) ppm

5.3.2.9 Fluorescence spectrometric analysis of N-[2-(anthracen-2-ylamino)-2-oxoethyl]-3,5-dioxocyclohexanecarboxamide

N-[2-(Anthracen-2-ylamino)-2-oxoethyl]-3,5-dioxocyclohexanecarboxamide (0.0005 g) was dissolved in 1 mL of DMSO and 200 μ L was transferred on to Costar™ 96-Well Black plates (Fisher Scientific, UK) in triplicates along with 200 μ L of DMSO in triplicates as the blank. The samples were run on the Spectramax GeminiXS, setting the instrument to read fluorescence. In the first instance the excitation wavelength was fixed at 300 nm and an emission sweep was done between 300-750 nm with no cut-offs and a wavelength increment of 5 nm. The maximum emission was determined as 520 nm. In the next instance this was set as the emission wavelength and the excitation wavelength was varied from 300-750 nm. **Figure 5.2 (top)** shows the excitation spectrum of DMSO and **Figure 5.2 (bottom)** shows the excitation spectrum of the compound, which has an excitation of 385 nm.



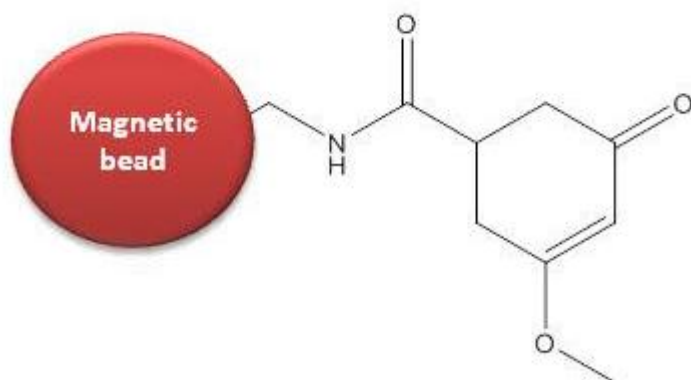
Well B2
 Lambda at Maximum 490.00



Well B3
 Lambda at Maximum 385.00

Figure 5.2: Fluorescence excitation spectra of N-[2-(anthracen-2-ylamino)-2-oxoethyl]-3,5-dioxycyclohexanecarboxamide in DMSO and DMSO.

5.3.2.10 Synthesis of reagent tagged magnetic probe:



Amine linked magnetic beads (0.2 mL) were washed with 2-[N-morpholino]ethane sulphonic acid (MES) (0.1 M, pH 4.5, 1 mL) three times. 3-methoxy-5-oxocyclohex-3-ene-1-carboxylic acid (0.1 g) was dissolved in 10 mL of MES. Separately a solution was prepared by dissolving 1-ethyl-3-(3-dimethylaminopropyl)carbodiimide (EDC) (0.1 g) and N-hydroxy succinimide (NHS) (0.15 g) in 10 mL of deionised water. 5 mL of this solution was added to the previous solution and incubated for 2 hours at room temperature with tilt rotation to get the final compound.

Since the compound has a magnetic bead, analysis with NMR or mass spectrometry was not possible. Therefore an infrared spectrum was taken and compared to the starting material, which is discussed in detail in results and discussion.

IR: 2925.97, 2850.11, 1502.87, 1433.08, 1381.50 cm^{-1}

5.4 Results and discussion:

5.4.1 Retrosynthetic approach for fluorescent probe to detect sulphenic acid:

The desired final fluorescent probe has been deconstructed according to the following retrosynthetic approach (**Figure 5.3**). Compound 1 can be obtained by coupling 3,5-diketohexahydrobenzoic acid (**Figure 5.3, 2**) with the free amine (**Figure 5.3, 3**). The latter can be obtained by acylation of the commercially available 2-aminoanthracene.

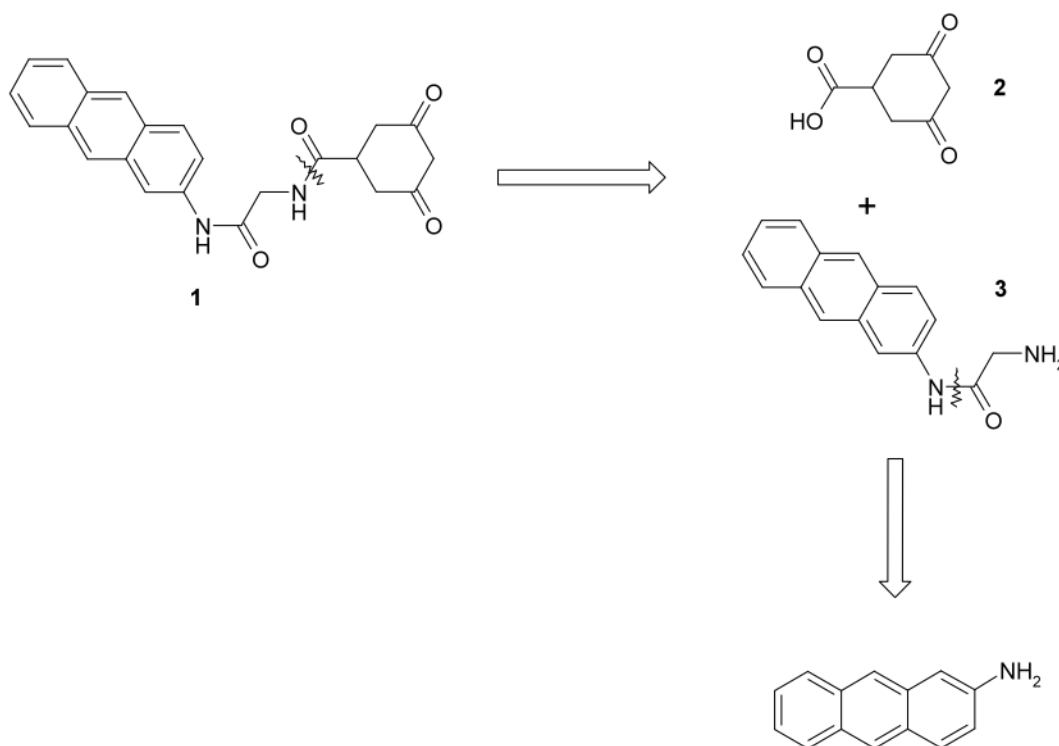


Figure 5.3: Schematic representation of retrosynthetic approach for sulphenic acid fluorescent probe (1).

5.4.2 First synthesis of synthon 3

Two different strategies have been adopted for the synthesis of synthon **3**. Firstly, the bifunctional chloroacetyl chloride was used to convert 2-aminoanthracene to the corresponding chloroacetamide **4** (Figure 5.4). Primary and secondary amines are known to react with chloroacetyl chloride to form amides (177, 178). Between the chlorides in the molecule the acyl chloride is known to be more reactive towards nucleophiles. It is also important to have a base such as triethyl amine (TEA) present as the reaction produces HCl, which will be neutralised by the presence of a base and will drive the reaction to completion (177). Coupling of 2-aminoanthracene with chloroacetyl chloride in DCM in the presence of TEA at room temperature led to the acylated compound **4** in a 93% yield.

2-Aminoanthracene and 9-Aminoacridine were chosen as two fluorescent molecules for the starting materials. While the synthesis was successful for 2-aminoanthracene the reaction failed to occur with 9-aminoacridine. Although experiments were carried out using different reaction conditions there was no success. One possibility for this could be because 9-aminoacridine has a nitrogen in its ring structure by which the lone pair on the NH₂ gets delocalised in the ring making it less reactive than 2-aminoanthracene. Therefore for further experiments only 2-aminoanthracene was used.

Subsequent reaction of compound **4** with urotropine (also known as hexamethylenetetramine) in THF, followed with hydrolysis using 2 M HCl in methanol gave the desired free amine **3** (Figure 5.4) with a 38% yield.

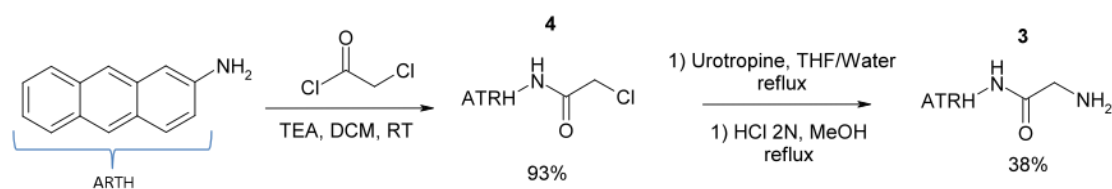


Figure 5.4: Reaction conditions for the synthesis of 2-amino-N-(anthracen-2-yl)acetamide

The production of primary amines from alkyl chlorides using urotropine is known as the Délepine reaction and is a very convenient way to produce primary amines selectively (179). Ammonia could also be used to synthesise amines from alkyl chlorides. However, if ammonia is used instead, the formation of the corresponding secondary and tertiary amines as side products is very likely, unless ammonia is used in excess, which might not be tolerated depending on the substrate. The reaction mechanism for the amine formation with urotropine is outlined below in **Figure 5.5**.

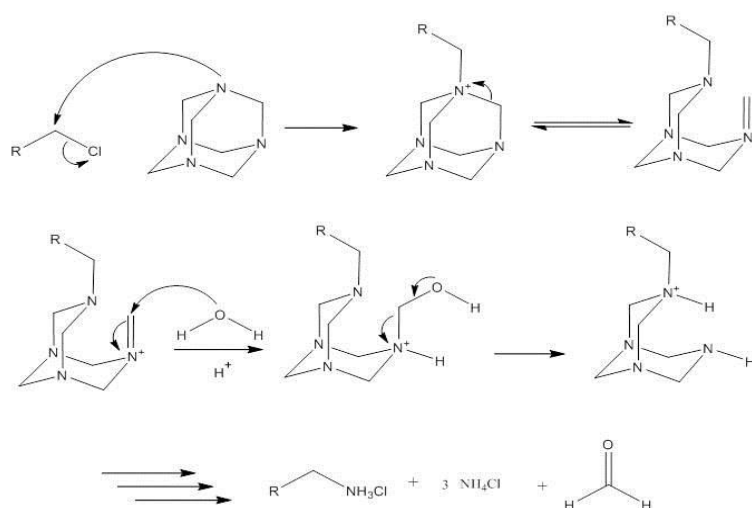


Figure 5.5: Reaction mechanism for the formation of an amine

The formation of the hexamethylenetetramine salt proceeds via an S_N2 reaction. While the starting materials are soluble in the organic solvent the salt crystallizes out. This compound is then treated to acid hydrolysis where the salt decomposes to yield the amine hydrochloride, ammonium chloride and formaldehyde (179). This reaction was quite difficult to optimise and the yield of the product was relatively low. Although different solvents were used and the reaction was left for longer periods with urotropine in excess, the yield did not improve. One

reason could be that because the starting material as well as urtropine is bulky in nature steric hindrance caused the relatively low reactivity between the compounds. However, in this case, the yield for the formation of the primary amine was moderate (38 %) and not always reproducible. Therefore an alternative route was explored for the synthesis of synthon **3**.

5.4.3 Second strategy for the synthesis of synthon **3**

2-aminoanthracene was reacted with an N-protected glycine derivative. It is important to use glycine where the NH₂ group has been protected in order to prevent side reactions. Boc-glycine was thus reacted with ethyl chloroformate in THF at 0 °C to form the mixed anhydride, which was then reacted with 2-aminoanthracene to yield the desired acetylated compound **5** (**Figure 5.7**) in a 90% yield after dry column chromatography. The reaction mechanism for the mixed anhydride formation is outlined below in **Figure 5.6** (178).

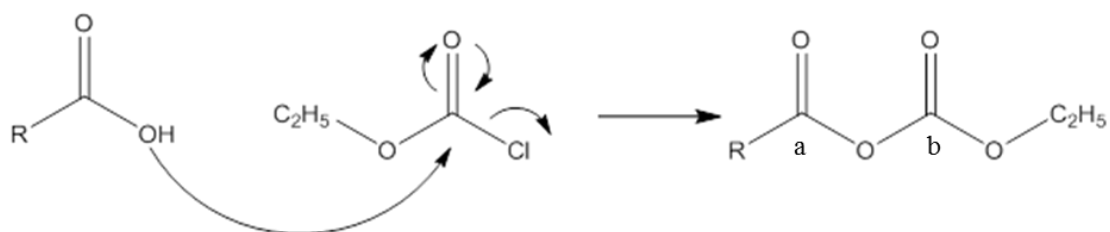


Figure 5.6: Reaction mechanism for mixed anhydride formation

The carboxylic acid was deprotonated by the base TEA, and the slightly nucleophilic oxygen reacts on ethyl chloroformate to produce the mixed anhydride. When the amine is added to the reaction mixture, it could then react on both carbons **a** and **b**. However, carbon **a** is much more electrophilic than carbon **b** due to the presence of only one mesomer donor oxygen and therefore the amine will preferentially react with **a** to give the desired product. Boc deprotection using TFA in DCM finally gave free amine **3** in a 85% yield (**Figure 5.7**). It has to be noted that this second synthetic route allowed the synthesis of synthon **3** in a much shorter reaction time and with highly improved yield compared to the first one. However

optimising the reaction conditions were lengthy and purification steps were needed to remove unreacted starting material and side products.

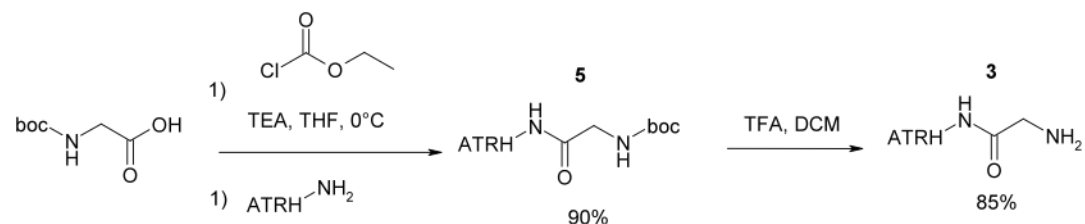


Figure 5.7: Reaction conditions for the synthesis of 2-amino-N-(anthracen-2-yl)acetamide via synthetic route 2

The reaction for the removal of the Boc group was very rapid. Initial experiments where the reaction was left for 1 hour at room temperature revealed 2 spots on the TLC, which were both, visualised when stained with ninhydrin. An NMR of this crude product led to the conclusion that both amide bonds had been cleaved off which left a mixture of 2-aminoanthracene and 2-amino-N-(anthracen-2-yl) acetamide. Therefore the reaction was closely monitored with TLC. As soon as the acid was added and the second spot was observed after 10 minutes of stirring, the reaction was stopped. To remove excess TFA the crude product was dissolved in ethanol twice and put on the rotary evaporator. The advantage of using an acid such as TFA for the boc deprotection is that it is soluble in a wide range of organic solvents and because of its volatility is easily removed without any work up procedures (180). The NMR of 2-amino-N-(anthracen-2-yl)acetamide is shown below in **Figure 5.8**.

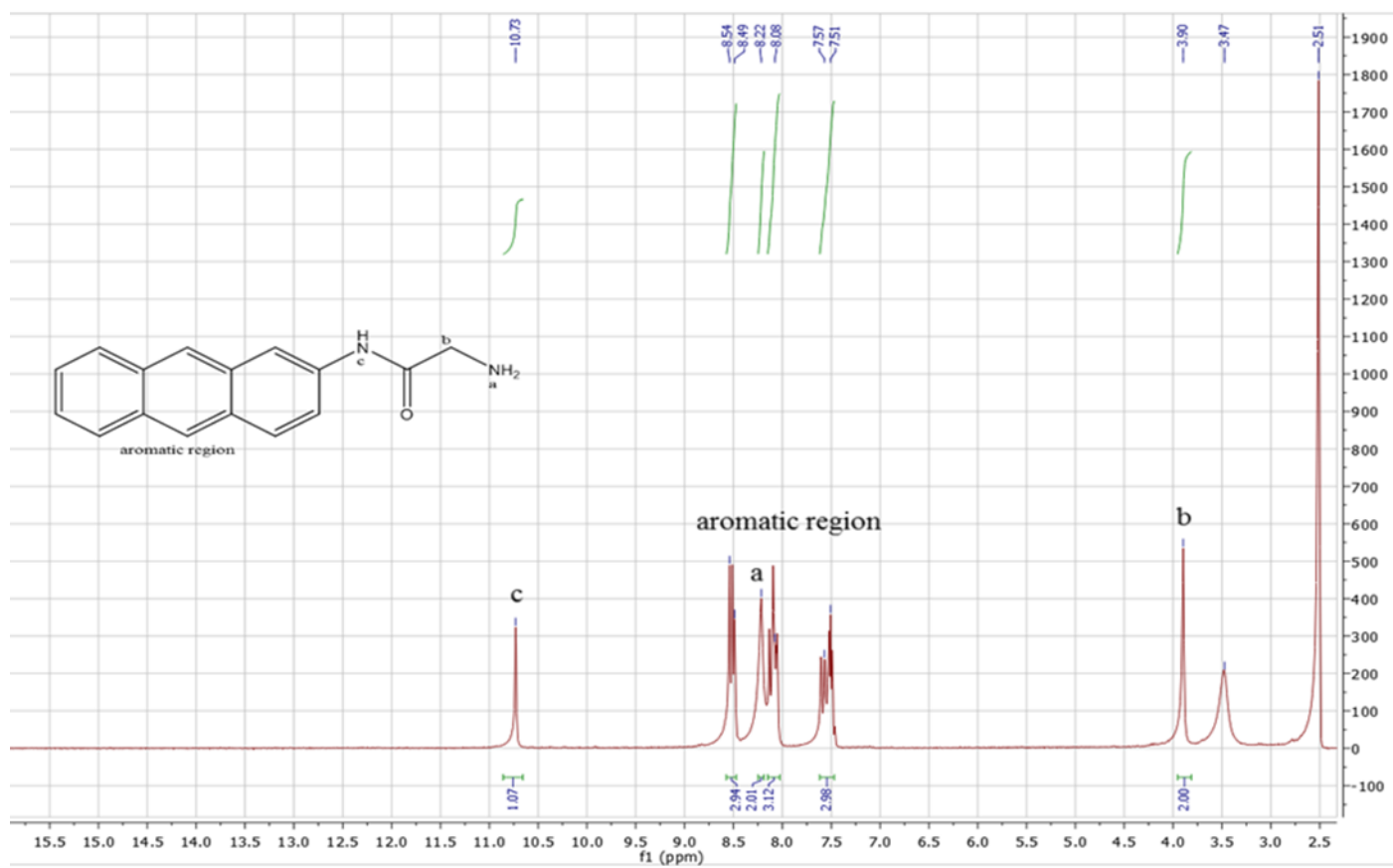


Figure 5.8: ^1H NMR spectrum of 2-amino-N-(anthracen-2-yl)acetamide

5.4.4 Synthesis of synthon 2

Synthon 2 was obtained by hydrogenation of 3,5-dihydroxybenzoic acid (61). Hydrogenation typically constitutes of the addition of pairs of hydrogen atoms to a molecule. Normally catalysts are required for the reaction to occur, as there is a high free energy of activation. There are two types of hydrogenation catalysts, homogenous and heterogeneous catalysts. Heterogeneous catalysts are the type that is mostly used for the majority of hydrogenation reactions. They are solids that form a distinct phase in the gas or liquid environment (181). Homogenous catalysts tend to dissolve in the liquid phase forming one single phase. Experiments for the hydrogenation of 3,5-dihydroxybenzoic acid were carried out using both types of catalysts. Palladium on carbon, palladium hydroxide on carbon, rhodium on carbon and Raney-Ni were used as heterogeneous catalysts and chlorotris(triphenylphosphine)rhodium(I) (Wilkinson's catalyst) was used to represent homogenous catalysts. The reaction conditions and corresponding yields are shown in the **Table 5.1** below.

Catalyst	Reaction conditions	Yield (%)
Pd/C	H ₂ O, 50 °C, 42 bar, overnight	0
Pd (OH) ₂ /C	H ₂ O, 50 °C, 42 bar, overnight	0
Rh/C	H ₂ O, 50 °C, 42 bar, overnight	0
Raney-Ni	H ₂ O, NaOH, 50 °C, 42 bar, overnight	62.3
Wilkinson's	H ₂ O, 50 °C, 42 bar, overnight	0

Table 5.1: Hydrogenation using different catalysts

A hydrogenation bomb was used to run each of these reactions. TLC analysis of the reaction mixtures suggested that only Raney-nickel was able to convert the starting material. The

identity of the product was confirmed by NMR. For the NMR of 3,5-diketohexahydrobenzoic acid a singlet for hydrogens 1 (with an integration of 2 for 2 protons), 1 Doublet for hydrogens 2 and 3 and 1 quintet for hydrogen 4 was expected (**Figure 5.9,A**). However the NMR of the synthesised product had only three peaks visible with a singlet at 5.20, which integrated for 1 proton. The CH₂ peaks are possibly around 2.5 and cannot be detected as the DMSO peak is also at 2.5. This suggests that in solution it mainly exists as its tautomeric form (**B, Figure 5.9**). The B form is more stable than the A form due to the formation of a hydroxyl-enone system where electrons can be delocalized, thus reducing the global energy of the system.

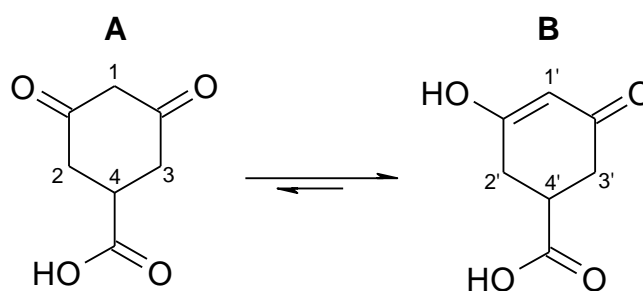


Figure 5.9: Tautomeric structures of 3,5-diketohexahydrobenzoic acid in solution.

5.4.5 Synthesis of the probe

Both synthons **2** and **3** had been obtained at this stage and needed to be coupled together. However, synthon **2** needed to be protected beforehand. Indeed, it holds two potential keto moieties which are highly electrophilic centers and can potentially react with the free amine of synthon **3** during the coupling step, leading to poor yields. Synthon **2** was thus protected using an enol ether function that was introduced by reacting it with catalytic amount of PTSA in methanol for 10 minutes at room temperature (**Figure 5.10**). This led to compound **6** in a 93% yield.

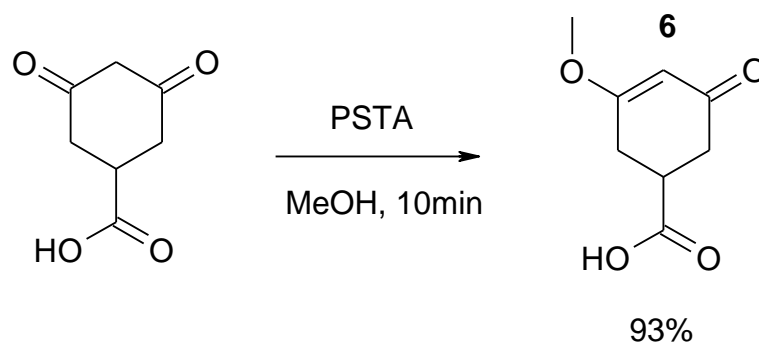


Figure 5.10: Protection of 3,5-diketohexahydrobenzoic acid

One possibility for the reaction mechanism is that PTSA forms a tosylate ester with methanol and then that the enol reacts with the methyl group, as tosylate is a good leaving group. The reaction time is very important for this reaction. When the reaction was left for longer period of time a second spot could be observed on the TLC. This is certainly due to the fact the carboxylic acid function can undergo esterification in the presence of a large excess of methanol and acidic catalysis. The proton NMR of the protected compound is shown below in **Figure 5.11**. The peak at 2.5 corresponds to the DMSO peak, which is the solvent used for the NMR. Proton a is the most deshielded proton as its situated between two electron withdrawing groups and therefore is found downfield on the spectrum. Next are the CH₃-protons as they are attached directly to electron withdrawing oxygen. The integration or the area under the peak indicates the number of protons present, which in this case are 3. The d proton is present as a multiplet because it has 4 other protons in its vicinity, which results from spin coupling. The protons b, c are the least deshielded and they appear the most upfield on the spectrum (182).

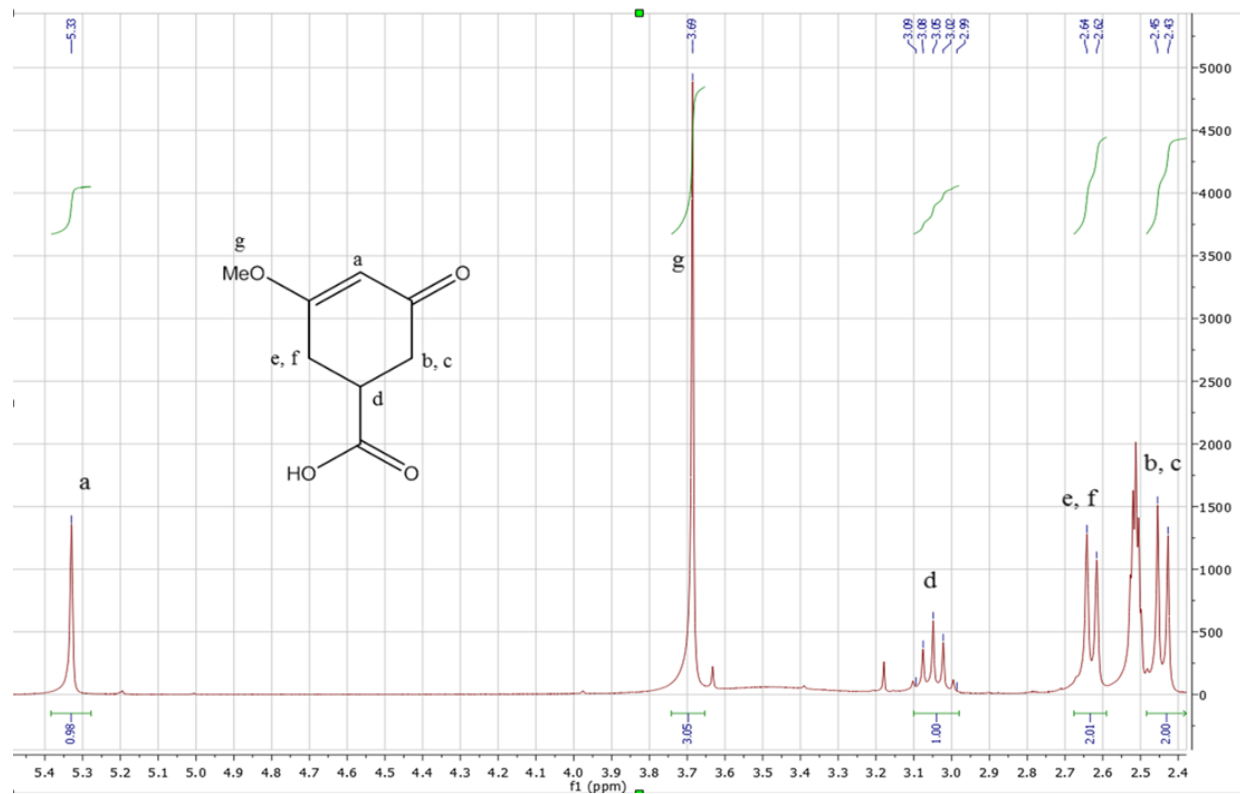


Figure 5.11: ^1H NMR spectrum of 3-methoxy-5-oxocyclohex-3-ene-1-carboxylic acid

Now that synthon had been protected and converted to **6** (Figure 5.12), it could be coupled to synthon **3**. For this, the same ethyl chloroformate method as described earlier was used, in DMF since compound **3** was poorly soluble in THF. Addition of the amine to the mixture led to the desired amide **7** (Figure 5.12) in a 43% yield after purification by dry column chromatography. Final deprotection of the enol ether using 1 M HCl led to the desired probe **1** with a 23% yield (Figure 5.12).

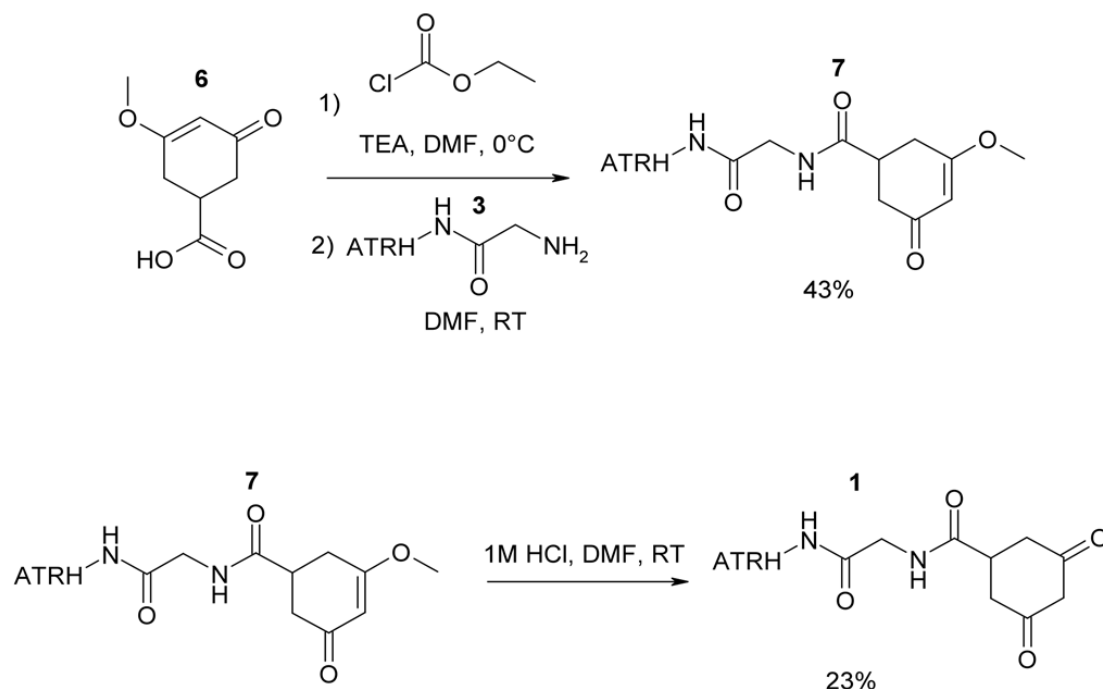


Figure 5.12: Reaction conditions for the synthesis of N-[2-(anthracen-2-ylamino)-2-oxoethyl]-3,5-dioxocyclohexanecarboxamide:

One of the challenges faced was when it came to the purification of the compound because DMF has a high boiling point the compound had to be heated to around 80 °C to evaporate all the solvent. When the compound was then checked on TLC the number of spots increased and the main spot, which could have been the compound, had disappeared as well. This could mean that the compound is not stable at high temperatures. To overcome this, a stronger vacuum pump was employed that could evaporate the solvent at 30 °C. TLC confirmed that the compound did not degrade at this temperature. The NMR with the assigned peaks of

compound **7** is shown in **Figure 5.13**. The final compound was characterised by ^1H NMR and will be used in the future to test on a single protein as well as on T cells to test its reactivity.

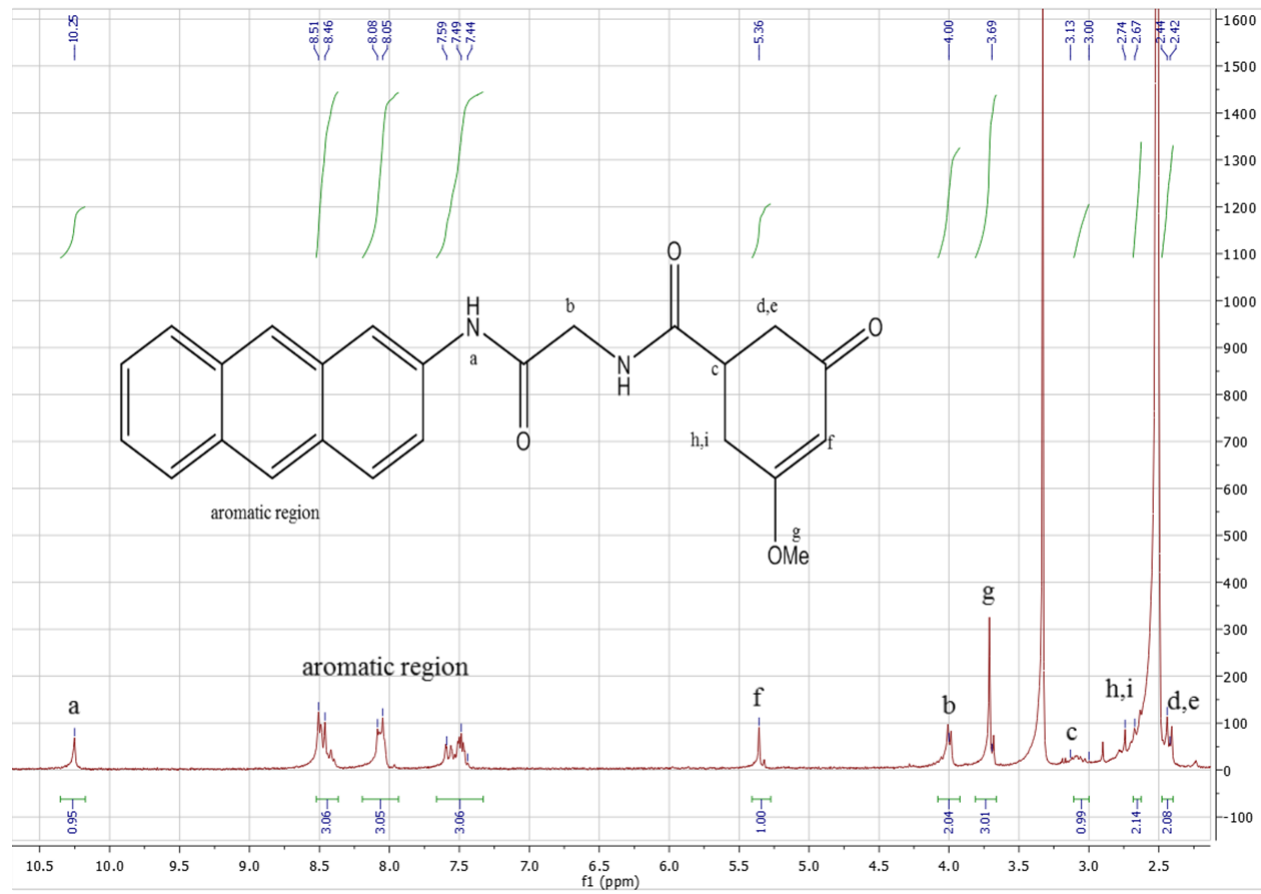


Figure 5.13: ¹H NMR spectrum of N-[(2-anthracen-2-ylamino)-2-oxoethyl]-3-methoxy-5-oxocyclohex-3-ene-1-carboxamide

5.4.6 Synthesis of sulphenic acid detecting magnetic probe:

Since the magnetic probe could not be characterised by NMR or mass spectrometry, infrared spectrometry was performed and compared with the starting material which is shown in **Figure 5.14** below. The red spectrum is the magnetic bead starting material, which has a broad peak around 3200 cm^{-1} that corresponds to the N-H stretch of amines. The product, which is shown in the blue spectrum lacks this peak but has two peaks, which correspond to the amine N-H stretch. The CO stretch from the carbonyl group of 3-methoxy-5-oxocyclohex-3-ene-1-carboxylic can be observed $\sim 1600\text{ cm}^{-1}$ as well as the aromatic ring vibrations $\sim 1500\text{-}1400\text{ cm}^{-1}$. Dissociation of amide bonds can be achieved using acids such as TFA and HCl. Therefore to cleave the amide bond 6 M HCl (10 mL) was added to the compound and left to react for 2 hours. Unfortunately these conditions proved to be too harsh and the magnetic beads were dissolved. The concentration of the acid was reduced to 2 M and the reaction was again carried out for 2 hours. The beads were isolated and washed and an IR was taken and compared to the starting material, which is shown in **Figure 5.15**.

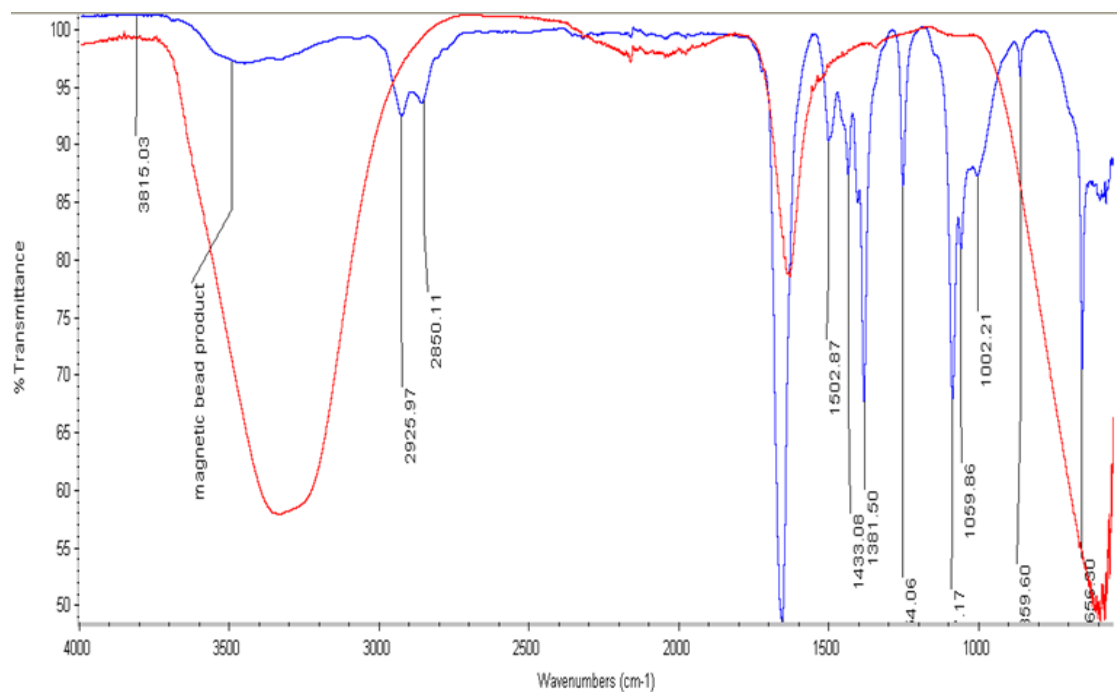


Figure 5.14: Infrared spectra of magnetic bead product with magnetic bead starting material.

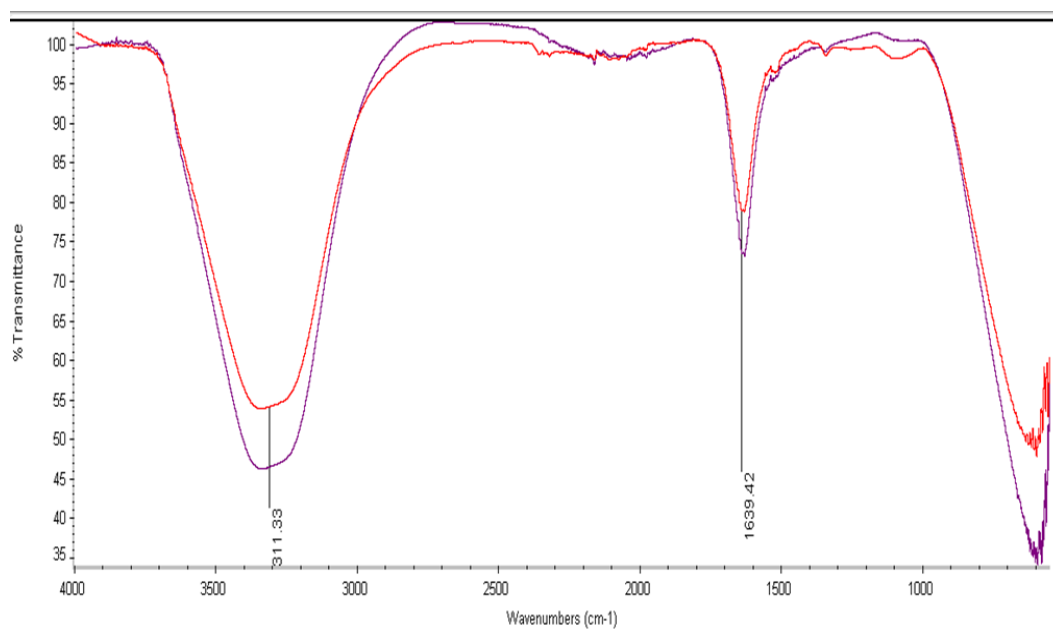


Figure 5.15: Infrared spectra comparison of starting material with material cleaved off with 2 M HCl.

The starting material (purple spectrum) and the beads after amide bond cleavage (red spectrum) look very similar which is indicative that the bond can be cleaved off with 2 M HCl and also that the peptide bond had previously been formed. EDC is used as a coupling agent in this reaction as it is a water soluble carbodiimide. NHS is used to stabilise the intermediate that is formed (178,183). The main disadvantage of this probe is that it cannot be characterised fully and can't be used in mass spectrometry. If the probe is to be used to isolate proteins from cells, that have sulphenic acid modifications it is important to cleave off the magnetic bead prior to mass spectrometric analysis. However, using acid in high concentrations would be harmful to the proteins. Therefore more work needs to be done in order to optimise this probe before it is ready to be tested.

In conclusion, two novel probes have been synthesised that have the potential to be used as tools in real time subcellular identification of sulphenic acid modified proteins.

Chapter 6.0 General Discussion

6.1 Discussion:

RSOH due to its unstable nature and high reactivity has been challenging to study until recently. The oxidation state of sulphur in SOH is 0 and therefore chemically it has both electrophilic and nucleophilic characteristics. The self-condensation to form thiosulphinic acid is an example of this dual nature (184). In cells oxidation to RSO₂H shows the nucleophilic nature of sulphenic acids. However RSOH exhibit a high reactivity towards nucleophiles and disulphide bond formation is an important function by which proteins are stabilised (185). Since sulphenic acids were first reported by Allison (140), they have only been identified in a small number of proteins. This is due to the fact that capturing these modifications remains difficult. Both direct and indirect methods have been employed to identify these modifications. Indirect methods rely on the reactivity of alkylating agents such as IAM and NEM to block thiols, reduction of SOH groups and consequent labelling of the reduced thiols with biotin maleimide (47). Since these methods are not very selective towards SOH, more recently dimedone based probes such as DCP-Bio1, DCP-Bio2, DCP-FL1 and Daz-1 have been employed to identify sulphenic acid modifications (1,10,56).

This thesis describes the optimisation of conditions for sulphenic acid modification in the purified protein human serum albumin (HSA) using the biotin tag probe DCP-Bio1. Mass spectrometry and dot blot experiments performed on GSH showed that sulphenic acid formation did not occur and that it favours disulphide bond formation. In contrast, under specific conditions sulphenic acid formation was observed in HSA using western blotting and mass spectrometry. Initial experiments using a modified ELSPA with HSA gave the first indication of SOH formation. Using this ELSPA it was demonstrated that addition of oxidants such as hydrogen peroxide could lead to the formation of sulphenic acids in a dose dependent manner. The addition of excess H₂O₂ lead to over oxidation to form sulphinic and sulphonic acids, which are not detectable by DCP-Bio1. It was also concluded from the results of the ELSPA that addition of DCP-Bio1 and H₂O₂ simultaneously resulted in more SOH being detected. Therefore for all experiments throughout this thesis this method was adapted. Using the electrophilic reagent NBD-Cl, previous studies have shown that HSA reacts with

hydrogen peroxide in a 1:1 ratio to form SOH (64). The disadvantages of using NBD-Cl are that this reagent lacks specificity to only detect SOH and therefore can lead to false positive detection. Using different concentrations of the probe as well as different concentrations of hydrogen peroxide it was possible to demonstrate that HSA reacts with hydrogen peroxide and DCP-Bio1 in a 1:1:1 ratio. To determine the effects of alkylating agents such as IAM on the formation of sulphenic acids experiments were done where excess of IAM was added before the and after the addition of DCP-Bio1. Results indicated that addition of IAM before DCP-Bio1 addition blocks thiols thus preventing oxidation. However, research done by Reisz and co workers suggest that alkylating agents could potentially react with SOH groups and thus compete with the probe for sulphenic acid binding (159). This could be another possibility for absence of a band.

Earlier studies which have used the nucleophilic reagent dimedone for mass spectral analysis showed that the site of modification in HSA is Cys34, which is the only free thiol available (118). The stability of this SOH moiety stems from the fact that it is situated in a hydrophobic crevice thereby protecting it from solvents and other thiols, thus preventing disulphide bond formations. This was confirmed by X-ray diffraction, which provided a three dimensional structure of HSA (143). Although mass spectrometric analysis of HSA using DCP-Bio1 did not show a modification at Cys34, it revealed modifications at Cys200 which normally takes part in disulphide bond formation. A possible explanation for this is that the Cys34 modification is in low abundance and therefore could not be detected by mass spectrometry. Since reducing agents are used prior to treatment of HSA, if some of it was still present in the sample this could potentially lead to the dissociation of some disulphide bonds and SOH formation.

This thesis also identifies sulphenic acid formation in human primary T cells for the first time and has shown that activation and oxidative stress can affect the formation of SOH. Under normal conditions cells maintain a reducing environment (**Figure 6.1, A**). Glutathione is a major antioxidant that helps in maintaining the redox status in the cells. Therefore it was hypothesised that if GSH was depleted in the cells it would cause oxidative stress in cells and

therefore led to an increase in SOH formation (**Figure 6.1, B**). BSO, which is widely used to deplete GSH in cells was used as it does not appear to have any toxicity towards primary cells (161). There was no loss of cell viability after treatment of primary T cells with BSO for 24 hours. Data obtained from both flow cytometry and DTNB assay indicated a significant decrease in surface thiols, which suggesting a more oxidised environment and therefore more SOH formation. Using DCP-Bio1 and western blotting techniques 5 bands were observed in primary T cells treated with BSO, at 25, 40, 45, 50 and 65 kDa. In resting T cells only three bands were observed at 25, 45 and 65 kDa. A non-specific band was detected in cell lysates following labelling with streptavidin-HRP. Carroll and co-workers have also reported these observations in Jurkat cell lysates and it was suggested that it could be an endogenously biotinylated protein (1).

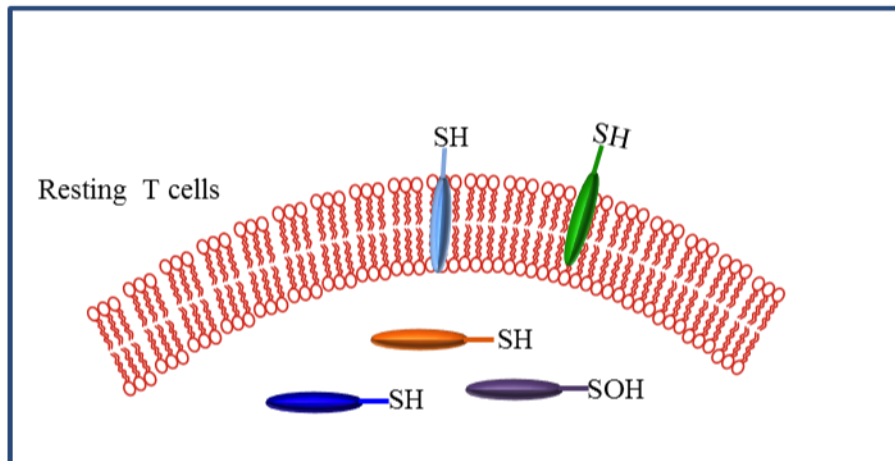
Since ROS are generated in response to mitogen-induced activation in resting T cells the next hypothesis was that when T cells were activated the number of sulphenic acid modified proteins would increase (**Figure 6.1, C**). In order to activate T cells 5 µg/mL PHA-L was used as it showed both increased levels of CD25 expression and IL-2 secretion after 24 hours of treatment. When T cells were activated to examine sulphenic acid modifications, although an increase in the number of protein bands was expected, only two bands could be observed at 25 kDa and 65 kDa. However, when cells were activated under oxidative stress, the number of bands increased. Mass spectrometry performed on the individual bands has identified some interesting proteins such as Flavin reductase (NADPH) for 25 kDa band, peroxiredoxin-1, arginase1, actin1 for 40 KDa band and HSA for 65 KDa band.

To visualise sulphenic acid formation in T cell, microscopy of the DCP-Bio1 and maleimide-labelled T cells was undertaken. The findings of this thesis suggests that DCP-Bio1 is cell permeable but perhaps could have some toxic effects on the cells which may limit the use of this probe in real time studies of sulphenic acid formation.

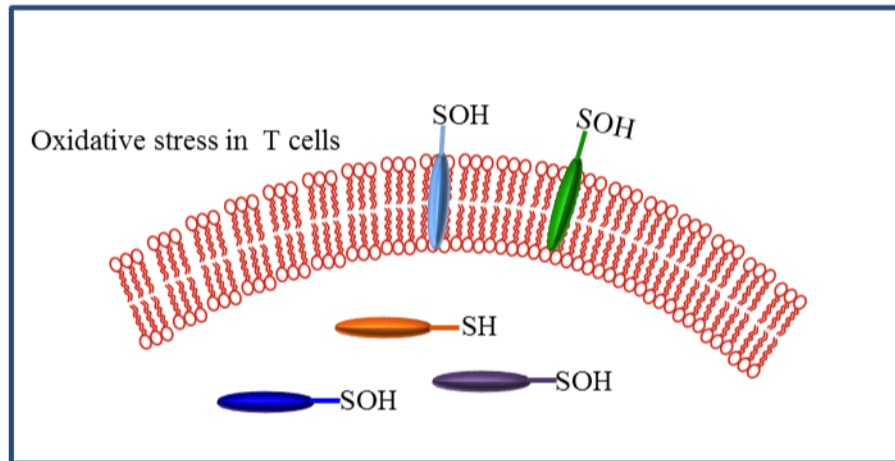
Finally, this thesis also looks at synthesising two novel probes; one fluorescent probe and one magnetic bead bound probe which have the potential to target sulphenic acid protein modifications. New probes are needed to visualise SOH formation in real time as the existing

probes exhibit certain limitations. The biotinylated DCP-Bio1, which was used throughout this thesis, showed some toxicity when confocal microscopy was performed on primary T cells. Although Poole and co-workers have developed a few fluorescent-tagged probes their bulky nature could mean limited cell permeability and steric hindrance prevent certain modifications from being detected. Therefore it was important to synthesise a fluorescent probe that is small to be cell permeable to visualise SOH formation in real time.

A



B



C

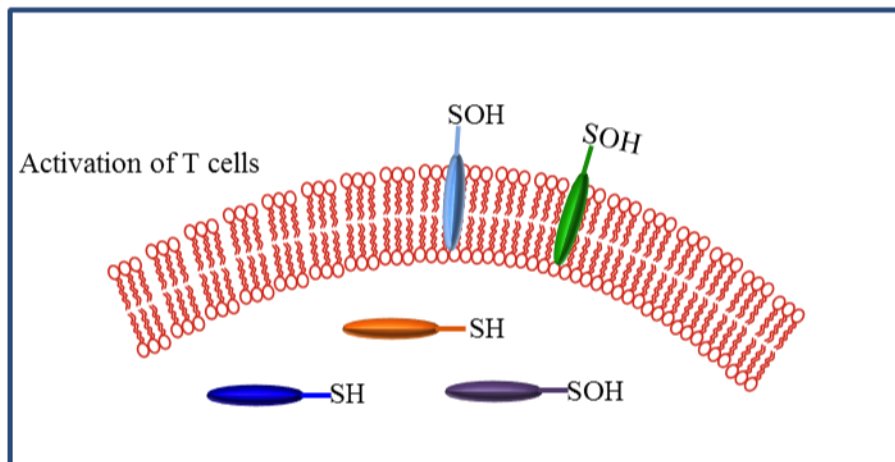


Figure 6.1: Schematic representation of T cells. A) resting B) oxidative stress and C) activated conditions.

6.2 Conclusion:

This thesis has described detection of sulphenic acid modifications in purified HSA using the biotinylated probe DCP-Bio1. It also describes the isolation of sulphenic acid modified proteins in resting; BSO depleted and activated human primary T cells for the first time. In addition, two novel probes, which have the potential to be used for sulphenic acid detection in real time, have been successfully synthesised.

6.3 Future work:

Although a fluorescent probe and a magnetic bead bound probe have successfully been synthesised they have not been tested on a purified protein or in cells. The first step towards establishing the usefulness of these molecules would be to investigate if they are able to detect sulphenic acids in a purified protein that has been well characterised such as HSA. It is also important to test the toxicity of the probe as it will be used to identify sub cellular sulphenic acids in real time. One of the limitations of the magnetic bead bound probe is that the magnetic bead has to be cleaved off prior to protein identification by mass spectrometry if it is able to identify modified proteins. However, the technique used in this thesis required 2 M HCl for cleavage which would be too harsh on proteins causing them to denature. Therefore alternative cleaving methods need to be investigated.

As a method has been developed to identify SOH in CD4+ T cells under resting, oxidative stress and activated conditions. This model could be used in the future to investigate changes in SOH formation in healthy controls versus patients with inflammatory disease. Although several proteins have been identified as potential targets for SOH modifications work needs to be done to confirm the specific proteins. For this, antibodies against specific proteins can be used and after immune precipitation, the PVDF membranes could be probed for each of them. Further work should also be done to improve the mass spectrometric detection methods in order that the probe-bound sulphenate is seen in tryptic peptides from probe precipitated specific proteins.

7.0 References

1. Leonard, E.S., Reddie, K.G., Carroll, S.K. (2009) Mining the thiol proteome for sulfenic acid modifications reveals new targets for oxidation in cells, *ACS Chemical Biology*, 4, 9, 783-799
2. Poole, L.B., Nelson, K.J. (2008) Discovering mechanisms of signalling-mediated cysteine oxidation, *Curr. Opin. Chem. Biol.*, 12, 18-24
3. Biswasa, S., Chidab, A.S., Rahman, I. (2006) Redox modifications of protein-thiols: Emerging roles in cell signalling, *Biochemical Pharmacology*, 7, 5, 551-564
4. Miseta, A., Csutora, P. (2000) Relationship between the occurrence of cysteine in proteins and the complexity of organisms, *Mol. Biol. Evol.*, 17, 1232-1239
5. Peter, I., Felder, C.E., Man, O., Silman, I., Sussman, J.L., Beckmann, J.S. (2004) Proteomic signatures: amino acid and oligopeptide compositions differentiate among phyla, *Proteins Struct. Funct. Bioinform.*, 54, 20-40
6. Nelson, D.L., Cox, M.M., Leninger, Principles of Biochemistry, 3rd edition, 118-126
7. Gupta, V., Carroll, K.S. (2014) Sulfenic acid chemistry, detection and cellular lifetime, *Biochem. Biophys. Acta*, 1840, 847-875
8. Carroll, S.K., Reddie, K.G. (2008) Expanding the functional diversity of proteins through cysteine oxidation, *Curr. Opin. Chem. Biol.*, 12, 746-754
9. Jacob, C., Giles, G.I., Giles, N.M., Sies, H. (2003) Sulphur and selenium: the role of oxidation state in protein structure and function, *Angew. Chem. Int. Ed.*, 42, 4742-4758
10. Reddie, K.G., Seo, Y.H., Muse, W.B., Leonard, S.E., Carroll, K.S. (2008) A chemical approach for detecting sulfenic acid-modified proteins in living cells, *Mol. Biosyst.*, 4, 521-531
11. Banerjee, R., Redox biochemistry (2008), John Wiley and sons,
12. Hogg, D.R. (1990) Chemistry of sulphenic acids and esters, in sulfenic acids and derivatives, JohnWiley and sons, Ltd., 2010, 361-402
13. Btuice, T.C., Sayigh, A.B. (1959) The structure of anthraquinone-1-sulphenic acid (Fries' acid) and related compounds, *J. Am. Chem. Soc.*, 81, 3416-3420
14. Benitez, L.V., Allison, W.S. (1974) The inactivation of the acyl phosphatase activity catalysed by the sulfenic acid form of glyceraldehyde-3-phosphate dehydrogenase by dimedone and olefins, *J. Biol. Chem.*, 249, 6234-6243
15. Salmeen, A., Anderson, J.N., Myers, M.P., Meng, T.C., Hinks, J.A., Tonks, N.K., Barford, D. (2003) Redox regulation of protein tyrosine phosphatase 1B involves a sulphenyl-amide intermediate, *Nature*, 423, 769-773
16. Van Montfort, R.L.M., Congreve, M., Tisi, D., Carr, R., Jhoti, H. (2003) Oxidation state of the active-site cysteine in protein tyrosine phosphatase 1B, *Nature*, 423, 773-777
17. Salmeen, A., Barford, D. (2005) Functions and Mechanisms of Redox Regulation of Cysteine based phosphatases, *Antioxid. Redox. Signal.*, 7, 560-577

18. Sarma, B.K., Muges, G. (2007) Redox regulation of protein tyrosine phosphatase 1B(PTP1B): a biomimetic study on the unexpected formation of a sulfenyl amide intermediate, *J. Am. Chem. Soc.*, 129, 8872-8881
19. Lee, J.W., Soonsanga, S., Helmann, J.D. (2007) A complex thiolate switch regulates the *Bacillus subtilis* organic peroxide sensor OhrR, *Proc. Natl. Acad. Sci.*, 104, 21, 8743-8748
20. Buhrman, G., Parker, B., Sohn, J., Rudolph, J., Mattos, C.(2005) Structural mechanism of oxidative regulation of phosphatase Cdc25B via an intramolecular disulfide bond, *Biochemistry*, 44, 5307-5316
21. Wardman, P., von Sonntag, D. (1995) Kinetic factors that control the fate of thiyl radicals in cells, *Methods Enzymol.*, 251, 31-45
22. Barton, J.P., Packer, J.E., Sims, R.J. (1973) Kinetics of the reaction of hydrogen peroxide with cysteine and cysteamine, *J. Chem. Soc., Perkin Trans. 2*, 1547-1549
23. Nagy, P., Ashby, M.T. (2007) Reactive sulfur species: Kinetics and mechanisms of the oxidation of cysteine by hypohalous acid to give cysteine sulfenic acid, *J. Am. Chem. Soc.*, 129, 14082-14091
24. Guerin, P., Menezo, Y. (1995) Hypotaurine and taurine in gamete and embryo environments: de novo synthesis via the cysteine sulfinic acid pathway in oviduct cells, *Zygote*, 3, 4, 333-343
25. Rabilloud, T., Heller, M., Gasnier, F., Luche, S., Rey, C., Aebersold, R., Benahmed, M., Louisot, P., Lunardi, J. (2002) Proteomics analysis of cellular response to oxidative stress: evidence for in vivo over oxidation of peroxiredoxins at their active site, *J. Biol. Chem.*, 277, 19396-19401
26. Wood, Z.A., Poole, L.B., Karplus, P.A. (2003) Peroxiredoxin evolution and the regulation of hydrogen peroxide signaling, *Science*, 300, 650-653
27. Yang, K.S., Kang, S.W., Woo, H.A., Hwang, S.C., Chae, H.Z., Kim, K., Rhee, S.G. (2002) Inactivation of human peroxiredoxin 1 during catalysis as the result of the oxidation of the catalytic site cysteine to cysteine-sulfinic acid, *J. Biol. Chem.*, 277, 38029-38036
28. Jeong, W., Park, S.J., Chang, T.S., Lee, D.Y., Rhee, S.G. (2006) Molecular mechanism of the reduction of cysteine sulfinic acid of peroxiredoxin to cysteine by mammalian sulfiredoxin, *J. Biol. Chem.*, 281, 14400-14407
29. Biteau, B., Labarre, J., Toledano, M.B. (2003) ATP-dependent reduction of cysteine-sulphinic acid by *S. cerevisiae* sulphiredoxin, *Nature*, 425, 980-984
30. Woo, H.A., Chae, H.Z., Hwang, S.C., Yang, K.S., Kim, K., Rhee, S.G. (2003) Reversing the inactivation of peroxiredoxins caused by cysteine sulfinic acid formation, *Science*, 300, 653-656
31. Rehder, D.S., Borges, C.R. (2010) Cysteine sulfenic acid as an intermediate in disulfide bond formation and nonenzymatic protein folding, *Biochemistry*, 49, 7748-7755

32. Soito, L., Williamson, C., Knutson, S.T., Fetrow, J.S., Poole, L.B., Nelson, K.J. (2011) PREX: peroxiredoxin classification index, a database of subfamily assignments across the diverse peroxiredoxin family, *Nucleic Acids Res.*, 39, D332–D337
33. Hall, A., Nelson, K.J., Poole, L.B., Karplus, P.A. (2011) Structure-based insights into the catalytic power and conformational dexterity of peroxiredoxins, *Antioxid. Redox Signal.*, 15, 795–815
34. Hofmann, B., Hecht, H.J., Flohé, L. (2002) Peroxiredoxins, *Biol. Chem.*, 383, 347
35. Cox, A.G., Winterbourn, C.C., Hampton, M.B. (2010) Mitochondrial peroxiredoxin involvement in antioxidant defence and redox signalling, *Biochem. J.*, 425, 313–325
36. Winterbourn, C.C. (2008) Reconciling the chemistry and biology of reactive oxygen species, *Nat. Chem. Biol.*, 4, 278–286
37. Toppo, S., Flohé, L., Ursini, F., Vanin, S., Maiorino, M. (2009) Catalytic mechanisms and specificities of glutathione peroxidases: variations of a basic scheme, *Biochim. Biophys. Acta, Gen. Subj.*, 179, 1486–1500
38. Brigelius-Flohé, R. (1999) Tissue-specific functions of individual glutathione peroxidases, *Free Radic. Biol. Med.*, 27, 951–965
39. Tosatto, S.C., Bosello, B., Fogolari, F., Mauri, P., Roveri, A., Toppo, S., Flohe, L., Ursini, F., Maiorino, M. (2008) The catalytic site of glutathione peroxidases, *Antioxid. Redox Signal.*, 10, 1515–1526
40. Flohe, L., Toppo, S., Cozza, G., Ursini, F. (2011) A comparison of thiol peroxidase mechanisms, *Antioxid. Redox Signal.*, 15, 763–780
41. Zheng, M., Wang, X., Templeton, L.J., Smulski, D.R., LaRossa, R.A., Storz, G. (2001) DNA microarray-mediated transcriptional profiling of the *Escherichia coli* response to hydrogen peroxide, *J. Bacteriol.*, 183, 4562–4570
42. Denu, J.M., Tanner, K.G. (1998) Specific and reversible inactivation of protein tyrosine phosphatases by hydrogen peroxide: evidence for a sulfenic acid intermediate and implications for redox regulation, *Biochemistry*, 37, 5633–5642
43. Zheng, M., Aslund, F., Storz, G. (1998) Activation of the OxyR transcription factor by reversible disulfide bond formation, *Science*, 279, 1718–1721
44. Carroll, K.S., Leonard, S.E. (2011) Chemical ‘omics’ approaches for understanding protein cysteine oxidation in biology, *Curr. Opin. Chem. Biol.*, 15, 88–102
45. Ying, J., Clavreul, N., Sethuraman, M., Adachi, T., Cohen, R.A. (2007) Thiol oxidation in signalling and response to stress: detection and quantification of physiological and pathophysiological thiol modifications, *Free. Radic. Biol. Med.*, 43, 1099–1108
46. Jaffrey, S.R., Snyder, S.H. (2001) The biotin switch method for the detection of S-nitrosylated proteins, *Sci. STKE*, 86, 1

47. Saurin, A.T., Neubert, H., Brennan, J.P., Eaton, P. (2004) Widespread sulfenic acid formation in tissues in response to hydrogen peroxide, *Proc. Natl. Acad. Sci. U.S.A.*, 101, 17982–17987
48. Eaton, P. (2006) Protein thiol oxidation in health and disease: techniques for measuring disulfides and related modifications in complex protein mixtures, *Free. Radic. Biol. Med.*, 40, 1889–1899
49. Persson, C., Sjöblom, T., Groen, A., Kappert, K., Engström, U., Hellman, U., Heldin, C.H., den Hertog, J., Östman, A. (2004) Preferential oxidation of the second phosphatase domain of receptor-like PTP- α revealed by an antibody against oxidized protein tyrosine phosphatases, *Proc. Natl. Acad. Sci. U.S.A.*, 101, 1886–1891
50. Karisch, R., Neel, B.G. (2013) Methods to monitor classical protein-tyrosine phosphatase oxidation, *FEBS. J.*, 280, 459–475
51. Birkett, D.J., Price, N.C., Radda, G.K., Salmon, A.G. (1970) The reactivity of SH groups with a fluorogenic reagent, *FEBS Lett.*, 6, 346–348
52. Ellis, H.R., Poole, L.B. (1997) Novel application of 7-chloro-4-nitrobenzo-2-oxa-1,3-diazole to identify cysteine sulfenic acid in the AhpC component of alkyl hydroperoxide reductase, *Biochemistry*, 36, 15013–15018
53. Takanishi, C.L., Ma, L.H., Wood, M.J. (2007) A genetically encoded probe for cysteine sulfenic acid protein modification in vivo, *Biochemistry*, 46, 14725–14732
54. Poole, L.B., Zeng, B.B., Knaggs, S.A., Yakubu, M., King, S.B. (2005) Synthesis of chemical probes to map sulfenic acid modifications on proteins, *Bioconjugate Chem.*, 16, 1624-1628
55. Poole, L.B., Ellis, H.R. (2002) Identification of cysteine sulfenic acid in AhpC of alkyl hydroperoxide reductase, *Methods in Enzymology*, 348, 122-136
56. Poole, L.B., Klomsiri, C., Knaggs, S.A., Furdai, C.M., Nelson, K.J., Thomas, M.J., Fetrow, J.S., Daniel, L.W., King, S.B. (2007) Fluorescent and affinity based tools to detect cysteine sulfenic acid formation in proteins, *Bioconjugate Chem.*, 18, 2004-2017
57. Toropainen, E., Ranta, V.P., Talvitie, A., Suhonen, P., Urtti, A. (2001) Culture model of human corneal epithelium for prediction of ocular drug absorption, *Invest. Ophthalmol. Visual. Sci.*, 42, 2942-2948
58. Michalek, R.D., Nelson, K.J., Holbrook, B.C., Yi, J.S., Stridiron, D., Daniel, L.W., Fetrow, J.S., King, S.B., Poole, L.B., Grayson, J.M. (2007) The requirement of reversible cysteine sulfenic acid formation for T cell activation and function, *J. Immunol.*, 179, 6456–6467

59. Wani, R., Qian, J., Yin, L., Bechtold, E., King, S.B., Poole, L.B., Paek, E., Tsang, A.W., Furdai, C.M. (2011) Isoform-specific regulation of Akt by PDGF-induced reactive oxygen species, *Proc. Natl. Acad. Sci. U.S.A.*, 108, 10550–10555
60. Carroll, K.S., Seo, Y.H. (2009) Facile synthesis and biological evaluation of a cell-permeable probe to detect redox-regulated proteins, *Bioorganic & Medicinal Chemistry Letters*, 19, 356-359
61. Van Tamelen, E.E., Hildahl, G.T (1956) The Synthesis of Tropone and Tropolone via a Norcarenone→Cycloheptadienone Rearrangement, *J. Am. Chem. Soc.*, 78, 4405-4412
62. Saxton, E., Bertozzi, C.R. (2000) Cell surface engineering by a modified Staudinger reaction, *Science*, 287, 2007-2010
63. Halliwell, B. (1988) Albumin: an important extracellular antioxidant?, *Biochem. Pharmacol.*, 37, 569-571
64. Carballal, S., Radi, R., Kirk, M.C., Barnes, S., Freeman, B.A., Alvarez, B. (2003) Sulfenic acid formation in human serum albumin by hydrogen peroxide and peroxynitrite, *Biochemistry*, 42, 9906-9914
65. Cowan-Jacob, S.W., Kaufmann, M., Anselmo, A.N., Stark, W., Grutter, M.G. (2003) Structure of rabbit muscle glyceraldehyde-3-phosphate dehydrogenase, *Acta Crystallogr. D Biol. Crystallogr.*, 59, 2218-2227
66. Paulsen, C.E., Truong, T.H., Garcia, F.J., Homann, A., Gupta, V., Leonard, S.E., Carroll, K.S. (2012) Peroxide-dependent sulfenylation of the EGFR catalytic site enhances kinase activity, *Nat. Chem. Biol.*, 8, 57–64
67. Speers, A.E., Cravatt, B.F. (2004) Profiling enzyme activities in vivo using click chemistry methods, *Chem. Biol.*, 11, 535–546
68. Truong, T.H., Carroll, K.S. (2012) Redox regulation of epidermal growth factor receptor signalling through cysteine oxidation, *Biochemistry*, 51, 9954–9965
69. Poole, L.B, Qian, J., Klosiri, C., Wright, M.W., King, S.B., Tsang, A.W., Furdai, C.M. (2011) Simple synthesis of 1,3-cyclopentanedione derived probes for labelling sulfenic acid proteins, *Chem. Commun.*, 47, 9203-9205
70. Janeway, C.A.Jr., Walport, M. (2001) *Immunobiology: The immune system in health and disease*, 5th ed., New York: Garland science
71. Kindt, T.J., Goldsby, A.R., Osborne, B.A, Kuby *Immunology* 5th edition
72. Lindstrom, T.M., Robinson, W.H. (2010) Rheumatoid arthritis: a role for immunosenescence?, *J. Am. Geriatr. Soc.*, 58, 1565-1575
73. Lacy, P., Stow, J.L. (2011) Cytokine release from innate immune cells: association with diverse membrane trafficking pathways, *Blood*, 118, 9-18
74. Zhang, J.M., Jianxiong, A. (2007) Cytokines, Inflammation and Pain, *Int. Anesthesiol Clin.*, 45(2), 27-37

75. Alberts, B., Lewis, J.A. (2007) *Molecular biology of the cell*, 4th edition.
76. Murphy, K., Travers, P., Walport, M. (2007) *Janeways immunology*, Garland Science, 7th edition
77. Ahlers, J.D., Belyakov, I.M. (2010) Molecular pathways regulating CD4(+) T cell differentiation, energy and memory with implications for vaccines, *Trends in Molecular Medicine*, 16(10), 478-491
78. Feili-Hariri, M., Falkner, D.H., Morel, P.A. (2005) Polarization of naïve T cells into Th1 or Th2 by distinct cytokine-driven murine dendritic cell populations: implications for immunotherapy, *Journal of Leukocyte Biology*, 78(3), p656-664
79. Jinfang, Z., William, E.P.(2008) CD4 T cells:fates, functions and faults, *Blood*, 112, 1557-1569
80. Joffre, O., Nolte, M.A., Spörri, R., Sousa, C.R. (2009) Inflammatory signals in dendritic cell activation and the induction of adaptive immunity, *Immunol. Rev.*, 227(1), 234-247
81. Cantrell, D.A. (2002) T-cell antigen receptor signal transduction, *Immunology*, 105, 369–374
82. Brownlie, R.J., Zamoyska, R. (2013) T cell receptor signalling networks: branched, diversified and bounded, *Nat. Rev. Immunol.*, 13, 257–269
83. Lin, J., Weiss, A. (2001) T cell receptor signalling, *Cell Sci.*, 114, 243–244
84. Kesarwani, P., Murali, A.K., Al-Khami, A.A., Mehrota, S. (2013) Redox regulation of T-cell function: from molecular mechanisms to significance in human health and disease, *Antioxid. Redox. Signal.*, 18(12), 1497-1534
85. King, M.R. , Ismail, A.S., Davis, L.S., Karp, D.R. (2006) Oxidative stress promotes polarization of human T cell differentiation towards a T helper 2 phenotype, *J. Immunol.*, 176, 2765-2772
86. Hadzic, T., Li, L., Cheng, N., Walsh, S.A., Spitz, D.R., Kudsn, C.M. (2005) The role of low molecular weight thiols in T lymphocyte proliferation and IL-2 secretion, *J. Immunol.*, 175, 7965-7972
87. Jaarsma, D., Haasdijk, E.D., Grashorn, J.A., Hawkins, R., van Duijn, W., Verspaget, H.W., London, J., Holstege, J.C. (2000) Human Cu/Zn superoxide dismutase (SOD1) overexpression in mice causes mitochondrial vacuolization, axonal degeneration, and premature motor neuron death and accelerates motor neuron disease in mice expressing a familial amyotrophic lateral sclerosis mutant SOD1, *Neurobiol. Dis.*, 7, 623–643
88. Case, A.J., McGill, J.L., Tygrett, L.T., Shirasawa, T., Spitz, D.R., Waldschmidt, T.J., Legge, K.L., Domann, F.E. (2011) Elevated mitochondrial superoxide disrupts normal T cell development, impairing adaptive immune responses to an influenza challenge, *Free Radic. Biol. Med.*, 50, 448–458

- 89.** Zou, Y., Chen, C.H., Fike, J.R., Huang, T.T. (2009) A new mouse model for temporal- and tissue-specific control of extracellular superoxide dismutase, *Genesis*, 47, 142–154
- 90.** Powers, S.K., Jackson, M.J. (2008) Exercise-induced oxidative stress: cellular mechanisms and impact on muscle force production, *Physiol. Rev.*, 88, 1243–1276
- 91.** Won, H.Y., Sohn, J.H., Min, H.J., Lee, K., Woo, H.A., Ho, Y.S., Park, J.W., Rhee, S.G., Hwang, E.S. (2010) Glutathione peroxidase 1 deficiency attenuates allergen-induced airway inflammation by suppressing Th2 and Th17 cell development, *Antioxid. Redox Signal.*, 13, 575–587
- 92.** Rubartelli, A., Bajetto, A., Alavena, G., Wollman, E., Sitia, R. (1992) Secretion of thioredoxin by normal and neoplastic cells through a leaderless secretory pathway, *J. Biol. Chem.*, 267, 24161-24164
- 93.** Di Trapani, G., Perkins, A., Clarke, F. (1998) Production and secretion of thioredoxin from transformed human trophoblast cells, *Mol. Hum. Reprod.*, 4(4), 369-375
- 94.** Nilsson, J., Soderberg, O., Nilsson, K., Rosen, A. (2000) Thioredoxin prolongs survival of B-type chronic lymphocytic leukaemia cells, *Blood*, 95(4), 1420-1426
- 95.** Rosen, A., Lundman, P., Carlsson, M., Bhavani, K., Srinivasa, B.R., Kjellstrom, G., Nilsson, K., Holmgren, A. (1995) A CD4⁺ T cell line-secreted factor, growth promoting for normal and leukemic B cells, identified as thioredoxin, *Int. Immunol.*, 7(4), 625-633
- 96.** Schenk, H., Vogt, M., Droge, W., Shulze-Osthoff, K. (1996) Thioredoxin as a potent costimulus of cytokine expression, *J. Immunol.*, 156(2), 765-771
- 97.** Nakamura, H., Nakamura, K., Yodiu, J. (1997) Redox regulation of cellular activation, *Annu. Rev. Immunol.*, 15, 351-369
- 98.** Holmgren, A., Lu, J. (2010) Thioredoxin and thioredoxin reductase: current research with special reference to human disease, *Biochem. Biophys. Res. Commun.*, 396, 120-124
- 99.** Shao, L., Diccianni, M.B., Tanaka, T., Gribi, R., Yu, A.L., Pullen, J.D., Camitta, B.M., Yu, J. (2001) Thioredoxin expression in primary T-cell acute lymphoblastic leukaemia and its therapeutic implication, *Cancer Res.*, 61, 7333–7338
- 100.** Meister, A. (1994) Glutathione-ascorbic acid antioxidant systems in animals, *J. Biol. Chem.*, 269, 9397-9400
- 101.** Ghezzi, P. (2011) Role of glutathione in immunity and inflammation in the lung, *Int. J. Gen. Med.*, 4, 105–113
- 102.** Griffiths, H.R., Grant, M.M. (2007) Cell passage-associated transient high oxygenation causes a transient decrease in cellular glutathione and affects T cell responses to apoptotic and mitogenic stimuli, *Environ. Toxicol. Pharmacol.*, 23(3), 335-339
- 103.** Phillips, D.C., Allen, K., Griffiths, H.R. (2002) Synthetic ceramides induce growth arrest or apoptosis by altering cellular redox status, *Arch. Biochem. Biophys.*, 407(1), 15-24

- 104.** Phillips, D.C., Woolard, K.J., Griffiths, H.R. (2003) The anti-inflammatory actions of methotrexate are critically dependent upon the production of reactive oxygen species, *Br. J. Pharmacol.*, 138(3), 501-511
- 105.** Grant, M.M., Scheel-Toellner, D., Griffiths, H.R. (2007) Contributions to our understanding of T cell physiology through unveiling the T cell proteome, *Clin. Exp. Immunol.*, 149(1), 9-15
- 106.** Phillips, D.C., Dias, H.K., Kitas, G.D., Griffiths, H.R. (2010) Aberrant reactive oxygen and nitrogen species generation in rheumatoid arthritis (RA): causes and consequences for immune function, cell survival and therapeutic intervention, *Antioxid. Redox. Signal.*, 12(6), 743-785
- 107.** Torrão, R.C., Bennett, S.J., Brown, J.E., Griffiths, H.R. (2014). Does metabolic reprogramming underpin age-associated changes in T cell phenotype and function?, *Free Radical Biology and Medicine*, 71, 26–35
- 108.** Torrão, R.C., Dias, H.K., Bennett, S.J., Dunston, C.R., Griffiths, H.R. (2013) Healthy ageing and depletion of intracellular glutathione influences T cell membrane thioredoxin-1 levels and cytokine secretion, *Chemistry Central Journal*, 7, 150
- 109.** Griffiths, H.R., Dunston, C.R., Bennet, S.J., Grant, M.M, Philips, D.C., Kitas, G.D. (2011) Free radicals and redox signalling in T cells during chronic inflammation and ageing, *Biochem. Soc. Trans.*, 39(5), 1273-1278
- 110.** Sahaf, B., Heydari, K., Herzenberg, L.A., Herzenberg, L.A. (2005) The extracellular microenvironment plays a key role in regulating the redox status of cell surface proteins in HIV-infected subjects, *Arch. Biochem. Biophys.*, 434, 26–32
- 111.** Gelderman, K.A., Hultqvist, M., Holmberg, J., Olofsson, P., Holmdahl, R (2006) T cell surface redox levels determine T cell reactivity and arthritis susceptibility, *Proc. Natl. Acad. Sci. U.S.A.*, 103, 12831–12836
- 112.** Hildeman, D.A., Mitchell, T., Teague, T.K., Henson, P., Day, B.J., Kappler, J., Marrack, P.C. (1999) Reactive oxygen species regulate activation-induced T cell apoptosis, *Immunity*, 10, 735–744
- 113.** Kesarwani, P., Murali, A.K., Al-Khami, A.A., Mehrota, S. (2013) Redox regulation of T-cell function: from molecular mechanisms to significance in human health and disease, *Antioxid. Redox. Signal.*, 18(12), 1497-1534
- 114.** Lahdenpohja, N., Savinainen, K., Hurme, M. (1998) Pre-Exposure to Oxidative Stress Decreases the Nuclear Factor- κ B Dependent Transcription in T Lymphocytes , *J. Immunol.*, 160(3), 1354-1358

- 115.** Smith, P.K., Krohn, R.I., Hermanson, G.T., Mallia, A.K., Gartner, F.H., Provenzano, M.D., Fujimoto, E.K., Goeke, N.M., Olson, B.J., Klenk, D.C. (1985) Measurement of protein using bicinchoninic acid, *Anal. Biochem.*, 150(1), 76-85
- 116.** Carballal, S., Alvarez, B., Turell, L., Botti, H., Freeman, B.A., Radi, R. (2007) Sulfenic acid in human serum albumin, *Amino acids*, 32, 543-551
- 117.** Clairborne, A., Yeh, J.I., Mallett, T.C., Luba, J., Crane, E.J.^{3rd}, Charrier, V., Parsonage, D. (1999) Protein sulfenic acids: diverse roles for an unlikely player in enzyme catalysis and redox regulation, *Biochemistry*, 8, 15407-15416
- 118.** Turell, L., Botti, H., Carballal, S., Radi, R., Alvarez, B. (2009) Sulfenic acid-A key intermediate in albumin thiol oxidation, *J. Chromatogr.*, 877, 3384-3392
- 119.** Bullmer, P.E., McNurlan, M.A., Milne, E., Heys, S.D., Buchan, V., Calder, A.G., Garlick, P.J. (1990) Measurement of albumin synthesis in humans: a new approach employing stable isotopes, *Am. J. Physiol.*, 259, 797-803
- 120.** Schnitzer, J.E., Sung, E., Hrvat, R., Bravo, J. (1992) Preferential interaction of albumin-binding proteins, gp30 and gp18, with conformationally modified albumins. Presence in many cells and tissues with a possible role in catabolism, *J. Biol. Chem.*, 267, 24544-24553
- 121.** Iwao, Y., Anraku, M., Hiraike, M., Kawai, K., Nakajou, K., Kai, T., Suenaga, A., Otagiri, M. (2006) The structural and pharmacokinetic properties of oxidized human serum albumin, advanced oxidation protein products (AOPP), *Drug metab. Pharmacokinet.*, 21, 140-146
- 122.** Halliwell, B., Gutteridge, J.M. (1990) The antioxidants of human extracellular fluids, *Arch. Biochem. Biophys.*, 280, 1-8
- 123.** Radi, R., Bush, K.M., Cosgrove, T.P., Freeman, B.A. (1991) Reaction of xanthine oxidase-derived oxidants with lipid and protein of human plasma, *Arch. Biochem. Biophys.*, 286, 117-125
- 124.** Takakura, K., Beckman, J.S., MacMillan-Crow, L.A., Crow, J.P. (1999) Rapid and irreversible inactivation of protein tyrosine phosphatases PTP1B, CD45 and LAR by peroxynitrite, *Arch. Biochem. Biophys.*, 369, 197-207
- 125.** Bryk, R., Griffin, P., Nathan, C. (2000) Peroxynitrite reductase activity of bacterial peroxiredoxins, *Nature*, 407, 211-215
- 126.** Trujillo, M., Budde, H., Pineyro, M.D., Stehr, M., Robello, C., Flohe, L., Radi, R. (2004) *Trypanosoma brucei* and *Trypanosoma cruzi* tryparedoxin peroxidises catalytically detoxify peroxynitrite via oxidation of fast reacting thiols, *J. Biol. Chem.*, 279, 34175-34182
- 127.** Wilson, J.M., Wu, D., Motiu-Degroot, R., Hupe, D.J. (1980) A spectrophotometric method for studying the rates of reaction of disulphides with protein thiol groups applied to bovine serum albumin, *J. Am. Chem. Soc.*, 102, 359-363

- 128.** Shafer, F.Q., Buettner, G.R. (2001) Redox environment of the cell as viewed through the redox state of the glutathione disulfide/glutathione couple, *Free Radic. Biol. Med.*, 30, 1191-1212
- 129.** Janatova, J., Fuller, J.K., Hunter, M.J. (1968) The heterogeneity of bovine albumin with respect to sulphhydryl and dimer content, *J. Biol. Chem.*, 243, 3612-3622
- 130.** Noel, J.K., Hunter, M.J. (1972) Bovine mercaptalbumin and non-mercaptalbumin monomers. Interconversions and structural differences, *J. Biol. Chem.*, 247, 7391-7406
- 131.** Era, S., Hamaguchi, T., Sogami, M., Kuwata, K., Suzuki, E., Miura, K., Kawai, K., Kitazawa, Y., Okabe, H., Noma, A. (1988) Further studies on the resolution of human mercapt and nonmercaptalbumin and on human serum albumin in the elderly by high performance liquid chromatography, *Int. J. Pept. Protein. Res.*, 31, 435-442
- 132.** Tomida, M., Ishimaru, J., Hayashi, T., Nakamura, K., Murayama, K., Era, S. (2003) The redox states of serum and synovial fluid of patients with temporomandibular joint disorders, *Jpn. J. Physiol.*, 53, 351-355
- 133.** Imai, H., Hayashi, T., Negawa, T., Nakamura, K., Tomida, M., Koda, K., Tajima, T., Koda, Y., Suda, K., Era, S. (2002) Strenuous exercise induced change in redox state of human serum albumin during intensive kendo training, *Jpn. J. Physiol.*, 52, 135-140
- 134.** Era, S., Kuwata, K., Imai, H., Nakamura, K., Hayashi, T., Sogami, M. (1995) Age related change in redox state of human serum albumin, *Biochim. Biophys. Acta*, 1247, 12-16
- 135.** Radi, R., Bush, K.M., Beckman, J.S., Freeman, B.A. (1991a) Peroxynitrite oxidation of sulphhydryls. The cytotoxic potential of superoxide and nitric oxide, *J. Biol. Chem.*, 266, 4244-4250
- 136.** Aboderin, A.A., Boedefeld, E. (1976) Reaction of chicken egg white lysozyme with 7-chloro-4-nitrobenz-2-oxa-1,3-diazole. II. Sites of modification, *Biochim. Biophys. Acta*, 420, 177-186
- 137.** Cañasl, B., López-Ferrer, D., Ramos-Fernández, A., Camafeita, E., Calvo, E. (2006) Mass spectrometry technologies for proteomics, *Brief Funct. Genomic Proteomic*, (4), 295-320
- 138.** Lu, B., Xu, T., Park, S.K., McCatchy, D.B., Liao, L., Yates, J.R. (2009) Shotgun protein identification and quantification by mass spectrometry in neuroproteomics, *Methods Mol. Biol.*, 566, 229-259
- 139.** Dickinson, D.A., Forman, H.J. (2002) Cellular glutathione and thiols metabolism, *Biochem. Pharmacol.*, 64, 1019-1026
- 140.** Allison, S.W. (1976) Formation and reactions of sulfenic acids in proteins, *Accounts of Chemical Research*, 9, 293-299
- 141.** He, X.M., Carter, D.C. (1992) Atomic structure and chemistry of human serum albumin, *Nature*, 358, 209-215

- 142.** Stewart, A.J, Bindauer, C.A., Berezenko, S., Sleep, D., Tooth, D., Sadler, P.J. (2005) Role of Tyr84 in controlling the reactivity of Cys34 of human albumin, *Febs. J.*, 272, 353-362
- 143.** Sugio, S., Kashima, A., Mochizuki, S., Noda, M., Kobayashi, K. (1999) Crystal structure of human serum albumin at 2.5Å resolution, *Protein Eng.*, 12, 439-446
- 144.** Nathan, C., Cunnigham-Bussel, A. (2013) Beyond oxidative stress: an immunologists guide to reactive oxygen species, *Nat. Rev. Immunol.*, 5, 349-61
- 145.** Ghezzi, P., Bonetto, V., Fratelli, M. (2005) Thiol-disulfide balance: from the concept of oxidative stress to that of redox regulation, *Antioxid. Redox Signal.*, 7, 964-72.
- 146.** Zheng, S., Yumei, F., Chen, A (2007) De novo synthesis of glutathione is a prerequisite for curcumin to inhibit HSC activation, *Free Radic. Biol. Med.*, 43(3), 444-453
- 147.** Wild, A.C., Moinova, H.R., Mulcahy, R.T. (1999) Regulation of gamma-glutamylcysteine synthetase subunit gene expression by the transcription factor Nrf2, *J. Biol Chem.*, 274(47):33627-33636
- 148.** Angelini, G., Gardella, S., Ardy, M., Ciriolo, M.R., Filomeni, G., Di Trapani, G., Clarke, F., Sitia, R., Rubartell, I A. (2002) Antigen-presenting dendritic cells provide the reducing extracellular microenvironment required for T lymphocyte activation, *Proc. Natl. Acad. Sci. U.S.A.*, 99, 1491–1496
- 149.** Gringhuis, S.I., Leow, A., Papendrecht-Van Der Voort, E.A., Remans, P.H., Breedveld, F.C., Verweij, C.L. (2000) Displacement of linker for activation of T cells from the plasma membrane due to redox balance alterations results in hyporesponsiveness of synovial fluid T lymphocytes in rheumatoid arthritis, *J. Immunol.*, 164, 2170-9.
- 150.** Reyes, B.M., Danese, S., Sans, M., Fiocchi, C., Levine, A.D.(2005) Redox equilibrium in mucosal T cells tunes the intestinal TCR signalling threshold, *J. Immunol.*, 175, 2158-2166
- 151.** Hogg, P.J. (2003) Disulphide bonds as molecular switches for protein function, *Trends. Biochem. Sci.*, 28,210-214
- 152.** He, Y.Y., Huang, J.L., Block, M.L., Hong, J.S.,Chignell, C.F. (2005) Role of phagocyte oxidase in UVA-induced oxidative stress and apoptosis in keratinocytes, *J. Invest. Dermatol.*, 125, 560-6.
- 153.** Kwon, J., Lee, S.R., Yang, K.S., Ahn, Y., Kim, Y.J., Stadtman, E.R., Rhee, S.G. (2004) Reversible oxidation and inactivation of the tumour suppressor PTEN in cells stimulated with peptide growth factors, *Proc. Natl. Acad. Sci. U.S.A.*, 101, 16419-16424
- 154.** Kwon, J., Qu, C.K., Maeng, J.S., Falahati, R., Lee, C., Williams, M.S. (2005) Receptor stimulated oxidation of SHP-2 promotes T-cell adhesion through SLP-76-ADAP, *EMBO J.*, 24, 2331-2341
- 155.** Abate, C., Patel, L., Rauscher, F.J, Curran, T. (1990) Redox regulation of fos and jun DNA binding activity in vitro, *Science*, 249, 1157-1161

- 156.** Nishi, T., Shimizu, N., Hiramoto, M., Sato, I. (2002) Spatial redox regulation of a critical cysteine residue of NF- κ B in vivo, *J. Biol. Chem.*, 277, 44548-44556
- 157.** Laragione, T., Bonetto, V., Casoni, F., Massignan, T., Bianchi, G., Gianazza, E. Ghezzi, P. (2003) *Proc. Natl. Acad. Sci. U.S.A.*, 100, 14737-41.
- 158.** Klarskov, K., Methogo, R.M., Dufresne-Martin, G., Leclerc, P., Leduc, R. (2005) Mass spectrometric peptide fingerprinting of proteins after Western Blotting on Polyvinylidene Fluoride and enhanced Chemiluminescence detection, *Journal of Proteomic Research*, 4, 2216-2224
- 159.** Reisz, J.A., Bechtold, E., King, S.B., Poole, L.B., Furdui, C.M. (2013) Thiol blocking electrophiles interfere with labelling and detection of protein sulfenic acids, *J. FEBS*, 23, 6150-6161
- 160.** Hancock, J.T, Desikan, R., Neill, S.J. (2003) CytochromeC, Glutathione and the possible role of redox potentials in apoptosis, *Ann. N. Y. Acad. Sci.*, 1010, 446-448
- 161.** Sechis, S., Alptekin, N., Dogru-Abbasoglu, S., Kocak-Toker, N., Toker, G., Uysal, M. (1997) The effect of chronic stress on hepatic and gastric lipid peroxidation in long term depletion of glutathione in rats, *Pharmacol. Res.*, 36, 55-57
- 162.** Nelson, B.H., (2004) IL-2, regulatory T cells and tolerance, *The Journal of Immunology*, 172, 3983
- 163.** Parsonage, D., Nelson, K.J., Ferrer-Sueta, G. Alley, S., Karplus, P.A., Furdui, C.M., Poole, L.B. (2015) Dissecting peroxiredoxin catalysis: Separating binding, peroxidation and resolution for a bacterial AhpC, *Biochemistry*, 54(7), 1567-1575
- 164.** Morais, M.A.B., Giuseppe, P.O., Souza, T.A.C.B., Alegria, T.G.P., Oliveira, M.A., Netto, L.E.S., Murakami, M.T. (2015) How pH modulates the dimer-decamer interconversion of 2-cys peroxiredoxins from the PRX1 subfamily, *JCB*, 1-10
- 165.** Iyamu, W.E., Perdew, H.A., Woods, G.M. (2012) Oxidant-mediated modification of the cellular thiols is sufficient for arginase activation in cultured cells, *Mol. Cell. Biochem.*, 360, 159-168
- 166.** Ckless, K., van der Vliet, A., Janssen-Heininger, Y. (2007) Oxidative-nitrosative stress and post translational protein modifications: Implications to lung structure function relations, *Am. J. Respir. Cell. Mol. Biol.*, 36, 645-653
- 167.** Hynes, R.O. (1992) Integrins: Versatility, modulation and signalling in cell adhesion, *Cell*, 69, 11-25
- 168.** Sobierajska, K., Skurzynski, S., Stasiak, M., Kryczka, J., Cierniewski, C., Swiatkowska, M. (2014) Protein disulfide isomerase directly interacts with β -Actin C374 and regulates cytoskeleton reorganisation, *JCB*, 289(9), 5758-5773
- 169.** Bruice, T.C., Sayigh, A.B. (1959) The Structure of Anthraquinone-1-sulfenic Acid (Fries' Acid) and Related Compounds, *J. Am. Chem. Soc.*, 81, 3416-3420

- 170.** Pal, B.C., Uziel, M., Doherty, D.G., Cohn, W.E. (1969) Isolation and characterisation of a pyrimidine sulfenic acid via scission of the sulfur-sulfur bond in the methyl analog of bis(4-thiouridine)disulfide, *J. Am. Chem. Soc.*, 91, 3634-3638
- 171.** Heckel, A., Pfeleiderer, W. (1983) Lumazinesulfenates-a new class of stable sulfenic acids, *Tetrahedron Lett.*, 24, 5047-5050
- 172.** Yoshimura, T., Tsukurimichi, E., Yamazaki, S., Soga, S., Shimasaki, C., Hasegawa, K. (1992) Synthesis of a stable sulfenic acid, trans-decalin-9-sulfenic acid, *J. Chem. Soc. Chem. Commun.*, 1337-1338
- 173.** Goto, K., Holler, M., Okazaki, R. (1997) Synthesis, structure and reactions of a sulfenic acid bearing a bowl-type substituent: the first synthesis of a stable sulfenic acid by direct oxidation of a thiol, *J. Am. Chem. Soc.*, 119, 1460-1461
- 174.** Miller, H., Claiborne, A. (1991) Peroxide modification of monoalkylated glutathione reductase. Stabilisation of an active side cysteine sulfenic acid, *J. Biol. Chem.*, 266, 19342-19350
- 175.** Fraenkel-Conrat, H. (1955) The reaction of tobacco mosaic virus with iodine, *J. Biol. Chem.*, 217, 373-381
- 176.** Seo, Y.H., Carroll, K.S. (2009) Profiling protein thiol oxidation in tumour cells using sulfenic acid specific antibodies, *Proc. Natl. Acad. Sci. U.S.A.*, 106, 16163-16168
- 177.** Montalbetti, C.A.G.N., Falque, V. (2005) Amide bond formation and peptide coupling, *Tetrahedron*, 61, 10827-10852
- 178.** Xang-Hong, S., Zhao, W., Yong, X., Ting-Hong, Y., Mei, D., You-Zhi, X., Yu-Quan, W., Luo-Ting, Y. (2012) Synthesis and biological evaluation of novel Benzothiazole-2- thiol derivatives as potential anticancer agents, *Molecules*, 17, 3933-3944
- 179.** Blazevic, N., Kolbah, D., Belin, B., Sunjic, V., Kajfez, F. (1979) Hexamethylenetetramine, a versatile reagent in organic synthesis, *Synthesis*, 161-176
- 180.** Lundt, B.F., Johansen, N.L., Vølund, A., Markussen, J. (1978) Removal of t-Butyl and t-Butoxycarbonyl Protecting Groups with Trifluoroacetic acid, *International Journal of Peptide and Protein Research*, 12(5), 258-268
- 181.** Rylander, P.N. (1985) Hydrogenation methods, 1-25
- 182.** Hornback, J.M. *Organic Chemistry* 2nd edition.
- 183.** Sheehan, J.C., Cruickshank, P.H., Boshart, G.L. (1960) A convenient synthesis of water-soluble carbodiimides, *Notes*, 2525-2528
- 184.** Davis, F.A., Jenkins, L.A., Billmers, R.L. (1986) Chemistry of sulfenic acids. 7. Reasons for the high reactivity of sulfenic acids. Stabilization by intramolecular hydrogen-bonding and electronegativity effects, *J. Org. Chem.*, 51, 1033-1040
- 185.** Rehder, D.S., Borges, C.R. (2010) Cysteine sulfenic acid as an intermediate in disulfide bond formation and nonenzymatic protein folding, *Biochemistry*, 49, 7748-7755